Estimating Cargo Airdrop Collateral Damage Risk

THESIS

Vincent R. Cammarano
Captain, United States Air Force

AFIT-LSCM-ENS-11-02

DEPARTMENT OF THE AIR FORCE
AIR UNIVERSITY

AIR FORCE INSTITUTE OF TECHNOLOGY

Wright-Patterson Air Force Base, Ohio

DISTRIBUTION STATEMENT A
APPROVED FOR PUBLIC RELEASE; DISTRIBUTION UNLIMITED.

The views expressed in this thesis are those of the author and do not reflect the official policy or position of the United States Air Force, Department of Defense, or the United States Government.

AFIT-LSCM-ENS-11-02

ESTIMATING CARGO AIRDROP COLLATERAL DAMAGE RISK

THESIS

Presented to the Faculty

Department of Logistics Management

Graduate School of Engineering and Management

Air Force Institute of Technology

Air University

Air Education and Training Command

In Partial Fulfillment of the Requirements for the

Degree of Master of Science in Logistics and Supply Chain Management

Vincent R. Cammarano

Captain, United States Air Force

March 2011

APPROVED FOR PUBLIC RELEASE; DISTRIBUTION UNLIMITED.

AFIT-LSCM-ENS-11-02

ESTIMATING CARGO AIRDROP COLLATERAL DAMAGE RISK

Vincent R. Cammarano
Captain, United States Air Force

Approved:

_____///SIGNED///_____	_24 Mar 11__
Dr. Jeffery K. Cochran, USAF (Advisor) Professor of Operations Research	Date
_____///SIGNED///_____	_24 Mar 11__
Dr. Raymond R. Hill (Member) Professor of Operations Research	Date

AFIT-LSCM-ENS-11-02

Abstract

The purpose of this research is to determine an appropriate method for estimating cargo airdrop collateral damage risk. Specifically, this thesis answers the question: How can mission planners accurately predict airdrop collateral damage risk? The question is answered through a literature review and a thorough examination of a data set of real world airdrop scoring data. The data were examined to determine critical factors that affect airdrop error risks as well as to determine the characteristics of airdrop error patterns. Through this research it was determined that bivariate normal distributions with parameters of $\mu_x = 0, \mu_y = 0,\ \rho_{x,y} = 0$ and σ_x & σ_y pairs determined by empirical data are appropriate for modeling cargo airdrop errors patterns. Collateral risk is estimated by summing numerical integrations of a fit bivariate normal distribution for each drop type across rectangular representations of drop field objects in the field of concern. Airdrop altitude and chute type are found to make a statistically significant difference in airdrop error patterns while airdrop aircraft type does not appear to have a significant effect. This research methodology is implemented in an EXCEL spreadsheet tool that can be easily used by airdrop mission planners including an extension, requested by the research sponsors, to handle bundled drops that fall in a linear spread.

Acknowledgments

Completing this thesis has been a very difficult but rewarding challenge. I could not have hoped to have tackled such a daunting task without the marvelous support team who made this possible. I would like to thank my wife for her tireless love and support. My children for reminding me that life is not all about work, we must stop and make time to play…even while we are getting old. My thanks also to Capt Steve Dillenburger for his mathematical prowess and selfless assistance and to Dr. Raymond Hill for his valued advice and experienced perspectives. And I would be remiss without recognizing my thesis advisor Dr. Jeffery Cochran. Without his endless patience, wisdom, and guidance this thesis would not have existed. You all have made this experience one that I will never forget…Thank you!

Vincent R. Cammarano

Table of Contents

Page

Abstract iv

Acknowledgments v

List of Figures viii

List of Tables x

List of Acronyms xi

I. Introduction 1

Overview 1
Background 1
Problem Statement 3
Research Focus 3
Research Objectives 5
Assumptions and Limitations 6
Summary 8

II. Literature Review 9

The History of Airlift 9
Khe Sanh 10
An Loc 12
Types of Airdrops 12
Methods of Airdrops 13
Types of Parachutes 14
Airdrop Platforms 14
Airdrop Errors 15
Fitting Frequency Distributions 17
Circular Error Probable vs. Elliptical Error Probable 19
Risk 22

III. Methodology 23

Introduction 23
Initial Data Interpretation 23
Cleaning the Data 25
Symmetry 26
Transforming Data 28
Goodness of Fit Testing 29
Data Groups 29

IV. Results and Analysis 34

What the Data Looks Like 34
Symmetry Testing 36
Goodness of Fit Testing 38
The Bivariate Normal Probability Distribution 40
Determining Meaningful Data Groups 45
Determining Bivariate Normal Parameters 52
Calculating Airdrop Risk 54
Excel Model Validation 59
Example Risk Estimation Scenarios 61

V. Conclusions 69

Introduction 69
Limitations 72
Areas for future research 73

Appendix A. Airdrop Data 74

Appendix B. Airdrop Collateral Damage Risk Estimator 95

Appendix C. Quad Chart 88

Appendix D. Blue Dart 89

Bibliography 92

Vita 95

List of Figures

Page

Figure 2.1 CARP Diagram 16

Figure 2.2 Normal Probability Distribution 17

Figure 2.3 Area Under the Curve 17

Figure 2.4 CEP/EEP Comparison w/Equal Minor & Major Axis.....20

Figure 2.5 CEP/EEP Comparison w/Unequal Minor & Major Axis 21

Figure 2.6 CEP/EEP Comparison w/Grossly Unequal Minor & Major Axis 21

Figure 3.1 Data Sample 24

Figure 3.2 Data Grouping Levels 30

Figure 4.1 All Data Scatterplot.....34

Figure 4.2 All Data Scatterplots by Altitude Category 35

Figure 4.3 All Data Scatterplots by Chute Type 35

Figure 4.4 All Data Scatterplots by Aircraft Type 35

Figure 4.5 K-S Symmetry Test (Includes 0 Distances).....37

Figure 4.6 K-S Symmetry Test (0 Distances Removed) 37

Figure 4.7 Sample Normal Distribution Goodness of Fit Test Results.....39

Figure 4.8 The Bivariate Normal Distribution 42

Figure 4.9 Chute Type Homogeneity Test Results 46

Figure 4.10 Altitude Category Homogeneity Test Results.....47

Figure 4.11 Aircraft Type Homogeneity Test Results.....48

Figure 4.12 Rectangular Method Numerical Integration.....56

Figure 4.13 2-D Rectangular Method Numerical Integration.....56

Figure 4.14 Airdrop Collateral Damage Risk Estimator Screenshot 58

Figure 4.15 Scenario Test Results 60

Figure 4.16 Excel Aimpoint Input 63

Figure 4.17 Graphic Example of Risk Estimation Scenarios 63

Figure 4.18 Graphic of Scenario 1 Results 66

Figure 4.19 Graphic of Scenario 2 Results 67

Figure 4.20 Graphic of Scenario 3 Results 68

List of Tables

Page

Table 4.1 Level 2 Homogeneity of Group Variances Test Results 49

Table 4.2 Level 3 Homogeneity of Group Variances Test Results 50

Table 4.3 Level 4 Standard Deviation Parameters.....51

Table 4.4 Mean and 95% Confidence Intervals of X and Y 52

Table 4.5 Correlation of X and Y 53

Table 4.6 Level 3 Standard Deviation Parameters.....54

Table 4.7 Airdrop Collateral Damage Risk Estimator Validation.....59

Table 4.8 Scenario 1, 2, & 3 Results.....65

List of Acronyms

AGU: Airborne Guidance Unit
AFI: Air Force Instruction
AMC: Air Mobility Command
API: Actual Point of Impact
ARVN: The Army of the Republic of Vietnam
CARP: Computed Air Release Point
CDS: Containerized Delivery System
CEP: Circular Error Probable
DZ: Drop Zone
EEP: Elliptical Error Probable
GPES: Ground Proximity Extraction System
GPS: Global Positioning System
ICDS: Improved Container Delivery System
K-S: Kolmogorov-Smirnov
LAPES: Low Altitude Parachute Extraction System
LCHV: Low-Cost High-Velocity
LCLA: Low-Cost Low-Altitude
LCLV: Low-Cost Low-Velocity
MARC: Mathematical Analysis Research Corporation
NVA: North Vietnamese Army
JPADS: Joint Precision Airdrop System
JPDI: Joint Desired Point of Impact
PI: Point of Impact
U.S.: United States

ESTIMATING CARGO AIRDROP COLLATERAL DAMAGE RISK

I. Introduction

Overview

This chapter introduces the reader to what lies ahead in this thesis. This thesis develops and implements a methodology that can be used by U.S. Air Force to develop a reliable collateral damage risk analysis tool for airdrop mission planning purposes. First this chapter discusses background information on the airdropping of cargo. Next it covers the problem statement that this thesis targets. Then it relates the area of airdrop planning this thesis uses as its research focus followed by the research objectives. Finally it conveys the research assumptions and limitations that were necessary for the research problem to become tractable.

Background

Airdrop accuracy has been an ever-present challenge to military planners since the early days of resupply via aircraft airdrop. That is; how can we ensure that airdropped supplies are received by our ground forces and not the enemy like some of our early attempts during the Vietnam War (Tokar, 1998). During this and other engagements throughout history, techniques and technologies have been developed that have consistently increased airdrop accuracy and/or improved aircraft survivability against enemy fire. Techniques such as high-velocity airdrops for rugged cargo minimize the effects of winds on airdrop trajectory and maintain accuracy while allowing for higher release altitudes and increase aircraft survivability. Reefing techniques and equipment also allow for airdrops to be released from higher altitudes while maintaining

the accuracy of lower altitude airdrops again increasing aircrew safety. Reefing allows for an airdrop to begin descent at high velocity for target accuracy and then switch to low velocity in mid-descent to increase cargo survivability. This allows aircraft to drop cargo from higher altitudes with the accuracy of a lower altitude drop. Many of these techniques and technologies were born out of operational necessity. One of the most successful recent examples of accuracy improvement is the Joint Precision Airdrop System (JPADS).

The JPADS system uses a steerable parachute and an Airborne Guidance Unit (AGU) to control the cargo's descent and guide it to its Joint Desired Point of Impact (JDPI) (McGowen, 2006). The JPADS system offers many advantages over traditional airdrops: increased accuracy, reduced drop zone (DZ) size requirements, standoff cargo release, improved aircraft survivability, and immediate feedback on airdrop accuracy (Benney et al, 2005). One of the few recognized disadvantages of the JPADS system is the cost of the system itself relative to traditional "dumb" airdrops. In order to keep costs down recovering and reusing retrograde airdrop items is necessary, though not always feasible (Benney et al, 2005). JPADS is an important and necessary capability but its costs prevent it from solving some of the problems associated with resupply via airdrop. As a result of the significant cost and other factors JPADS cannot always be used for airdrops.

With the majority of combat airdrops still being accomplished with the relatively "dumb" airdrop techniques, planners must choose carefully when deciding on a JPDI and DZ. If it is too far from the point of use, recovery personnel could be exposed to enemy fire while recovering the cargo. If it is too close to friendly forces the risk of hitting

collateral hazards or friendly forces with cargo weighing several tons traveling at speeds of over 50 feet per second may become too great. How do mission planners know how close is too close? What is the chance that the cargo will impact a collateral object inside the DZ? These are some of the answers this thesis attempts to provide.

Problem Statement

Airdrop planners are asked to make decisions during mission planning that sometimes require a tradeoff between risk of hitting collateral objects and the distance from the airdrop cargo's point of use. This thesis aims to aid in the decision making process by providing a methodology and mission planning tool that airdrop planners can use to accurately predict airdrop collateral damage risk. This leads us to the problem statement for this thesis:

How can mission planners accurately predict airdrop collateral damage risk?

Research Focus

This research will examine recent airdrop score data collected from real world airdrops to assess factors that affect airdrop accuracy and characterize those effects. Airdrop scores are assigned after each operational airdrop by the personnel collecting the cargo from the DZ. During this scoring process a clock position relative to the DZ axis and a distance from the center of the DZ (JDPI) are recorded. This data is then reported to higher headquarters. These operational airdrop score data are the most reliable information we have on the current operational accuracy of cargo airdrops. They also

represent the errors in the current models used in calculating computed air release points (CARP) for airdrop cargo, CARP calculation errors or other uncontrollable errors.

There are many factors that affect airdrop accuracy such as aircraft altitude, speed, direction of travel, the timing of the release of cargo, the location of the cargo release, winds, cargo weight, number of chutes and type of parachutes used, etc. These factors have been studied and analyzed extensively and are taken into account when determining CARPs. But what happens after you have used the latest techniques and technology to determine the best known time and place in three dimensional space to release an airdrop, but the airdrop still misses its target? These errors are normal and are to be expected from any model. This thesis will describe these errors and characterize them in order to develop a method to evaluate risk.

There are and will always be some degree of errors associated with an airdrop. What happens when the pilot flies the aircraft one-half of a degree off from the DZ axis? What happens if the cargo is released one-half of a second early or late? What happens if the winds suddenly shift direction and/or velocity? The cargo will not hit exactly where it was intended to land. It will miss in some direction and some distance from the JPDI. These misses can be described in relation to the DZ axis as an ordered pair of (x,y) coordinates. A large enough collection of these data can provide the basis to describe risk around a JPDI.

What this thesis does is examine the airdrop (x,y) data to determine where the cargo actually lands in relation to where it was intended to land. What this study does not do is attempt to determine why the cargo missed the JPDI in the first place. The airdrop scores provided daily by operational units provide up-to-date information about the

current accuracy and two-dimensional distributional properties of these operational airdrops. By analyzing the data as a whole and by breaking down the data by airdrop method, altitude, and delivery aircraft we can gain useful insight into how far from the JPDI and in what direction relative to the DZ axis an airdrop will likely land. By understanding the two-dimensional probability miss distribution airdrops we can gain insight as to where collateral objects should and should not be located relative to a JPDI to minimize risk.

Research Objectives

This thesis has two main objectives. The first objective is to describe the two-dimensional distribution of airdrop errors through a literature review and by analyzing recent operational airdrop score data. Once the two-dimensional distribution of the errors can be adequately described, this description can be used to predict the risks associated with collateral objects being located in specific locations in relation to the JPDI and DZ axis. It would be simple to assume that an object located from a JPDI is as likely to be struck by an errant airdrop if it were 100 feet before an airdrop as if it were 100 feet to the right, but this thesis will show that the data suggests otherwise.

The second objective is to develop an accessible planning tool that enables airdrop planners to accurately gauge the risk of an airdrop striking collateral object concerns near a JPDI. This planning tool will require the location of the collateral object(s) in relation to the DZ axis and JPDI. Additionally, the dimensions of those objects would need to be known as well. This planning tool will also need to account for any known factors that change the distribution of an airdrop misses of a JPDI. The

objective of the planning tool will be for it to receive inputs from a mission planner and for the tool to provide an output to that mission planner. This output will be the probability of an airdrop striking a collateral object(s) near a JPDI. This probability can then be used as a decision aide in determining if the chosen JPDI is acceptable.

Assumptions/Limitations

There are a number of assumptions that were necessary to accomplish this research. Some of these assumptions were required because of the nature of the data and some were made to make the research tractable for this researcher. Some of these assumptions may become the "Areas for Future Research" in Chapter 6 of this thesis.

Assumptions:

- The data we have are the most accurate available on operational airdrop errors. When these data are analyzed and a two-dimensional distribution is fit to them, the results can be used to gauge the risk of striking collateral objects.
- The current airdrop models used to determine the computed aerial release points for airdrops are the most accurate available. In addition the errors from these models result in the average airdrop hitting the JPDI. In other words, there is no systematic problem with the airdrop models currently in use to determine aerial release points.
- The earth and collateral objects are flat. That is, for the purposes of this research the relative elevation of the drop zone and the height of collateral objects & elevations of areas inside the DZ have no bearing on the probability of an airdrop

striking them. This is of course not the case in practice. It stands to reason that when an airdrop is released towards an upward sloping hill it will have a tendency to land shorter than if the terrain where level or downward sloping. Other derivations in the long, left and right directions seem reasonable as well. Additionally, height of collateral objects will have an impact on the probability of an airdrop striking them. An object that is 25 x 25 feet and 10 feet tall would be less likely to be struck than an object with the same footprint and 100 feet tall located in the same space on the DZ. Unfortunately due to data constraints this cannot be accounted for.

Limitations:

Currently airdrops are scored by ground personnel at the DZ who report the location of the airdrop in relation to the JPDI with a clock position and a distance only, not as a relative (x,y) coordinate. For example, if an airdrop lands 100 yards short of the JPDI along the DZ axis the drop score would be recorded as 100 yards at 6 o'clock. This practice leads to estimation of the true angle into one of only 12 out of the 360°'s of a circle surrounding the JPDI. This makes estimating the true two-dimensional distribution based on this data more difficult and therefore assumptions about the true distribution between these clock positions must be made. In this thesis the data as presented will be analyzed to determine best estimates of the parameters of a known two-dimensional distribution. This known two dimensional distribution will be used to estimate collateral damage risk.

The data that has been collected does not give information about the elevation changes in the area surrounding the JPDI. As discussed earlier these elevation changes have an effect on the distance an airdrop lands but cannot be accounted for due to the lack of information. This data limitation leads to the earlier assumption about the earth being flat for the purposes of this research.

Summary

This research aims to answer the question "How can mission planners accurately predict airdrop collateral damage risk?" It will do so by first conducting a thorough literature review and then providing an accurate assessment of the distribution of airdrops around their respective aimpoints using scoring data from recent real world airdrops. This literature review and airdrop data assessment will then become the basis for developing an accessible and flexible tool for use by mission planners. The objective of this tool will be to provide a collateral damage risk probability output given a minimum set of inputs by the user that affect that risk. These factors could be the location and size of collateral objects in a drop zone, the height from which an airdrop is released or the type of airdrop chutes used.

II. Literature Review

The History of Airlift

History has shown that the logistical resupply of military forces is a critical component to the success or failure of operations. Of course, the most efficient and cost effective methods are usually preferred. Typically, sea and ground transportation are used before airlift is considered for these reasons. There have been times in history where these were no longer acceptable making airlift the only remaining option.

After the defeat of Germany in World War II the country was divided into four separate sectors. Each sector was controlled by one of the allied nations: the United States, France, Great Britain, and the Soviet Union. The capitol city of Berlin resided within the Soviet sector but was itself divided into two zones with the western half controlled by the Soviets and the eastern half controlled by the remaining western allied countries. Political tensions between the Soviet Union and the western allies reached a breaking point when on June 22, 1948 the Soviet controlled land-based resupply routes where halted by order of the Soviet leader Joseph Stalin. Some in the U.S. wished to force the issue and use military soldiers to escort the supply convoys but there was a difficult but peaceful option to consider, aerial resupply. Through careful planning and strictly adhered to execution policies the allies were able to supply all of the basic needs of the eastern half of Berlin using strictly airlift. The Soviets finally relented on May 12, 1949 and reopened the roads into eastern Berlin. Their attempt to rid Berlin of western Allied presence had only resulted in their embarrassment. By the official end of the operation the allies had provided more than 2.3 million tons of cargo using more than 277,685 flights to accomplish the task. During the operation, known in the U.S. as

"Operation Vittles" aircraft took off and landed from Berlin every three minutes in highly synchronized around the clock operations. Typical cargo included coal, food, medical supplies, and industrial supplies and equipment. One interesting cargo type was memorable not only for its type but also its method of delivery. Pilot Gail Halvorsen came to be known as the "Candy Bomber" for his crews airdropping of their candy rations using handkerchiefs as parachutes (Feltus, 2007).

Khe Sanh

Just as sea and ground transportation are preferred logistical methods over airlift, conventional airlift is preferred over airdrops. There have been numerous examples throughout history where airdrops were the only option and through these experiences the modern methods of airdrop have been developed. As the saying goes, "Necessity is the mother of invention."

As early as 1940 the U.S. Army identified the need, developed the techniques and procedures, and began purchasing the necessary equipment to conduct airdrop operations (Tokar, 1998). In his monograph "*Provide by Parachute: Airdrop in Vietnam, 1954-1972*", Tokar relates the impact that airdrop logistics had during three battles in Vietnam: Dien Bien Phu, Khe Sanh, and An Loc. In it he discusses how the French outpost at Dien Bien Phu was lost despite aerial resupply efforts, how the battle of Khe Sanh proved the necessity of airdrop capabilities and how U.S. aerial resupply efforts were critical to the success of the Army of the Republic of Vietnam against the North Vietnamese siege of the city of An Loc in 1972.

The Khe Sanh Combat Base was located in the northwest corner of South Vietnam near the North Vietnamese supply route known as the "Ho Chi Minh Trail".

Khe Sanh had approximately 7,000 soldiers assigned to it and in late November 1967 it appeared that the North Vietnamese Army (NVA) was preparing for an attack on it. The U.S. military leadership felt that aerial resupply of the soldiers there was feasible in case of a NVA attack. On 21 January, 1968 the NVA attacked Khe Sanh and its outposts. The aerial resupply commenced using mainly C-130 Hercules and C-123 Provider airlift aircraft. On February 10, a Marine C-130 was hit by NVA fire and destroyed; as a result the U.S. suspended landings of the C-130 at Khe Sanh. This event led to a change in tactics for aerial resupply. The Air Force began using its Low Altitude Parachute Extraction System (LAPES) and the Ground Proximity Extraction System (GPES) for delivering rugged supplies like food and ammunition. LAPES uses parachutes to extract cargo pallets from the aircraft at extremely low altitudes while the GPES uses a ground-based hook system to pull the cargo from the aircraft. Although weather conditions prevented the full employment of these systems, by the end of the attack 67 successful LAPES/GPES airdrop resupply missions had been conducted. The remaining rugged cargo was dropped using traditional paradrop techniques while delicate cargo was delivered with C-123's landing on the treacherous runway. The NVA continued their attack on Khe Sanh until 30 March and a land resupply route was not established until 8 April. The aerial resupply of Khe Sanh was critical to saving the lives of the nearly 7,000 soldiers stationed there and for assisting to repel the NVA attack. The airlift averaged 235 tons of cargo delivered per day for a total of 17,100 tons over the 77 day siege (Vaughan 2000). This battle demonstrated that given the right conditions, aerial resupply of a combat force was possible, even for extended periods of time.

An Loc

During the NVA siege of the city of An Loc in 1972 the U.S. capability to resupply via airdrop was once again put to the test. During this time frame the U.S. was in its "Vietnamization" phase of the conflict. During this phase the U.S. role in Vietnam was considered non-combat. So when the NVA began a siege of the South Vietnamese city of An Loc U.S. support of the Army of the Republic of Vietnam (ARVN) forces was mainly logistical. The NVA had cut off all supply lines and the only plausible method of resupply was via airdrop. During the initial phases of the siege low altitude resupply was used but due to heavy aircraft damage and losses new techniques were developed. These included two stage parachutes, high-velocity airdrops, and high-altitude low-opening methods. These methods all allowed for increased accuracy from altitudes that were outside of the enemy anti-aircraft artillery range. By the end of the siege, equipment, tactics and procedures had improved to the point that greater than 95% of the airdrops were landing within the drop zones boundaries. This siege showed the need for a reliable and accurate high-altitude airdrop system and spurred on its development (Tokar, 1998).

Types of Airdrops

There are four types of airdrops used by the US Air Force: guided (also called smart airdrops), low-velocity, high-velocity, and free fall (AFI 11-231, 2005). For guided airdrops the cargo load is guided to the airdrop joint desired point of impact (JPDI) typically using a parachute control and guidance system connected to the load. One of the more common systems in use today is the Joint Precision Airdrop System (JPADS). This system enables airdrop loads to be dropped from high altitudes out of the range of the enemy with high accuracy. Although the exact accuracy of JPADS is

classified it is accurate enough that cargo drop zone requirements are drastically reduced when the system is used. An additional benefit of JPADS is that the load can be released vertically offset from the Drop Zone (DZ) and can be guided during descent enabling the aircraft greater survivability against enemy defenses.

With low-velocity airdrops there is no guidance system. Typically, parachutes are used to slow the descent of the airdrop load and to reduce the impact velocity. Low-velocity airdrops are used for more delicate cargo that would not be capable of withstanding the more accurate high-velocity airdrop.

For high-velocity airdrops a smaller parachute or parafoil is used to stabilize the descent of the airdrop. These smaller parachutes do not slow the descent by the same amount as the low-velocity parachutes, but they ensure that the load impacts the ground at the proper angle. High-velocity airdrops are affected less by the winds and are typically more accurate than low-velocity airdrops if all other factors remain equal. The cargo dropped with this method is more rugged and can withstand the higher force of impact.

With free fall airdrops the load is released from the aircraft with no parachutes. This type of airdrop is typically used for dropping propaganda leaflets over enemy territory.

Methods of Airdrops

With all four of the above types of airdrops there are several methods for releasing the cargo from the aircraft for its descent to the JPDI: extraction, gravity and door bundle drops. Extraction parachutes are smaller chutes that are deployed to pull the load from the aircraft on its system of floor rollers. Gravity airdrops are when the pilot

changes the angle of the aircraft such that gravity pulls the load from the aircraft. Finally the cargo load can simply be pushed out of the aircraft manually called a door bundle drop (AFI 11-231, 2005).

Types of Parachutes

There are two basic categories of parachutes that the US Air Force uses: personnel and cargo; since cargo airdrops are the focus of this thesis we will focus on the latter. In this section we will introduce and give general information about the most common cargo parachute types in use today by the US Air Force. Air Force Instruction (AFI) 11-231 *Computed Air Release Point Procedures* lists 9 main types of equipment parachutes. They are listed as G-11A, G-11B, G-11C, G-12D, G-12E, G-13, G-14, 12' High Velocity, 22' High Velocity, and the 26' High Velocity. The G-series parachutes are generally used for low-velocity low altitude airdrops and the 12', 22', and 26' high-velocity parachutes are generally used for high-velocity high altitude airdrops. The ballistics of different types of parachutes varies. Each parachute is designed for a specific purpose and has its own peculiar characteristics (AFI 11-231, 2005). As a result airdrops using different chutes behave differently.

Airdrop Platforms

There are three main airdrop platforms in use by the US Air Force today. They are the C-130 Hercules, the C-17 Globemaster III, and the C-5 Galaxy. The C-130 Hercules primarily performs the tactical portion of the airlift mission. The aircraft is capable of operating from rough, dirt strips and is the prime transport for air dropping troops and equipment into hostile areas. The C-130E & H variants can carry 6 standard pallets of cargo or 16 Container Delivery System (CDS) bundles and the newer stretched

version of the C-130J can carry 8 standard pallets of cargo or 24 CDS bundles. The C-17 Globemaster III is capable of rapid strategic delivery of troops and all types of cargo to main operating bases or directly to forward bases in the deployment area. The C-17 can also perform tactical airlift and airdrop missions and can carry 18 standard pallets of cargo or 40 CDS bundles. The C-5 Galaxy is one of the largest aircraft in the world and the largest airlifter in the US Air Force inventory. The C-5 can carry more than any other airlifter. It has the ability to carry 36 standard pallets. (Factsheets, 2010)

Airdrop Errors

Airdrop errors occur when an airdrop does not land at its intended point of impact (PI). These errors can be described by a distance from the PI and an angle with respect to the drop zone (DZ) axis or by (x,y) coordinates. These errors can be caused by problems with the computed air release point, pilot error, crew error or any number of other causes.

The calculation of a CARP takes in account many factors to determine the optimal location in the air to release an airdrop from the aircraft. A cargo release at this location should result in the cargo landing at the intended PI. Small errors in the factors listed below (and others like those in Figure 2.1) can result in the cargo missing its intended PI (Kogler, 1989).

- drop zone conditions
- ballistics of the cargo
- weight of the load
- DZ elevations
- wind and other meteorological conditions

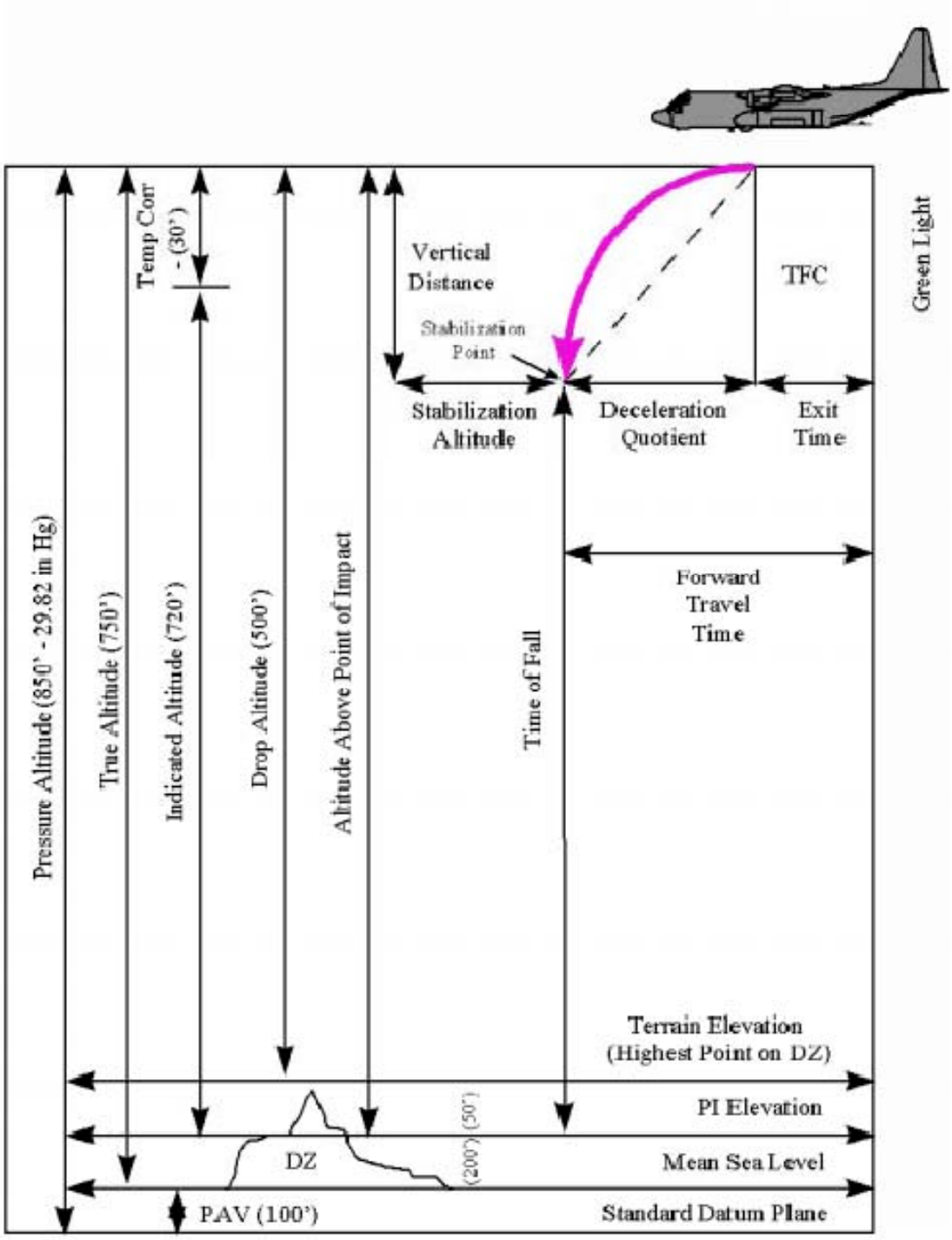

Figure 2.1: CARP Diagram (AFI 11-231, 2005)

Other minor errors by the pilot, loadmaster, etc. can contribute as well. All of these deviations would be very difficult to predict individually. But the results of these

deviations should be quantifiable when real-world airdrop accuracy data is analyzed. These deviations can be summarized as the actual PI distance to the intended PI and angle from the DZ axis with respect to the DZ axis. This information can be plotted two-dimensionally to gain insight into the typical error patterns. One method of describing an error pattern is determining if any known frequency distributions can suitably fit the empirical data.

Fitting Frequency Distributions

A random variable assumes numerical values associated with the random outcomes of an experiment, where one (and only one) numerical value is assigned to each sample point (McClave, 2000). A continuous random variable, such as distance, can assume values corresponding to any of the points contained in one or more intervals. The graphical form of the probability distribution for a continuous random variable *x* is a smooth curve that might appear as shown in Figure 2.2.

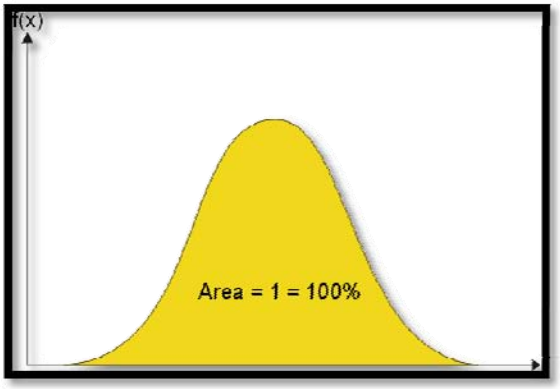

Figure 2.2: Normal Probability Distribution

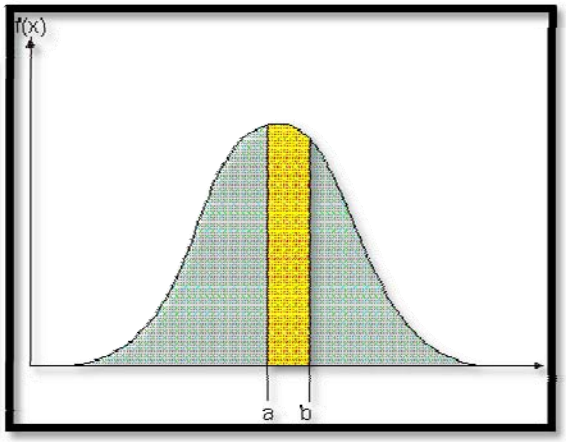

Figure 2.3: Area Under the Curve

Figure 2.2 displays a normal probability distribution of a continuous random variable *x*. The areas under the curve correspond to probabilities for *x*. The area under the curve

between points *a* and *b* (Figure 2.3) is the probability that *x* assumes a value between points *a* and *b*. The shape of the curve in Figure 2.2 is called a normal distribution. There are many shapes of probability distributions and those shapes describe how the values of the variable are distributed. As we shall see, the normal distribution plays a large role in this research.

When building a model it is often useful to use known distributions types rather than empirical distributions. There are many different known frequency distribution types. Some of the more common types are the Empirical, Continuous, Normal, Lognormal, Exponential, Gamma, Binomial, Poisson, Beta, Triangular, Erlang, and Weibull. This can be accomplished using a four step process outlined by Banks et al. (2010).

1. Collect data from the real system of interest.
2. Select a family of probability distributions that should closely represent the data gathered in step 1.
3. Choose parameters that determine a specific instance of the distribution family.
4. Evaluate the chosen distribution and the selected parameters for goodness of fit either informally via graphical methods or formally using statistical tests. If this step does not provide an acceptable level of goodness of fit the process begins again at step 2 until an adequate fit can be found. If no adequate distribution is found the Empirical form of the distribution can be used.

As recommended in step 4, goodness of fit tests can be used to test candidate distributions against the empirical data. If either the graphical or formal methods provide

a satisfactory fit to the empirical data, then the theoretical distribution can be used in place of the empirical data for modeling purposes.

A goodness of fit test determines how well a known distribution matches the distribution of the real system's data that has been collected. Goodness of fit tests provide helpful guidance for evaluating the suitability of a particular distribution with given parameters. It is especially important to note the effect of sample size. If a very small data set is analyzed then a goodness of fit test is unlikely to reject any candidate distribution. Conversely, if a large data set is analyzed then a goodness of fit test is likely to reject all candidate distributions. It is therefore recommended that failing to reject a candidate distribution should be taken as one piece of evidence in favor of choosing that distribution, and rejecting an input model as only one piece of evidence against that distribution (Banks et al, 2010).

Circular Error Probable vs. Elliptical Error Probable

Circular Error Probable (CEP) is the Army's standard measure of accuracy for ballistics and is likewise applied to airdrop accuracy. The CEP is a circular region centered on an aimpoint whose perimeter contains the expected percentage of hits. For example, a CEP 90 would be expected to contain 90% of the hits around an aimpoint with only 10% of hits falling outside of the defined CEP 90 circle. This measurement works well for defining distributions of ballistics with a circular confidence region but may be slightly inaccurate for elliptical regions as expressed by the Mathematical Analysis Research Corporation in "Calculation of the CEP" (MARC, 1987). According to the research the CEP is based on the lengths of the semi-major and semi-minor axes of the Elliptical Error Probable (EEP). The CEP can be calculated as follows:

$$CEP\ Radius = 0.75\ x\ [(EEP\ Major\ Axis)^2 +\ \ (EEP\ Minor\ Axis)^2]$$

In the research they conclude that the CEP and EEP are essentially equivalent for the case where the EEP's major axis equals its minor axis. In this scenario the CEP is actually slightly more conservative than the EEP as can be seen in Figure 2.4 below.

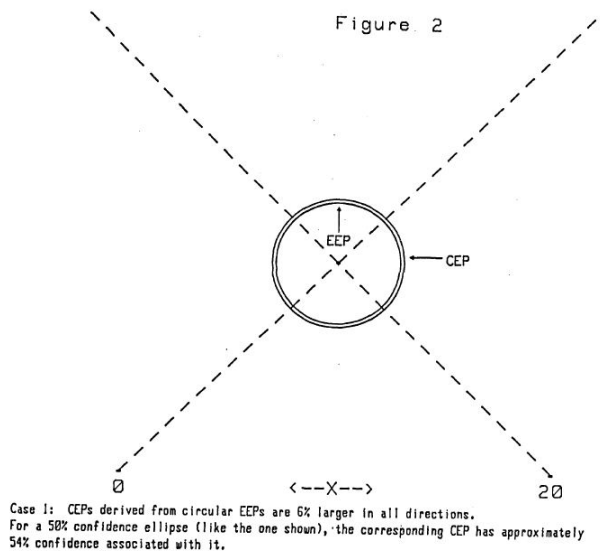

Figure 2.4: CEP/EEP Comparison w/Equal Minor & Major Axis (MARC, 1987)

For the case where the EEP's major axis is longer than the minor axis the CEP can begin to capture probability in the minor axis directions that the EEP misses but it also misses probability in the major axis directions that the EEP catches as seen in figure 2.5.

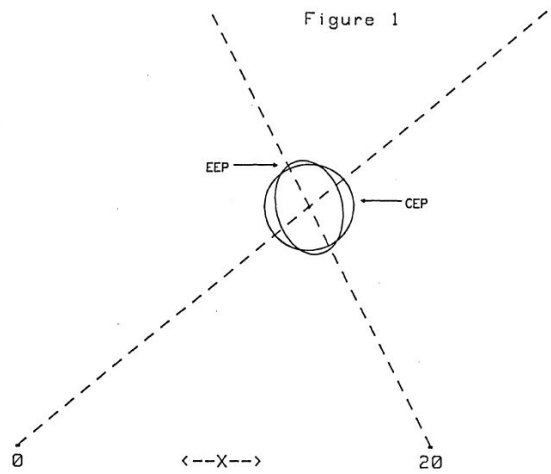

Figure 2.5: CEP/EEP Comparison w/Unequal Minor & Major Axis; Source: (MARC, 1987)

In a more extreme case the CEP can actually begin to overestimate the amount of probability contained within its perimeter because the amount of probability it misses in the major direction is more than the amount of probability that is gains in the minor direction as seen in Figure 2.6 (MARC, 1987).

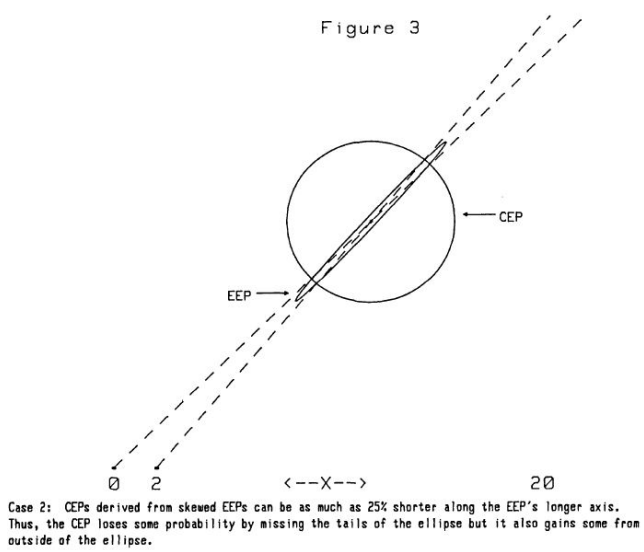

Figure 2.6: CEP/EEP Comparison w/Grossly Unequal Minor & Major Axis (MARC, 1987)

Risk

Risk is defined as the chance of loss or injury. In a situation that has both favorable and unfavorable outcomes, risk is the probability that an unfavorable outcome occurs (Garvey, 2009). Risk can therefore be described as a probabilistic event that is viewed as being negative. Risk can be classified in a number of different ways. One classification system of risk breaks risk up into the six categories below (Frame, 2003).

1. Pure (or insurable risk): focuses exclusively on the occurrence of bad things
2. Business risk: risk that involves the possibility of a loss or a gain
3. Project risk: risk associated with project management
4. Operational Risk: addresses the risks associated with carrying out operations
5. Technical Risk: risks associated with advanced technologies
6. Political Risk: risks associated with political motives

For this research the focus will of course be on Operational Risk. Operational risk is different from other classes of risk because we are concerned about managing a necessary process and the dangers that are inherent in it. Operational risk is separated from other forms of risk because we are dealing with a well known risk that is part of ongoing operations. In the case of airdrops the risk of striking collateral objects is a well known problem. The question then turns to how do we manage that risk?

A risk management framework can be described with these five steps:

1. Step 1: Plan for Risk
2. Step 2: Identify Risk
3. Step 3: Examine Risk Impacts, Both Qualitative and Quantitative
4. Step 4: Develop Risk-Handling Strategies
5. Step 5: Monitor and Control Risks

This thesis provides quantitative airdrop data risk predictions to aid in the risk management endeavor.

III. Methodology

Introduction

This research attempts to answer the question "How can mission planners more accurately predict airdrop collateral damage risk?" To begin to answer this question two research objectives were developed.

The first objective is to determine the best way describe the two-dimensional distribution of current airdrop errors through research and analyzing recent operational airdrop score data. Air Mobility Command (AMC)/A2 provided a historical airdrop data set gathered in theater from January to August 2010 that contained over 700 data points. This data will be analyzed here with to describe the data in a way that can be used later for our second objective.

The second objective of this research is to develop an accessible planning tool that enables airdrop planners to accurately gauge the risk of an airdrop striking collateral object concerns near a JPDI. The mission planners require a simple tool that can quickly output an accurate estimate of a risk probability to aid in their decision making and mission planning process. To accomplish this, Microsoft's Excel spreadsheet tool is used. Information gained from the first objective is used to build a tool in Excel that provides the necessary output after given the necessary inputs by the user.

Initial Data Interpretation

The data provided by AMC/A2 contained real-world airdrop scoring data collected in theater during actual combat operations. The data contained information from over 700 actual combat airdrops. The data also included the type of aircraft used, chute type and altitude from which the airdrop was released. The drop score was

recorded as the clock angle in relation to the DZ axis as well as the distance from the JPDI. A sample of the data format can be seen in Figure 3.1 below. For all of the data points see Appendix B.

AIRCRAFT	TYPE	ALT	CHUTES	DISTANCE	CLOCK
C-17	CONV	3,000	26'RS	250	7
C-17	CONV	3,000	26'RS	0	0

Figure 3.1: Data Sample

These data points represent the real world results and are a good indication of the accuracy of current operational military airdrop techniques and technology. Current methods and technologies are used to calculate and compensate for all known and controllable dynamics that effect airdrop accuracy such as wind, aircraft altitude, aircraft speed, cargo characteristics and chute type. These calculation methods and technologies lead to a release of the airdrop from the aircraft at the best known position in the air for the airdrop to land at the JPDI. There is however a certain amount of error in this process and the data that has been provided can be used to characterize and describe this error.

After an initial inspection of the data the first thing we noticed is the data were not provided as Global Positioning System (GPS) coordinates as initially expected. Instead the data were given simply as a distance measurement in yards and a clock position. These were both given in relation to the DZ axis (airdrop aircraft axis) and JPDI. This showed a limitation in the accuracy of the data that collected. An airdrop will land in some exact direction and at some exact distance from the JPDI. When ground personnel score the airdrop they estimate the angle to one of the 12 clock radials. This limitation also means that an assumption about the data's true two-dimensional distribution between clock radials must be made.

Cleaning the Data

The data set used for this research is real world airdrop scoring data. These scores are reported by the personnel on the ground collecting the airdrops. The data is recorded as a distance and angle from the intended point of impact. The angle is estimated to the closest clock position with 12 o'clock referenced to the DZ axis (aircraft heading). With the scores being recorded in an operational setting the likelihood of decreased accuracy is increased when compared to data collected in a controlled testing environment. Additionally as with any system of records there may be errors in data entry. It is therefore important that the data be scrutinized prior to analysis.

Upon examining the data a few types of errors were noticed:

1. Data with an aircraft type but no distance or clock position
2. Data with a distance recorded but no clock position
3. Data with an "X" prior to the distance

Data errors of type 1 were not included in the analysis as no information could be gained from these entries. Data errors of type 2 were also not included in the analysis with the exception of the entries with a distance of 0. For a distance of 0 the clock position recorded is of no consequence as the airdrop struck on target. These data points were assigned to clock position 12 and were included in the analysis. Data errors of type 3 were recorded with an "X" as a result of a question as to the reliability of the recorded drop scoring data. This designator was either recorded at the time of drop scoring or during database data entry. It was also noted that these data points were not used in

determining collateral damage risk under AMC's current methodology. As these data were considered unreliable by the data source and are not currently being used to determine risk, they were not used in characterizing the distribution of the airdrop data for this research.

Symmetry

As stated earlier the data provided for this research was recorded as a distance in yards and a clock position with the JPDI as the center point and the DZ axis as the reference clock position of 12 o'clock. Intuitively airdrops that miss the JPDI will not only strike along these 12 clock radials but will rather strike in some continuous two-dimensional distribution about the JPDI. The precise angles and distances of these misses would enable a more accurate estimation method of the true distribution of airdrop misses but unfortunately that data is not available. The clock angles and distances collected are therefore our best estimates of the true two-dimensional miss distribution that is to be modeled.

An assumption for this research is that there is not a systematic problem with the models that are used to calculate aerial release points for airdropped cargo. This assumption leads to the natural conclusion that the center of a two dimensional distribution of actual airdrop misses will be the JPDI. If this were true one should be able to see this by analyzing the one dimensional distribution of the miss data along the clock positions. With the data sorted by clock position it should be apparent that the majority of the miss distances along each clock position should be gathered close to zero and the remaining misses should fall off the farther they are from zero you go.

Another piece of evidence that would support this assumption would be that the two dimensional distribution should be relatively symmetric around the JPDI. Given the form of the supplied data one method to test for symmetry that can be used is the Kolmogorov-Smirnov (K-S) test.

As one of the best known and most frequently used distribution goodness of fit tests, the K-S test is very useful. By calculating the maximum distance between two sets of data it is possible to argue that the data are from the same distribution (Clarke/Disney, 1985). The K-S two-sample test is an extremely robust nonparametric (distribution-free) statistical technique which allows one to compare two distributions for significant differences. Thus, it is ideally suited to many modeling problems. It will detect any difference between two distributions caused by location, dispersion, or skewness. The test is based on the idea that the cumulative distributions of both samples should be fairly close to each other if they were drawn from the same distribution. It is a relatively simple test and is not based on restrictive assumptions (Friedman, 1985).

By using the K-S test we can compare the one-dimensional distribution of clock radials to one another. If the two clock radials pass the K-S test we argue that they could be from the same distribution and are therefore symmetrical. If we repeat the K-S test on all possible combinations of radials we can begin to determine if there is symmetry in the two-dimensional distribution of the data. A symmetrical two-dimensional distribution would again support the idea that the model used to determine CARP's is relatively accurate and the errors from these models produce a symmetrical scatter of airdrops around the JPDI.

Transforming Data

The recorded data were provided as the distance from JPDI to the actual point of impact (API) and the error azimuth relative to the DZ axis. We can transform this new data into a set of (x,y) coordinates where the y-axis is the original DZ axis, the origin is the JPDI and the coordinates for the actual point of impact is the (x,y). We can do this using basic trigonometry.

In can be shown that the lengths of the sides of a right triangle are related to the length of the hypotenuse and the angles within the triangle. For example referencing a standard right triangle let's assume that angle "A's" source is the origin of our grid (also the JPDI), the hypotenuse (side "h") is the distance from the JPDI to the API, side "b" is on top of the x-axis, and angle "B's" source is the API. Using this standard right triangle as an example the length of side "a" can be calculated by the following formula:

$$h * \sin(A) = a$$

Also, the length of side "b" can be calculated by the following formula:

$$h * \cos(A) = b$$

In this example the length of side "a" will become the "y" coordinate of our data point and the length of side "b" will become the "x" coordinate of our data point. By performing this procedure to each of the data points we can develop a new data set of bivariate (x,y) data.

This bivariate data can then be plotted onto a (x,y) scatterplot that displays the relationship between the JPDI (the origin) and the actual points of impact (the (x,y)'s). This data can also be tested using goodness of fit tests to determine if they conform reasonably well to any known distributions.

Goodness of Fit Testing

Goodness of fit testing is used to determine how closely a known distribution of given parameters approximates a data set. Using a theoretical distribution can give advantages over an empirical distribution and we prefer to use a theoretical distribution for many reasons. One advantage of theoretical distributions is that they can provide information beyond the range of the sample data whereas empirical distributions are limited by the range of the sample (Ebeling, 2005). Since the samples used for this research are a relatively small subset of the population of airdrop data and taken during a limited time interval they may not fully describe the population by themselves. We are more interested in what the sample is telling us about the entire population than in the peculiarities of the sample itself (Ebeling, 2005). Therefore we will use research and the sample to determine a reasonable theoretical distribution. Once this reasonable theoretical probability distribution is determined this distribution can be used in place of the data for modeling purposes. The risk model developed will be based on this theoretical distribution and risk assessments can then be made with the model.

Data Groups

Many factors could affect cargo airdrop accuracy including terrain, aircraft type, airdrop altitude, airdrop heading, airdrop method (i.e. conventional, ICDS, JPADS), and chute type (low velocity, high velocity) among others. The data provided includes information on each airdrop including aircraft type, chute type, airdrop altitude, distance the airdrop landed from the JPDI and the closest clock position from the JPDI to the impact point referenced to the DZ axis (aircraft heading).

We are interested in factoring out all variables that affect airdrop accuracy so that what we are left with are airdrop errors in a particular category. With the data set given for this research there are three main categories with which the data can be grouped:

1. Aircraft Type
    - C-130H, C-130J, or C-17
2. Chute Type
    - HV (26' RS, LCHV), LV(G-12E, LCLV), or LCLA
3. Airdrop Altitude
    - ≤ 1,000', 1,001' to 2,000', or 2,001' to 3,000'

These factors can be divided by hierarchical levels as displayed in Figure 3.2 below:

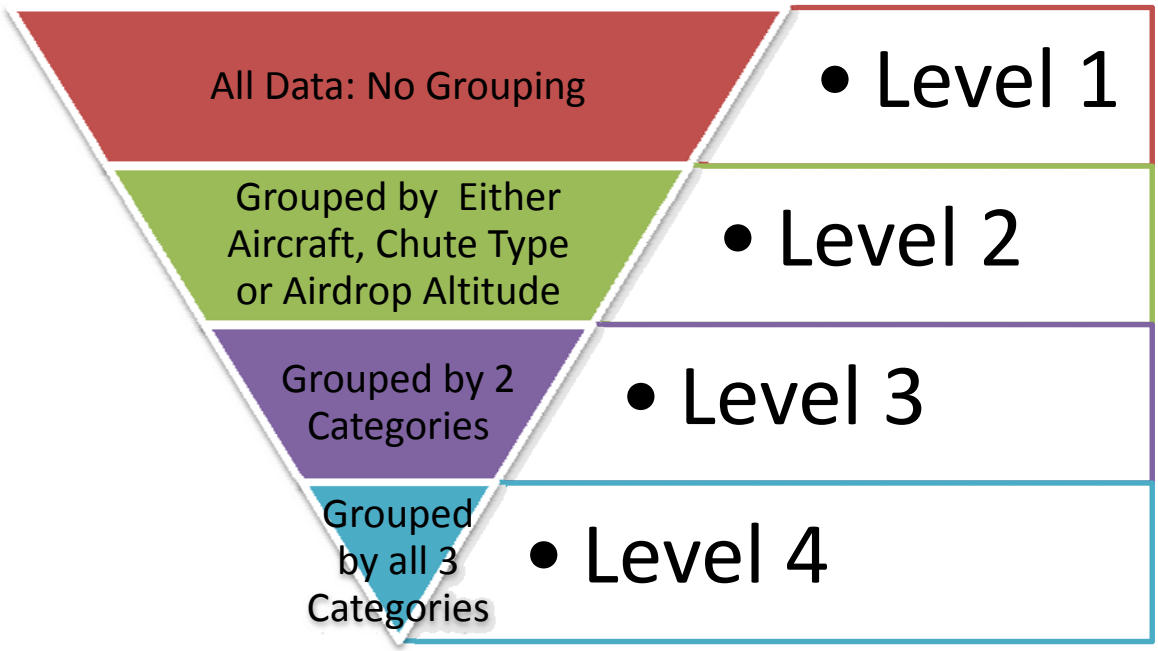

Figure 3.2: Data Grouping Levels

Level 1 data grouping includes all data points regardless of aircraft type, chute type or airdrop altitude. This level of data grouping should represent the general behavior of the all of the airdrops. The Level 2 data grouping divides all of the data into groups based on aircraft type, chute type, or airdrop altitude. If the factor the data is grouped by changes the behavior of airdrop, this level of data grouping should enable a more accurate picture of the different behaviors in the separate groups. The Level 3 data grouping groups the data by exactly two factors. Data grouped by Aircraft and Chute type would be an example of a Level 3 grouping. Level 4 data grouping would group the data by all 3 factors at the same time breaking the data down by aircraft, chute type, and airdrop altitude. Some combinations of factors were not observed in the data set at Level 4. If these factors are significant to the behavior of the airdrops once again a more accurate picture of the data may be possible by characterizing the data in each of these groups. That is of course, provided the data set contains enough data points to support this level of analysis. Figure 3.2 displays how increasing the data grouping level decreases the sample sizes available at each level. Without adequately large samples the validity of the sample becomes questionable.

In addition to limitations due to increasingly small sample sizes as levels increase there is another aspect of data grouping to consider. What if the intuitive data groupings are unnecessary because two intuitive groups are not statistically different? If this were the case there would be no need to differentiate the two groups and their respective error patterns would effectively be the same. As a result of similar error patterns, risk estimates for these groups could be calculated in the same way as well.

For the purposes of this research one of the aspects that can be examined to characterize the data is the standard deviation of the lateral miss distance (x) and the standard deviation of the longitudinal miss distance (y). By comparing these standard deviations between proposed groups we can determine if there is any statistical difference between them. If the statistical tools show that there is a difference between groups it would be desirable to separate the data to determine risk within those groups. The opposite is also true. If the there is no statistical difference between groups then the groupings could be detrimental to the accuracy of the risk assessments due the resulting decrease in sample size.

The JMP 8.0 statistical software package incorporates homogeneity of variance tests. When JMP tests for homogeneity of variances the software runs and outputs the results from four types of tests. The tests are summarized in the JMP manual as follows:

- *O'Brien's* test constructs a dependent variable so that the group means of the new variable equal the group sample variances of the original response. An ANOVA on the O'Brien variable is actually an ANOVA on the group sample variances (O'Brien 1979, Olejnik and Algina 1987).
- *The Brown-Forsythe* test show the F-test from an ANOVA in which the response is the absolute value of the difference of each observation and the group median (Brown and Forsythe 1974).
- *Levene's* test shows the F-test from an ANOVA in which the response is the absolute value of the difference of each observation and the group mean (Levene 1960).

- *Bartlett's* test compares the weighted arithmetic average of the sample variances to the weighted geometric average of the sample variances. The geometric average is always less than or equal to the arithmetic average with equality holding only when all sample variances are equal. The more variation there is among the group variances, the more these two averages differ. A function of these two averages is created, which approximates a χ^2 distribution. Large values correspond to large values of the arithmetic/geometric ratio, and hence to widely varying group variances. Bartlett's test is not very robust to violations of the normality assumption (Bartlett and Kendall, 1946).

For all four of the above tests JMP 8.0 calculates an F and a p-value. This p-value is the probability of obtaining by chance alone an F-value larger than the one calculated if, in reality, the variances are equal across all levels. Observed significance probabilities of 0.05 or less are often considered evidence of unequal variances across the levels (JMP 8.0 Help, 2008).

IV. Results and Analysis

What the Data Looks Like

As discussed in the previous chapter the airdrop data were given as distances and clock positions. The data were then converted to ordered (x,y) pairs using the aforementioned geometric formulas. The data in the (x,y) pairs were the input into the JMP v8.0 software suite for graphing. This software was used to create the scatterplot and 90% density ellipse in Figure 4.1 below.

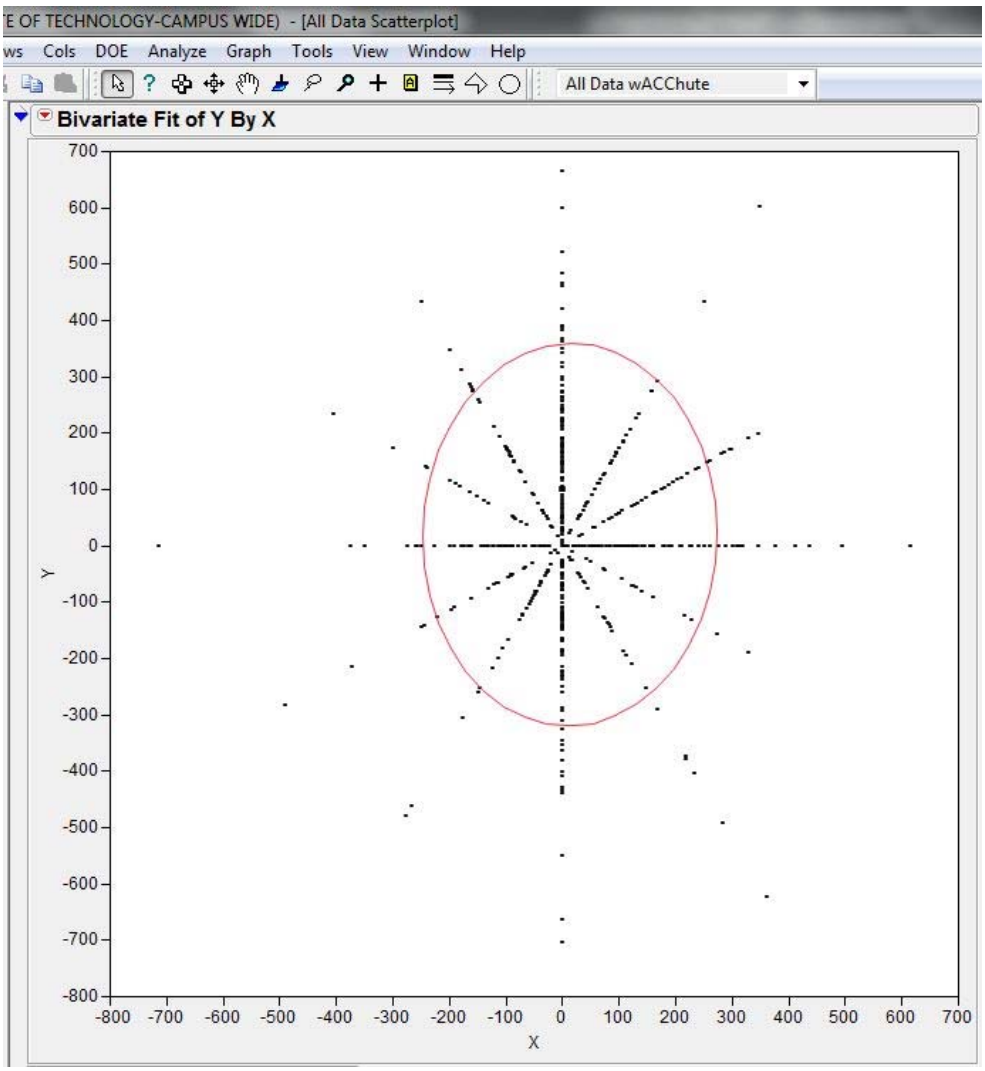

Figure 4.1: All Data Scatterplot

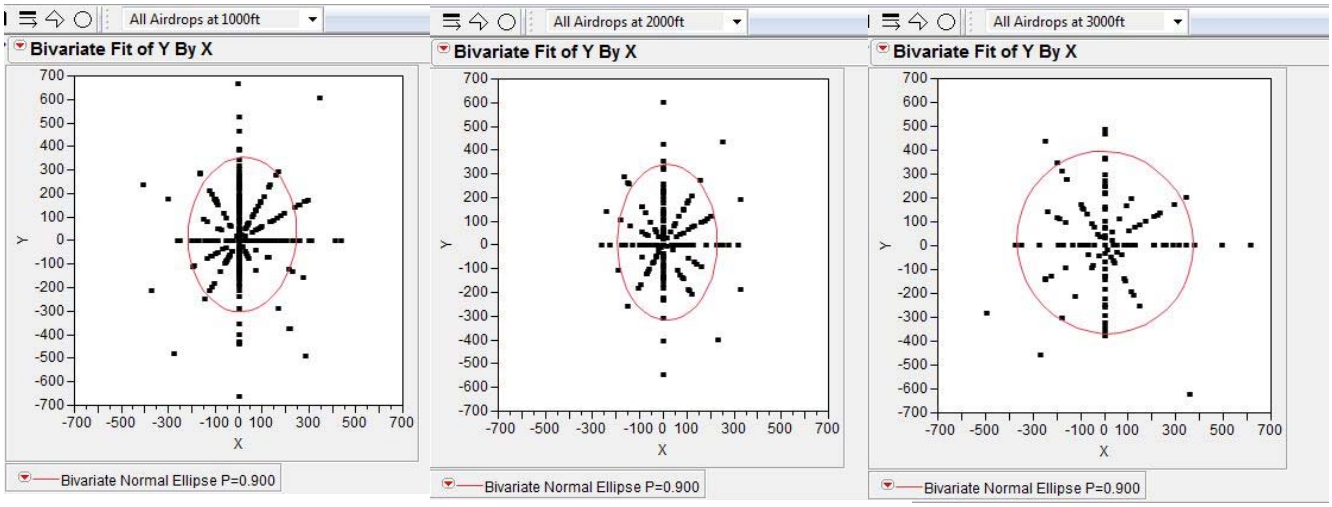

Figure 4.2: All Data Scatterplots by Altitude Category

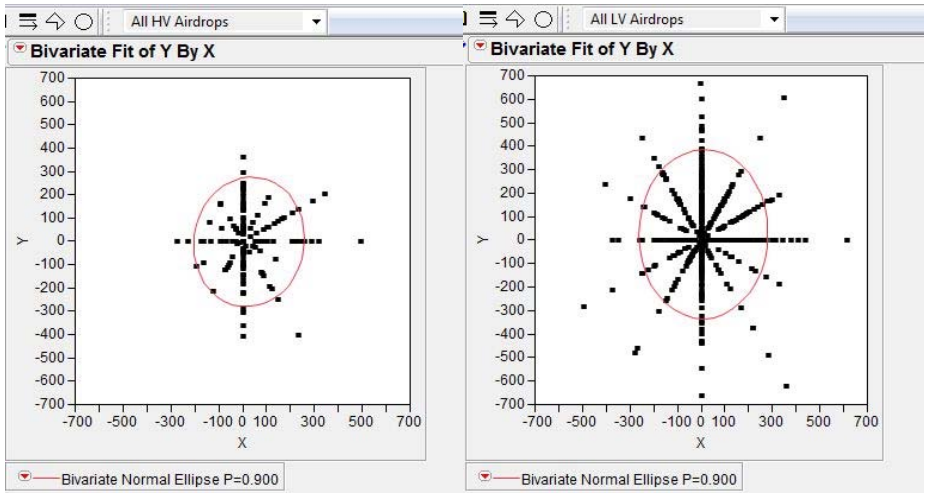

Figure 4.3: All Data Scatterplots by Chute Type

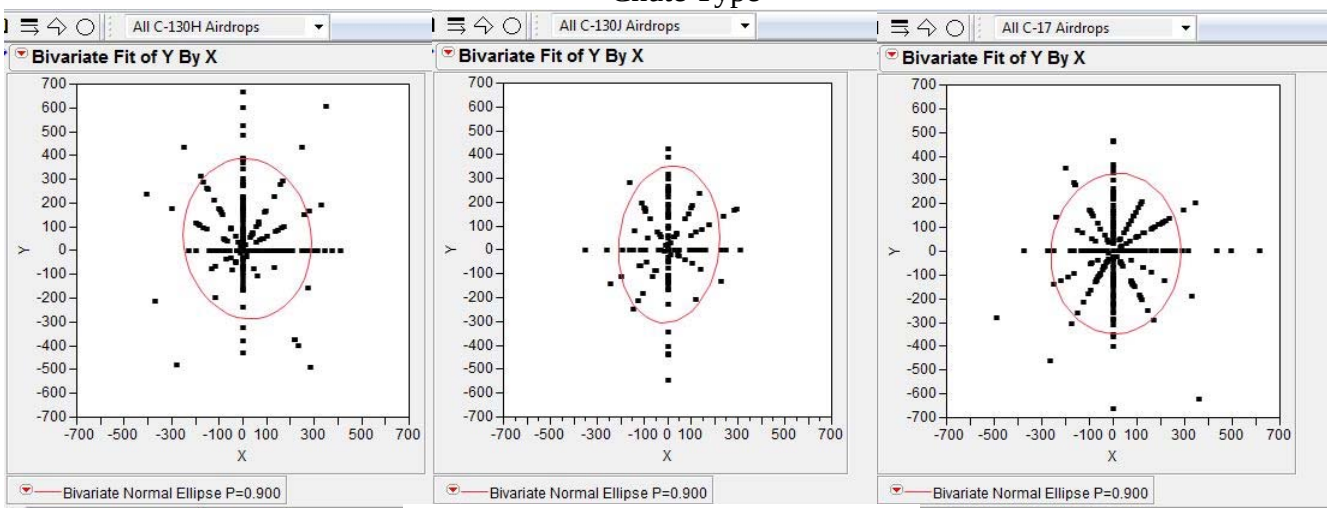

Figure 4.4: All Data Scatterplots by Aircraft Type

After visual examination of the scatterplot and density ellipses it was noted that the data appeared along each of the 12 clock radials. The data was concentrated more heavily towards the center of the scatterplot with a diminishing number of airdrops landing further from the center we examined. It was also noted that a 90% confidence region takes the shape of an ellipse with its semi-major radius along the Y axis and its semi-minor radius along the X axis. The 90% confidence ellipse is also reasonably centered at the origin and is not skewed either left or right.

The shape of the confidence region suggests that the true error pattern for airdrops is elliptical. The shape also suggests that there may be different factors causing errors in the X and Y directions. For example the timing of airdrop release should play a major role in the error in the Y direction where winds may play a larger role in the errors in the X directions. It is also intuitive that as a result of the elliptical confidence region probabilities of collateral objects being struck may not be the same for objects at a set distance in the X vs. Y directions.

Symmetry Testing

As introduced in the previous chapter the Kolmogorov-Smirnov (K-S) test was used to test if the airdrop scoring data were relatively symmetrical. Each of the twelve clock radials data were compared against each of the other radials using an online K-S test calculator provided by the College of Saint Benedict & Saint John's University (CSBSJU, 2010). The initial results can be seen in Figure 4.5 below.

			K-S Test p-values (with 0 distances included)									
1				95% significance level used								
2	0.414							Data are not from the same distribution				
3	0.499	0.016						Data may be from the same distribution				
4	0.942	0.48	0.33					Data are from the same distribution				
5	0.457	0.623	0.099	0.871								
6	0.968	0.122	0.17	0.985	0.681							
7	0.812	0.033	0.946	0.447	0.093	0.358						
8	0.878	0.558	0.468	0.927	0.847	0.976	0.51					
9	0.551	0.018	0.893	0.28	0.077	0.341	0.893	0.379				
10	0.285	0.965	0.119	0.55	0.56	0.341	0.152	0.874	0.139			
11	0.333	0.899	0.022	0.325	0.788	0.034	0.043	0.755	0.006	0.472		
12	0	0	0	0.094	0.009	0	0.002	0.013	0	0.001	0.001	
Radials	1	2	3	4	5	6	7	8	9	10	11	12

Figure 4.5: K-S Symmetry Test (includes 0 distances)

The results show that the data are reasonably symmetrical with the 12 o'clock radial appearing non-symmetric with every other radial. Upon investigation of this phenomenon a potential reason for the difference was noted. In nearly all cases when a zero distance was recorded in the data it was assigned to the 12 o'clock radial. As a result this radial's distance distribution was unlike any of the other radials. In order to compensate for this problem all zero distances were eliminated from every radial to prevent biasing. The K-S tests were performed once again and the results can be seen in Figure 4.6 below.

			K-S Test p-values (without 0 distances)									
1				95% significance level used								
2	0.414							Data are not from the same distribution				
3	0.579	0.019						Data may be from the same distribution				
4	0.942	0.48	0.351					Data are from the same distribution				
5	0.457	0.623	0.11	0.871								
6	0.968	0.122	0.197	0.985	0.681							
7	0.812	0.033	0.974	0.447	0.093	0.358						
8	0.878	0.558	0.513	0.927	0.847	0.976	0.51					
9	0.551	0.018	0.874	0.28	0.077	0.341	0.893	0.379				
10	0.285	0.965	0.14	0.55	0.56	0.341	0.152	0.874	0.139			
11	0.333	0.899	0.026	0.325	0.788	0.034	0.043	0.755	0.006	0.472		
12	0.633	0.517	0.016	0.863	0.815	0.331	0.092	0.92	0.033	0.271	0.605	
Radials	1	2	3	4	5	6	7	8	9	10	11	12
			K-S Test p-values (without 0 distances)									

Figure 4.6: K-S Symmetry Test (0 distances removed)

As the table shows, the vast majority of the radial comparisons appear to support the idea that their data come from the same distribution. These results support the notion that the airdrop data displays reasonable symmetry. This evidence should also support the use of some symmetrical theoretical two-dimensional probability distribution to represent the true population probability distribution. But what symmetrical theoretical two-dimensional distribution should be an appropriate representation for the error patterns in airdrops?

Goodness of Fit Testing

The JMP 8.0 statistical software was used to analyze the airdrop data to help determine an appropriate two dimensional distribution to represent the cargo airdrop error patterns. The data were examined using the distribution analyzing functionality of JMP 8.0. The X values and Y values were fitted against known distributions. The data was then categorized by altitude, chute type or aircraft type and tested again. An example of the JMP 8.0 test results can be seen in Figure 4.7 below.

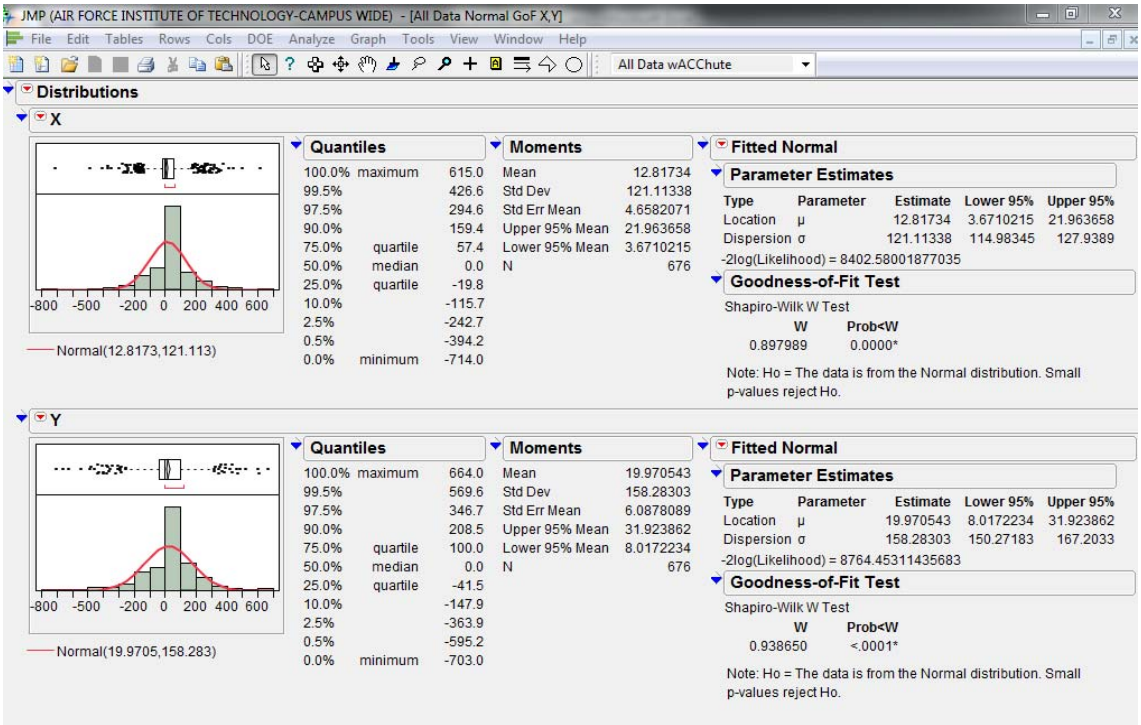

Figure 4.7: Sample Normal Goodness of Fit Test Results

As mentioned previously if a large data set is analyzed then a goodness of fit test is likely to reject all candidate distributions (Banks, 2010). In fact JMP 8.0's functionality was used to test 12 other commonly known distributions against the data and none of the fitted distributions passed a goodness of fit test. The distributions tested were the Normal, Lognormal, Weibull, Weibull (with threshold), Extreme Value, Exponential, Gamma, Beta, Smooth Curve, Johnson Su, Johnson Sb, Johnson Sl, and Glog. Of the 13 distributions tested the Normal distribution ranked as the third best fitting distribution by the JMP 8.0 software. As a result of the failure to acceptably fit any common distribution to the data, the result of the Normal distribution ranking third out of 13 distributions tested, we did not eliminate the bivariate normal distribution from

further consideration. As we will see there are other reasons why the bivariate normal distribution would be a good choice as a model of airdrop error distributions.

The Bivariate Normal Probability Distribution

One commonly used bivariate probability distribution is the bivariate normal. The bivariate normal probability distribution occurs often in sampling-type problems. One area of its application has to do with gunfire ballistics. It is theorized that due to barrel whip, aiming errors, wind effects, projectile irregularities and other reasons, that a gun aimed at a particular point will generally hit another point and the probability distribution for the impact point can be modeled as a pair of random variables (X,Y) where X is the horizontal deviation of the impact point and Y is the range deviation of the impact point (Clarke/Disney, 1985). The bivariate normal probability distribution has also been used for naval aircraft ballistics simulations (Bingham, 1970) and is the best known and most widely used bivariate distribution (Wilson, 1997).

Also according to Wilson:

> "When seeking to model the behavior of a bivariate random vector (X,Y), we often have information about the marginal means μ_x and μ_y, and the correlation coefficient $\rho_{x,y}$; and in this situation it is sometimes appropriate to assume that (X,Y) has the bivariate normal p.d.f."

In many ways the modeling of airdrops is similar to gunfire. The actual point of impact of an airdrop is affected by multiple factors in much the same way that multiple factors effect gunfire. Factors like aiming error, random wind shifts, chute variations, and payload irregularities all have corollaries to gunfire.

In Berry and Laugginger 1975 a computer simulation was used to verify the assumption of a bivariate normal probability distribution of bomb drop errors. In the thesis *A Computer Simulation of Release Parameter Effects Upon Bomb Impact Distributions* Berry and Laugginger found that the assumption of bivariate normal held for the majority of the tested scenarios where the input variables were varied according to a normal distribution (Berry and Laugginger, 1975).

There are other theoretical reasons why a bivariate normal distribution would be appropriate for use in modeling airdrop errors. In any situation where a model is fitted and measures of unexplained variation in the form of a set of residuals (errors) are available for examination the residuals should have zero mean and be normally distributed (Draper/Smith, 1966). This applies to our research as well. In our case the model that is fitted is the CARP calculations that occur prior to airdrop release. The residuals from these models manifest as the recorded drop scores. In this instance however, the residuals can occur in either the lateral (X) or longitudinal (Y) directions. If the CARP models currently in use account for all of the factors that affect airdrop accuracy it would be reasonable to expect the residuals from these models to be bivariate normally distributed. As a result of the theoretical evidence and the failure of any other theoretical distribution to statistically fit the airdrop data the bivariate normal distribution was chosen as our distribution to represent cargo airdrop errors and for our collateral damage risk estimation. The bivariate normal has many desirable properties and its characteristics are well known as we will see next.

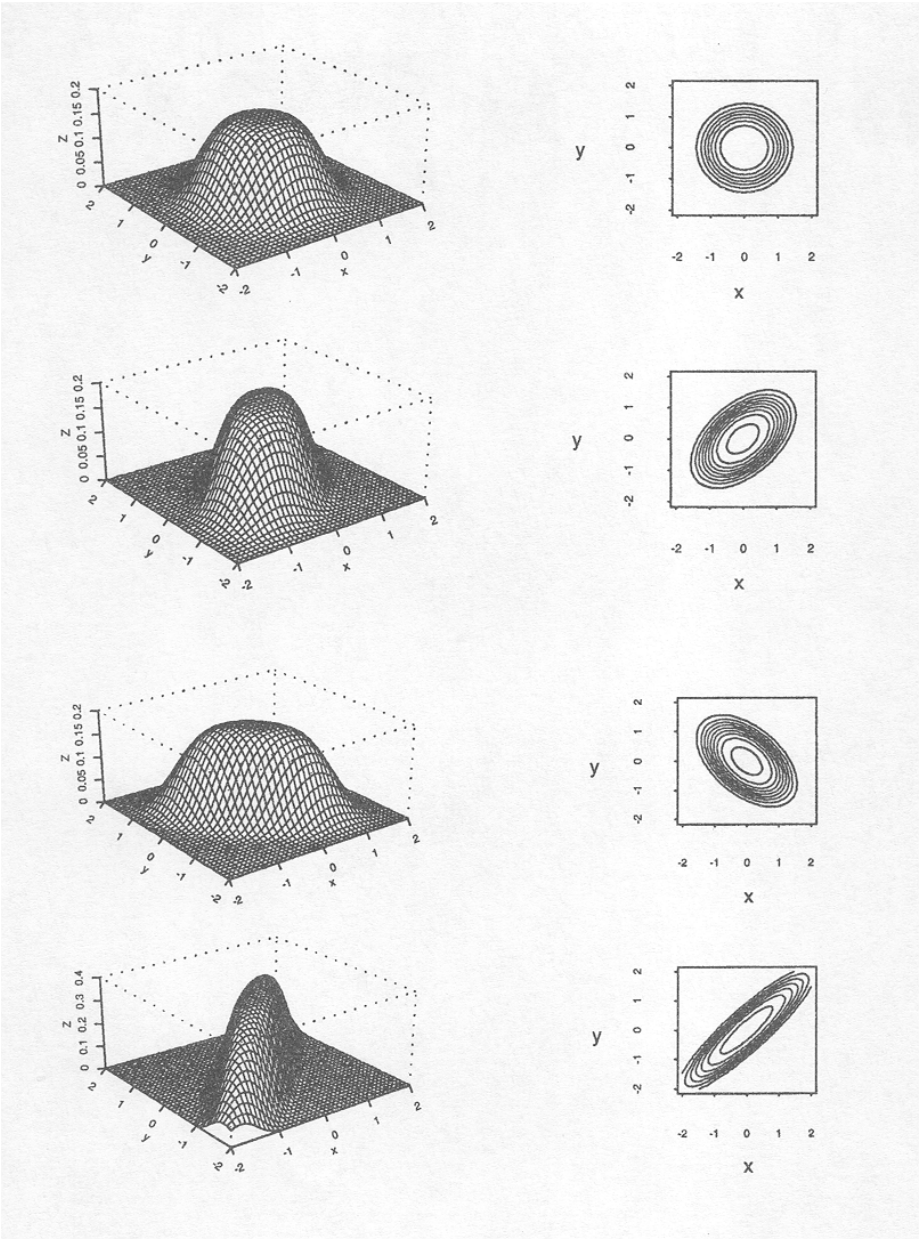

Figure 4.8: The Bivariate Normal Distribution (Duchateau, 2011)

The bivariate normal distribution can take on different shapes dependent upon its parameters as seen in Figure 4.8. By varying the μ_x and μ_y the center of the distribution can be varied. For our purposes a $\mu_x = 0$ and $\mu_y = 0$ suggests that an average airdrop hits on target. We will later show that the evidence does not prove this to be untrue. By adjusting the σ_x and σ_y the shape can be made more round or more elliptical. When $\sigma_x = \sigma_y$ the error pattern appears round as in Figure 4.4's first illustration. When σ_x and σ_y become more and more different the shape becomes more elliptical. Finally by adjusting ρ the angle of the ellipse with respect to the x and y axis can be varied as displayed by Figure 4.8's second illustration. As we will see the evidence provided by the airdrop data supports a ρ = 0. The combination of these variables makes this distribution quite flexible for modeling airdrop errors. If for example, airdrops in a particular category were found to typically land long then the μ_y could be set to compensate. Or if the σ_x and σ_y were found to be the same or very different an accurate model could still be built.

All bivariate probability distributions share common features (Clarke/Disney, 1985).

- $f(x, y) \geq 0 \; for \; all \; x, y.$
- $\iint_{-\infty}^{\infty} f(x, y) dy \, dx = 1$
- $f(x, y)$ is continuous for all except possibly finitely many values of x or y.

Additionally when X and Y are independent the joint probability can be calculated as (Clarke/Disney, 1985):

$$Pr[x_1 < x < x_2 \; and \; y_1 < y < y_2] = \int_{x_1}^{x_2} \int_{y_1}^{y_2} f(x,y)\, dy\, dx$$

These functions can be used to determine the area (probability) below the joint density surface with corner points (x_1, y_1),(x_1, y_2), (x_2, y_1) and (x_2, y_2). The total area under the joint density surface equals one so that if the corner points were $(\infty, -\infty)$, (∞, ∞), $(-\infty, -\infty)$ and $(-\infty, \infty)$ the probability would be one. Any rectangular probability can be calculated using this formula with the exact probability dependent on the actual shape of the particular instance of the bivariate normal probability distribution and the values of the corner points of the rectangle. In other words, by enclosing a collateral object with four corner points and describing the airdrop errors with a bivariate normal distribution, the probability that the collateral object will be hit can be determined through the functions given.

$$Pr[x_1 < x < x_2 \; and \; y_1 < y < y_2] = \int_{x_1}^{x_2} \int_{y_1}^{y_2} f(x,y)\, dy\, dx$$

The joint probability distribution of (X,Y) is given as:

$$f(x,y) = \frac{1}{2\pi \cdot \sigma_1 \sigma_2 \sqrt{1-\rho^2}} exp \frac{-\left[\left(\frac{x-\mu_1}{\sigma_1}\right)^2 - 2\rho\left(\frac{x-\mu_1}{\sigma_1}\right)\left(\frac{x-\mu_2}{\sigma_2}\right) + \left(\frac{y-\mu_2}{\sigma_2}\right)^2\right]}{2(1-\rho^2)}$$

$$-\infty < x < \infty$$

$$-\infty < y < \infty$$

where μ_1 and σ_1 are the mean and standard deviation of drop errors in the X direction, and μ_2 and σ_2 are the mean and standard deviation of drop errors in the Y direction; f(x,y) is known as the bivariate normal probability distribution (Devore, 1987). These formulas are implemented in a Microsoft Excel spreadsheet as a tool for estimating cargo airdrop risk. By entering the bivariate normal distribution parameters into the spreadsheet the

airdrop error pattern will be described. Then, by entering the corner points around a collateral object, the probability of that object being struck by the cargo airdrop can be estimated.

Determining Meaningful Data Groupings

With a theoretical distribution to represent the airdrop error patterns we next need to decide how many different airdrop error patterns exist. Is one pattern applicable to all airdrops or do factors such as aircraft type, chute type or airdrop altitudes contribute to the parameters of the airdrop error distribution pattern? As described earlier the standard deviation of X and Y can be compared among groups using JMP 8.0's homogeneity of variance tests. If the test results show significant differences among groups' standard deviation of X and Y then we conclude that there is a quantifiable difference between the groups' error patterns. These different error patterns suggest the groups should be modeled separately for determining collateral damage risk.

The airdrop error data were first grouped by aircraft type (C-130H, C-130J, or C-17), chute type (26'RS, G-12E, LCHV, LCLA, or LCLV), or airdrop altitude (1,000', 2,000', or 3,000'). The group variances were then tested for homogeneity using JMP 8.0. An example output can be seen in Figure 4.9.

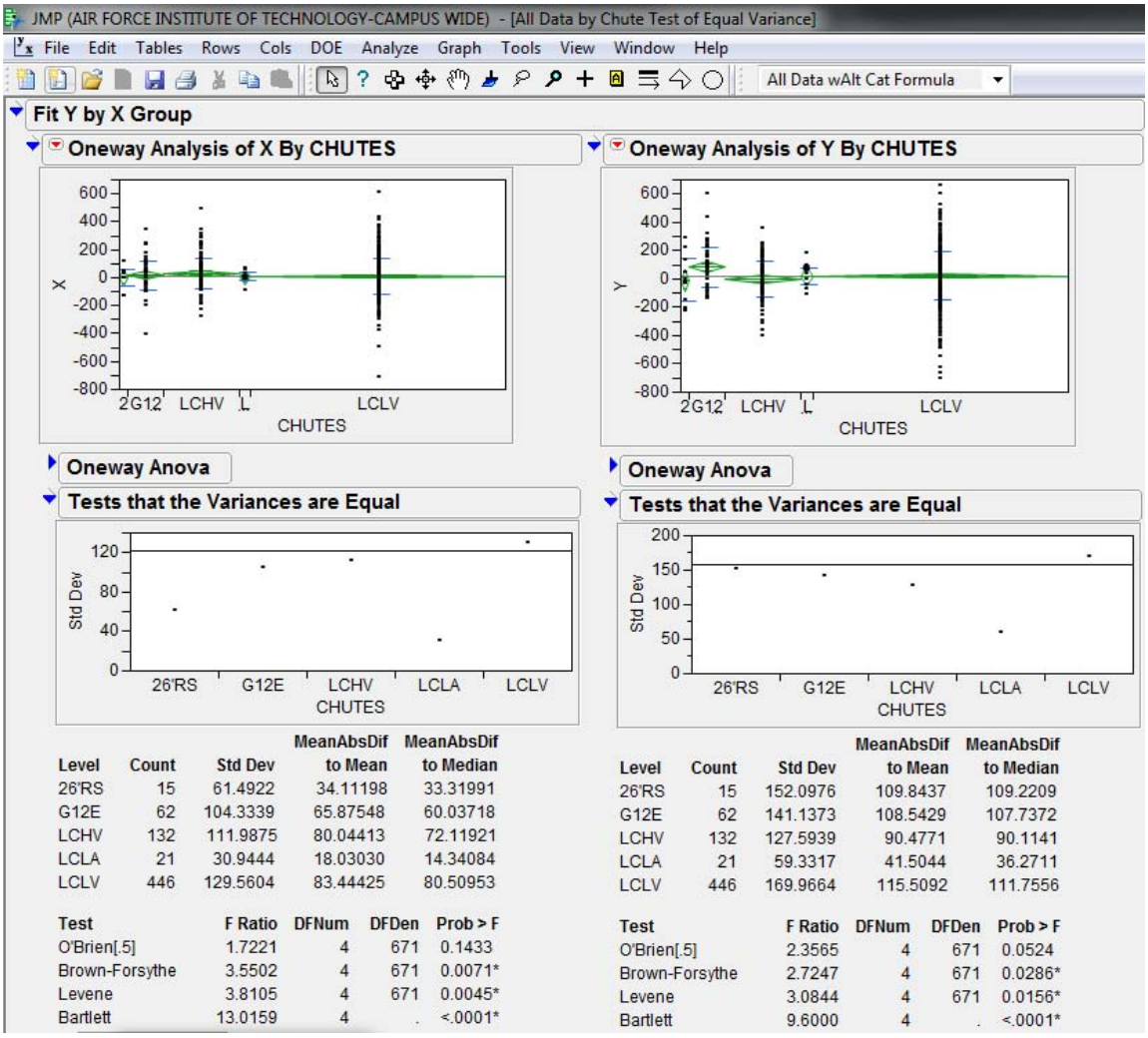

Figure 4.9: Chute Type Homogeneity Test Results

As noted by the p-values for the O'Brien, Brown-Forsythe, Levene and Bartlett tests there appears to be a definite difference among chute categories. Therefore, we conclude that chute type be taken into consideration when attempting to determine airdrop risk.

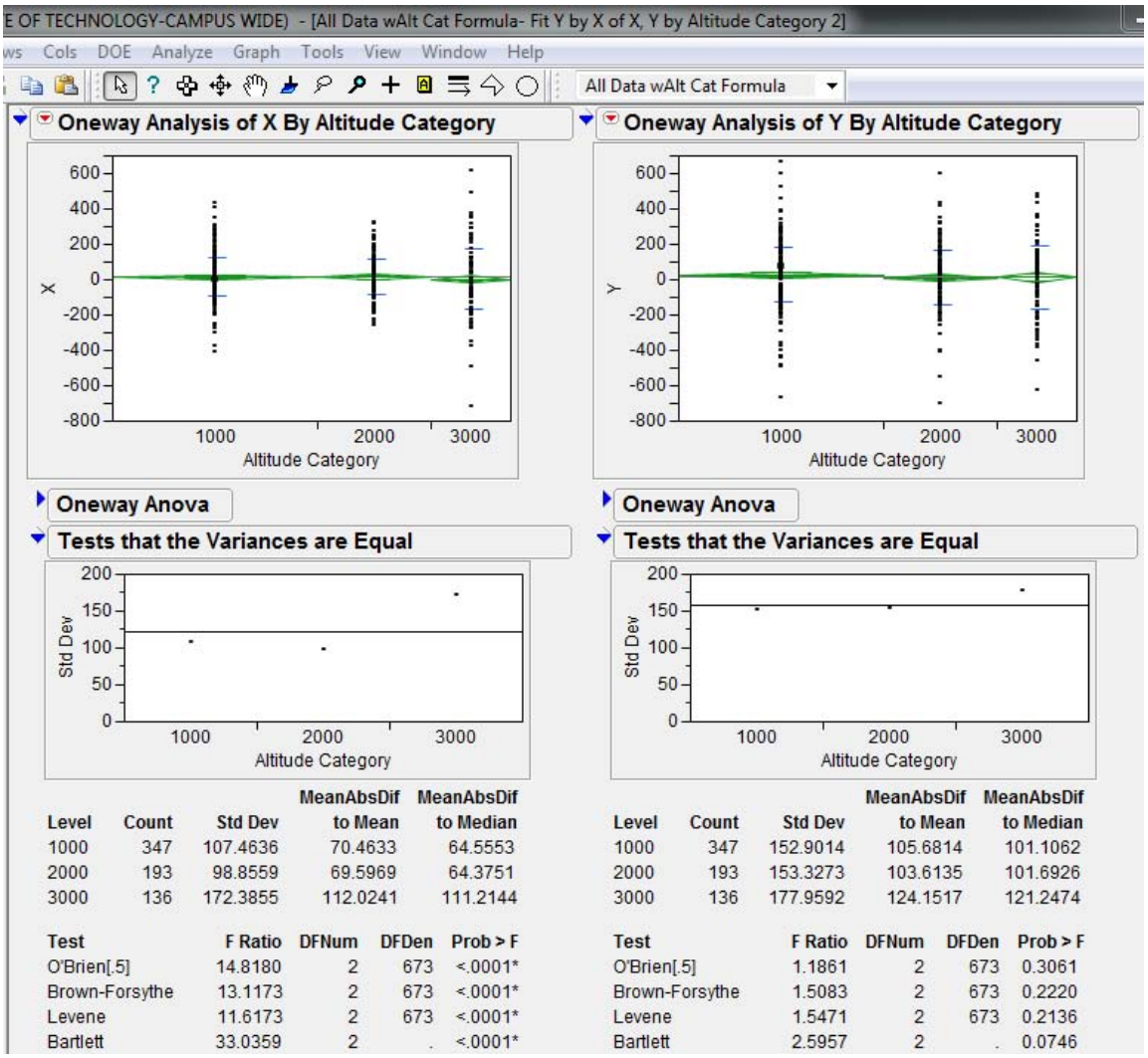

Figure 4.10: Altitude Category Homogeneity Test Results

As noted by the p-values for the O'Brien, Brown-Forsythe, Levene and Bartlett tests there appears to be a definite difference among altitude categories in the X direction but the difference in the Y direction is not as clearly distinct.

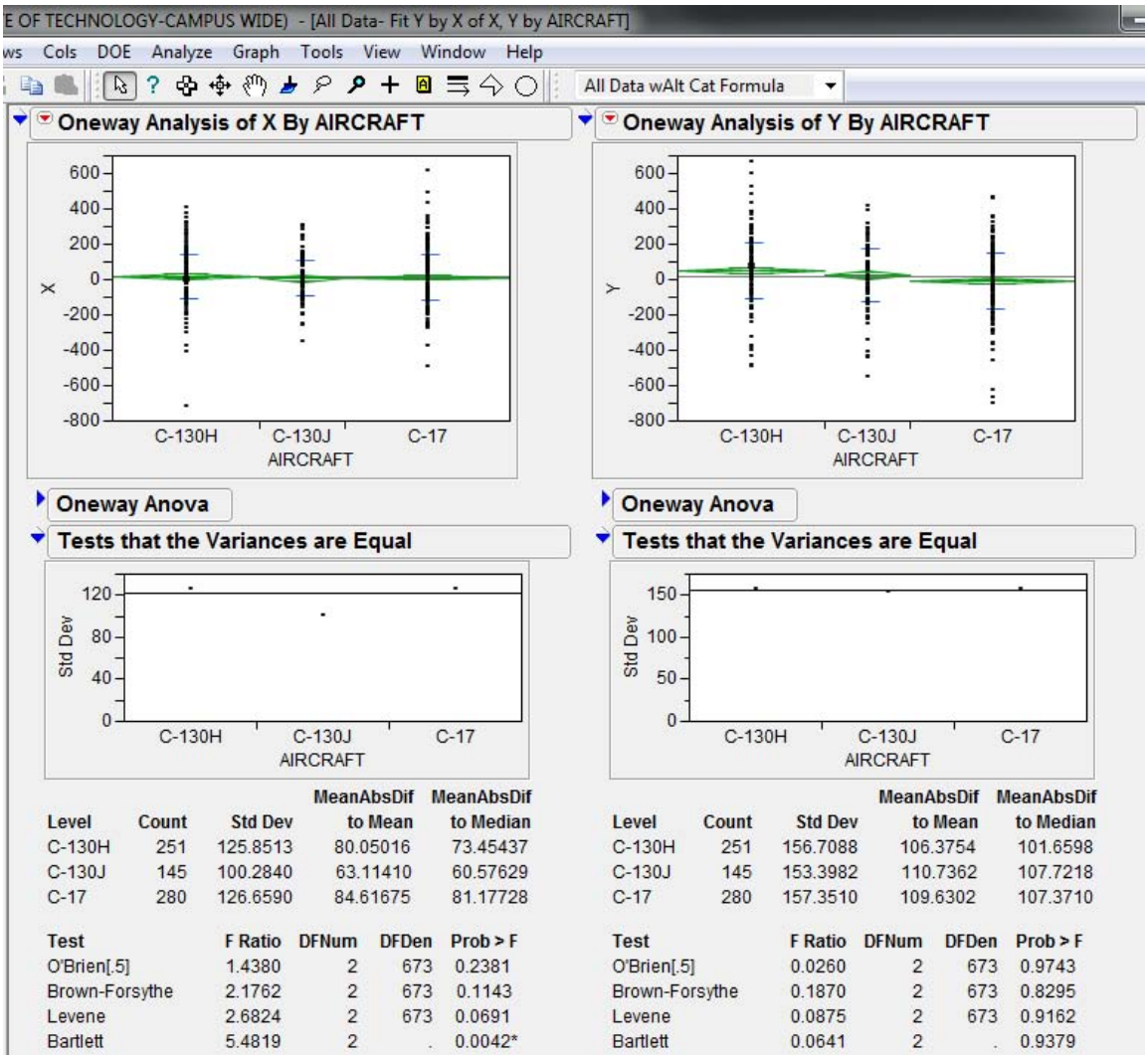

Figure 4.11: Aircraft Type Homogeneity Test Results

As noted by the p-values for the O'Brien, Brown-Forsythe, Levene and Bartlett tests there appears to be no definitive difference among aircraft types in the X direction and the difference in the Y direction appears to display homogeneity. The results of the homogeneity tests are summarized and discussed next.

				Significant	
LEVEL 2				**Difference in (x,y)**	
Altitude	**# of Data Pts**	**Std Dev (x) in yds**	**Std Dev (y) in yds**	**Std Dev Among Cat's?**	**Correlation**
1,000 ft	347	107.5	152.9	(Yes, Inconclusive)	0.04
2,000 ft	193	98.9	153.3	(Yes, Inconclusive)	0.00
3,000 ft	136	172.4	178.0	(Yes, Inconclusive)	-0.03
				Significant	
LEVEL 2				**Difference in (x,y)**	
Chute Type	**# of Data Pts**	**Std Dev (x) in yds**	**Std Dev (y) in yds**	**Std Dev Among Cat's?**	**Correlation**
HV	147	108.2	129.7	(Yes,Yes)	0.05
LV	508	126.7	167.9	(Yes,Yes)	0.01
LCLA	21	30.9	59.3	(Yes,Yes)	0.04
				Significant	
LEVEL 2				**Difference in (x,y)**	
A/C Type	**# of Data Pts**	**Std Dev (x) in yds**	**Std Dev (y) in yds**	**Std Dev Among Cat's?**	**Correlation**
C-130H	251	125.9	156.7	(Inconclusive,No)	-0.05
C-130J	145	100.3	153.4	(Inconclusive,No)	0.09
C-17	280	126.7	157.4	(Inconclusive,No)	0.02

Table 4.1: Level 2 Homogeneity of Group Variances Test Results
$\alpha = 0.05$

The results for the homogeneity of variance test were summarized in Table 4.1. Where (Inconclusive) are noted the results among the four homogeneity tests were not in agreement and therefore determining homogeneity among groups were not as clear cut. The altitude categories showed clear differences in the X dimension but not in the Y dimension. Based on these tests it is recommended to group the data by altitude for risk modeling as there is clear evidence of differences in the X dimension. This should lead to a more accurate estimate of error distributions among categories. As previously mentioned the chute type showed clear evidence of differences among groups and therefore grouping the data by chute type should also be accomplished for risk modeling. The aircraft categories did not prove to have convincingly different variances in the X

dimension. The Y dimension proved to be statistically homogeneous. Based on these results I would recommend not grouping the data by aircraft type for risk modeling due to the airdrop error distribution patterns among aircraft types appearing to be the same.

In addition to the Level 2 data groupings above the data were also separated into the Level 3 groups of (Aircraft Type & Altitude), (Aircraft Type & Chute Type) and (Altitude & Chute Type). A summary of the results of the JMP homogeneity tests can be seen in Table 4.2.

					Significant Difference in (x,y)
LEVEL 3		**# of Data Pts**	**Std Dev (x) in yds**	**Std Dev (y) in yds**	**Std Dev Among Cat's?**
C-17	**HV**	97	101.2	142.0	(Inconclusive,Inconclusive)
	LV	183	129.5	172.4	(Inconclusive,Inconclusive)
	1000'	97	92.2	151.9	(Yes, Inconclusive)
	2000'	90	105.1	145.3	(Yes, Inconclusive)
	3000'	93	170.2	174.8	(Yes, Inconclusive)
C-130H	**HV**	16	119.7	139.2	(Inconclusive,Inconclusive)
	LV	214	132.0	163.8	(Inconclusive,Inconclusive)
	LCLA	21	31.3	59.7	(Inconclusive,Inconclusive)
	1000'	172	112.8	152.9	(Yes, Inconclusive)
	2000'	55	113.7	147.2	(Yes, Inconclusive)
	3000'	24	207.7	202.6	(Yes, Inconclusive)
C-130J	**HV**	34	58.2	138.5	(Inconclusive,Inconclusive)
	LV	111	110.2	158.3	(Inconclusive,Inconclusive)
	1000'	78	113.1	147.1	(Yes, Inconclusive)
	2000'	48	58.7	169.9	(Yes, Inconclusive)
	3000'	19	124.6	141.4	(Yes, Inconclusive)
HV	**1000'**	6	76.8	116.5	(Yes,Yes)
	2000'	79	84.5	125.0	(Yes,Yes)
	3000'	62	129.9	138.0	(Yes,Yes)
LV	**1000'**	321	110.8	157.6	(Yes,Yes)
	2000'	113	108.4	170.4	(Yes,Yes)
	3000'	74	191.8	205.8	(Yes,Yes)
LCLA	**1000'**	21	30.9	59.3	(Yes,Yes)

Table 4.2: Level 3 Homogeneity of Group Variances Test Results
$\alpha = 0.05$

Based on the above homogeneity test results it appears that the best Level 3 grouping of data is the Chute Type and Altitude combination. These groups show clear

differences in the standard deviations of both X and Y dimensions. This is also consistent with the findings of the homogeneity tests at Level 2.

Data groupings at Level 4 were also considered for homogeneity of variance testing, however as seen in Table 4.3, many of the sample sizes at this grouping level became extremely small. It was determined that any information gained from these small data samples would not properly describe a two-dimensional probability distribution and therefore further data analysis at this level was not pursued.

LEVEL 4		# of Data Pts	Std Dev (x) in yds	Std Dev (y) in yds
C-17 HV	All Data	97	101.2	142.0
	1000'	3	98.7	145.7
	2000'	41	70.2	118.8
	3000'	53	116.7	159.3
C-17 LV	All Data	183	129.5	172.4
	1000'	94	91.3	152.4
	2000'	49	123.4	169.6
	3000'	40	196.3	218.2
C-130J HV	All Data	34	58.2	138.5
	1000'	1	N/A	N/A
	2000'	25	56.2	135.1
	3000'	8	55.6	123.4
C-130J LV	All Data	111	110.2	158.3
	1000'	77	113.8	147.1
	2000'	23	59.7	203.6
	3000'	11	144.0	125.1
C-130EH LCLA	All Data	21	31.3	59.7
	1000'	21	31.3	59.7
	2000'		N/A	N/A
	3000'		N/A	N/A
C-130EH HV	All Data	16	119.7	139.2
	1000'	2	0.0	29.0
	2000'	13	130.4	152.8
	3000'	1	N/A	N/A
C-130EH LV	All Data	215	131.8	163.5
	1000'	150	120.1	161.9
	2000'	42	109.7	143.9
	3000'	23	209.3	206.3

Table 4.3: Level 4 Standard Deviation Parameters

Determining Bivariate Normal Parameters

If we know the form of the theoretical relationship of a bivariate distribution but do not know the parameters, it would be best to fit this theoretical distribution to the data (Box/Draper, 1987). Since a theoretical distribution has been selected to represent the airdrop errors and we know that airdrop chutes and altitudes have an effect on the airdrop error distribution we now need to describe how the distribution changes with changes in chute type and airdrop altitude. Through analysis of the variances between data groupings we have also determined the most meaningful groupings of the airdrop data provided for this research. The data suggests that grouping by airdrop altitude and chute type provides meaningful data groups. These meaningful data groups are of a generally large enough size that their distribution parameters should provide reasonable estimates of the true population's distribution parameters.

In order to begin estimating probabilities (volumes) beneath a bivariate normal probability distribution we must first understand where that distribution is centered at. For this we examined the given data set and determined the means of X and Y and their 95% confidence intervals. The results are summarized in Table 4.4.

	# of Data			Lower	Upper	Lower	Upper	C.I. of X	C.I. of Y
	Points	Mean X	Mean Y	95% C.I. X	95% C.I. X	95% C.I. Y	95% C.I. Y	Includes 0?	Includes 0?
All Aircraft	676	12.8	20.0	3.7	22.0	8.0	31.9	No	No
C-17 HV	97	21.3	7.9	0.9	41.7	-20.7	36.5	No	Yes
C-17 LV	183	-0.7	-7.9	-19.6	18.2	-33.0	17.3	Yes	Yes
C-130J HV	34	1.3	25.6	-19.0	21.5	-22.8	73.9	Yes	Yes
C-130J LV	111	7.2	24.8	-13.5	27.9	-5.0	54.5	Yes	Yes
C-130EH LCLA	21	8.4	14.1	-6.9	21.7	-9.0	45.4	Yes	Yes
C-130EH HV	16	42.2	6.1	-21.6	106.0	-68.1	80.2	Yes	Yes
C-130EH LV	215	18.2	56.2	0.5	35.9	34.2	78.1	No	No

Table 4.4: Mean and 95% Confidence Intervals of X and Y

Table 4.4 shows that most of the calculated confidence intervals include 0 with notable exceptions. When all of the data are considered simultaneously the data suggest that an average airdrop may not strike at (0,0). However, the confidence interval's lower boundaries are very close to 0 and for our purposes we are going to say they are effectively 0. This conclusion essentially means that an average airdrop will strike on target at (0,0).

The airdrops display an elliptical pattern. By examining the correlation of X and Y we can determine if that ellipse is in line with the DZ axis or if it is at some angle to it. In Table 4.5 below it can be seen that there is no correlation between X and Y suggesting that the true airdrop error pattern's ellipse is in line with the DZ axis.

				Significant	
LEVEL 2				**Difference in (x,y)**	
Altitude	**# of Data Pts**	**Std Dev (x) in yds**	**Std Dev (y) in yds**	**Std Dev Among Cat's?**	**Correlation**
1,000 ft	347	107.5	152.9	(Yes, Inconclusive)	0.04
2,000 ft	193	98.9	153.3	(Yes, Inconclusive)	0.00
3,000 ft	136	172.4	178.0	(Yes, Inconclusive)	-0.03
				Significant	
LEVEL 2				**Difference in (x,y)**	
Chute Type	**# of Data Pts**	**Std Dev (x) in yds**	**Std Dev (y) in yds**	**Std Dev Among Cat's?**	**Correlation**
HV	147	108.2	129.7	(Yes,Yes)	0.05
LV	508	126.7	167.9	(Yes,Yes)	0.01
LCLA	21	30.9	59.3	(Yes,Yes)	0.04
				Significant	
LEVEL 2				**Difference in (x,y)**	
A/C Type	**# of Data Pts**	**Std Dev (x) in yds**	**Std Dev (y) in yds**	**Std Dev Among Cat's?**	**Correlation**
C-130H	251	125.9	156.7	(Inconclusive,No)	-0.05
C-130J	145	100.3	153.4	(Inconclusive,No)	0.09
C-17	280	126.7	157.4	(Inconclusive,No)	0.02

Table 4.5: Correlation of X and Y

After determining the means of X and Y and their correlations the only remaining parameters of a bivariate normal are the standard deviation of X and Y. The data were grouped by chute type and altitude. After grouping the standard deviations in the X and Y dimensions were calculated. The results were recorded in Table 4.6.

LEVEL 3		# of Data Pts	Std Dev (x) in yds	Std Dev (y) in yds
HV	1000'	6	76.8	116.5
	2000'	79	84.5	125.0
	3000'	62	129.9	138.0
LV	1000'	321	110.8	157.6
	2000'	113	108.4	170.4
	3000'	74	191.8	205.8
LCLA	1000'	21	30.9	59.3

Table 4.6: Level 3 Standard Deviation Parameters

As the table shows, even at data grouping Level 3 some of the data groups become small. However, the behavior of standard deviations at this level does appear intuitive. Note how the standard deviations in both the X and Y dimension generally decrease as altitude decreases. Due to the size of the samples at this level of grouping it is recommended that this be the lowest level used for calculating airdrop risk. The values in Table 4.6 can be used as bivariate normal parameter inputs in the estimation of airdrop collateral damage risk. This will be discussed next.

Calculating Airdrop Risk

With the airdrop error probability distribution being described by the bivariate normal distribution with the parameters determined with the data analysis results in Table 4.4 the risk of striking an object in a DZ can be determined by applying the formulas below:

$$f(x,y) = \frac{1}{2\pi \cdot \sigma_1 \sigma_2 \sqrt{1-\rho^2}} exp \frac{-\left[\left(\frac{x-\mu_1}{\sigma_1}\right)^2 - 2\rho\left(\frac{x-\mu_1}{\sigma_1}\right)\left(\frac{x-\mu_2}{\sigma_2}\right) + \left(\frac{y-\mu_2}{\sigma_2}\right)^2\right]}{2(1-\rho^2)}$$

$$Pr[x_1 < x < x_2 \; and \; y_1 < y < y_2] = \int_{x_1}^{x_2} \int_{y_1}^{y_2} f(x,y)\, dy\, dx$$

Application of the above formulas will allow any collateral object's risk of being struck by an airdrop to be determined. By fitting a rectangular shape around the shape of the collateral object, determining the rectangles corner point coordinates (x_1, y_1), (x_1, y_2), (x_2, y_1), and (x_2, y_2), and calculating the area under the bivariate normal surface the probability of striking the collateral object can be estimated. The risk of striking multiple collateral objects can be estimated this way as well. Since the probability of striking non-overlapping collateral objects are independent events their probabilities can be simply summed together to determine the probability of striking any of the collateral objects. Numerical integration must be used because there is no closed form solution to the bivariate normal distribution's probability density function.

This research employed the rectangular method numerical integration technique. Rectangular numerical integration estimates the volume under a curve by breaking the area up into smaller rectangles, determining their area, and summing the areas of all of the rectangles. A simple univariate example is shown in Figure 4.12.

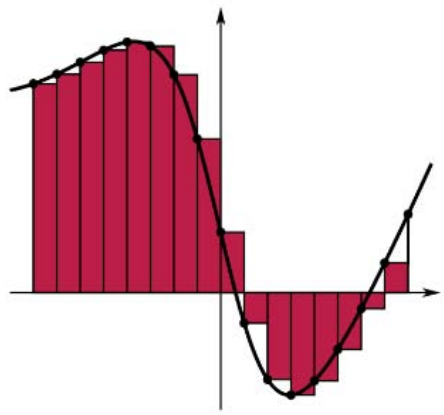

Figure 4.12: Rectangular Method Numerical Integration (KSmrq, 2011)

For estimating the risk of a rectangular collateral object under a bivariate normal distribution surface we apply the same principle to two dimensions. Instead of determining the area as before we must now calculate volume. To do this we divide the rectangular collateral object into smaller rectangles, determine their individual volumes, and sum them to estimate the total volume under the bivariate density surface. A visual example of the rectangular numerical integration method implemented in two dimensions can be seen in Figure 4.13.

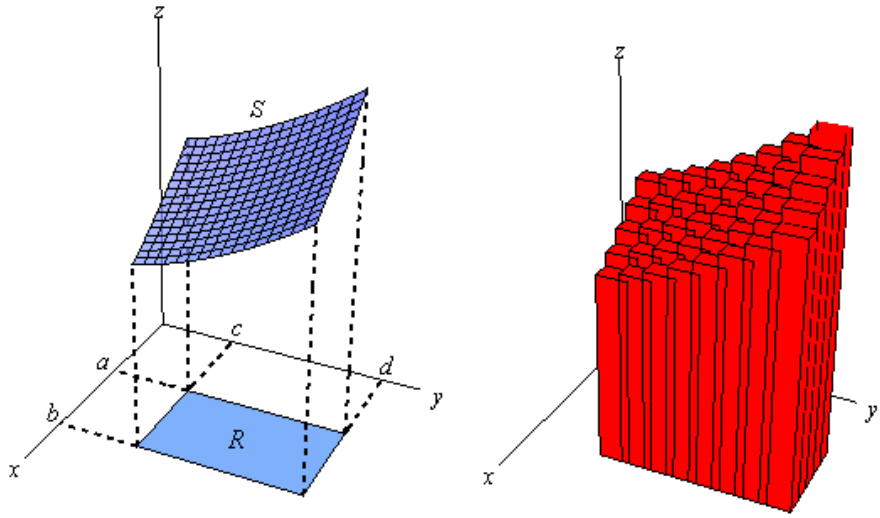

Figure 4.13: 2-D Rectangular Method Numerical Integration (Dawkins, 2011)

The total volume under the entire bivariate normal surface equals one because we know with absolute certainty that the airdrop will hit the earth at some distance and some direction from the JPDI (the bivariate normal's surface approaches but never arrives at zero). The portion of that volume that resides above the collateral object yet below the bivariate normal surface is its probability of being struck by an airdrop. As discussed previously, when multiple non-overlapping rectangular collateral objects are present the volumes above each collateral object can be summed to determine the probability that an airdrop will strike one of the objects.

A Microsoft Excel implementation of the above method was developed for the calculation of airdrop collateral damage risk estimates (Dillenburger, 2011). The Excel spreadsheet "Airdrop Collateral Damage Risk Estimator" uses numerical integration to estimate the probability of striking the inputted collateral objects around an airdrop aimpoint based on the defined bivariate normal probability function's surface. The shape of the airdrop error bivariate normal probability distribution is determined by parameters inputted by the Excel file's user. A tab with data similar to Table 4.4 is provided for the user to choose and input the appropriate σ_x and σ_y parameters. After inputting the parameters, the user has the option to enter the (x_1, x_2, y_1, y_2) rectangular coordinates (in yards) for up to 20 collateral objects. These coordinates correlate to (a, b, c, d) in Figure 4.13. Following the entry of all necessary data the user simply clicks the "Start" button and the Collateral Damage Risk is estimated and displayed. The displayed probability is estimated numerically similar to Figure 4.8 (right graphic). The displayed output is the estimated probability that a single airdropped piece of cargo will strike any of the input collateral objects. This probability could then be used for airdrop planning decisions.

	A	B	C	D	E	F
1	Collateral Objects	Left Boundary	Right Boundary	Lower Boundary	Upper Boundary	Likelihood of Strike
2	1	600	650	750	850	0.00000
3	2	650	750	550	600	0.00000
4	3	300	350	350	400	0.00046
5	4	650	700	100	200	0.00003
6	5	-50	50	-50	50	0.03948
7	6	150	200	-50	0	0.00658
8	7	50	150	-250	-100	0.03625
9	8	200	300	-450	-150	0.01960
10	9	800	850	350	400	0.00000
11	10	400	450	-500	-450	0.00006
12	11					
13	12					
14	13					
15	14					
16	15					
17	16					
18	17					
19	18					
20	19					
21	20					
22						
23						
24			Total Risk	0.10246	Start	
25						

	Inputs	Default Values
Aimpoint(x)	0	0
Aimpoint(y)	0	0
Std Dev(x)	110.8	121.1
Std Dev (y)	157.6	158.3
Correlation (x/y)	0	0
Power	1	1
Stepsize	0.1	0.01

Red cells should not be changed from default without evidence that supports doing so!!!

Explanation of Inputs:

Aimpoint (x)/(y):	Aimpoints define where an average airdrop is expected to land. The entered aimpoints should be (0,0) unless new empirical airdrop data shows average airdrops do not land on target. Aimpoints other than 0 may indicate a problem with CARP calculation and/or airdrop methodology.
Std Dev (x)/(y):	Enter standard deviation lateral and longitudinal from the tab labeled "Distribution Tables".
Correlation (x/y):	Correlation (x/y) should be 0 unless new data proves otherwise. Correlation other than 0 may indicate a problem with CARP calculation and/or airdrop methodology.
Power:	Power should remain at 1.
Stepsize:	The stepsize describes the size of the squares used for numberical integration and should be sufficiently small to ensure accuracy. Too small of a number will slow computation of risk.

Figure 4.14: Airdrop Collateral Damage Risk Estimator Screenshot

Excel Model Validation

The Airdrop Collateral Damage Estimator uses a VBA program designed to estimate the volume beneath a bivariate normal density surface over a defined rectangular collateral object's perimeter. As this is a locally developed program validation was required to verify the program's accuracy. The Airdrop Collateral Damage Estimator was used to calculate a series of probabilities and the results were recorded and compared against the results from a commercially available mathematical software application "Scientific Workplace". The results can be seen below in Table 4.7. As the table shows the program's calculations are identical to those of the commercial software.

.

	Along the Y axis				Probability	Scientific
	Left Boundary	Right Boundary	Lower Boundary	Upper Boundary	of Strike	Workplace
1	-10	10	190	210	0.001628049	0.001628
2	-10	10	170	190	0.001896803	0.0018968
3	-10	10	150	170	0.002174666	0.0021747
4	-10	10	130	150	0.002453454	0.0024535
5	-10	10	110	130	0.002723821	0.0027238
6	-10	10	90	110	0.002975737	0.0029757
7	-10	10	70	90	0.003199085	0.0031991
8	-10	10	50	70	0.003384327	0.0033843
9	-10	10	30	50	0.003523174	0.0035232
10	-10	10	10	30	0.003609202	0.0036092
11	-10	10	-10	10	0.003638342	0.0036383
12	-10	10	-30	-10	0.003609202	0.0036092
13	-10	10	-50	-30	0.003523174	0.0035232
14	-10	10	-70	-50	0.003384327	0.0033843
15	-10	10	-90	-70	0.003199085	0.0031991
16	-10	10	-110	-90	0.002975737	0.0029757
17	-10	10	-130	-110	0.002723821	0.0027238
18	-10	10	-150	-130	0.002453454	0.0024535
19	-10	10	-170	-150	0.002174666	0.0021747
20	-10	10	-190	-170	0.001896803	0.0018968
21	-10	10	-210	-190	0.001628049	0.001628

Table 4.7: Airdrop Collateral Damage Risk Estimator Validation

To demonstrate the expected behavior of probabilities output by the Airdrop Collateral Damage Estimator a sample collateral object of constant size measuring 20 yards by 20 yards was input. A sample airdrop scenario was developed where the sample collateral object was located on a distant location on the y axis and moved along the y axis, through the aimpoint and finally to a distant location on the other end of the y axis. The probabilities of an airdrop striking the collateral object were calculated and recorded for each of the non-overlapping locations along the y axis. This process was again repeated along the x axis and at a 45 degree angle between the x and y axis.

As the Airdrop Collateral Damage Estimator is calculating a bivariate normal distribution and the marginal distributions from a bivariate normal distribution are normally distributed, we would expect the distribution of risk probabilities from these three scenarios to display a normal distribution. A graphic of the results from these scenarios can be seen in Figure 4.15.

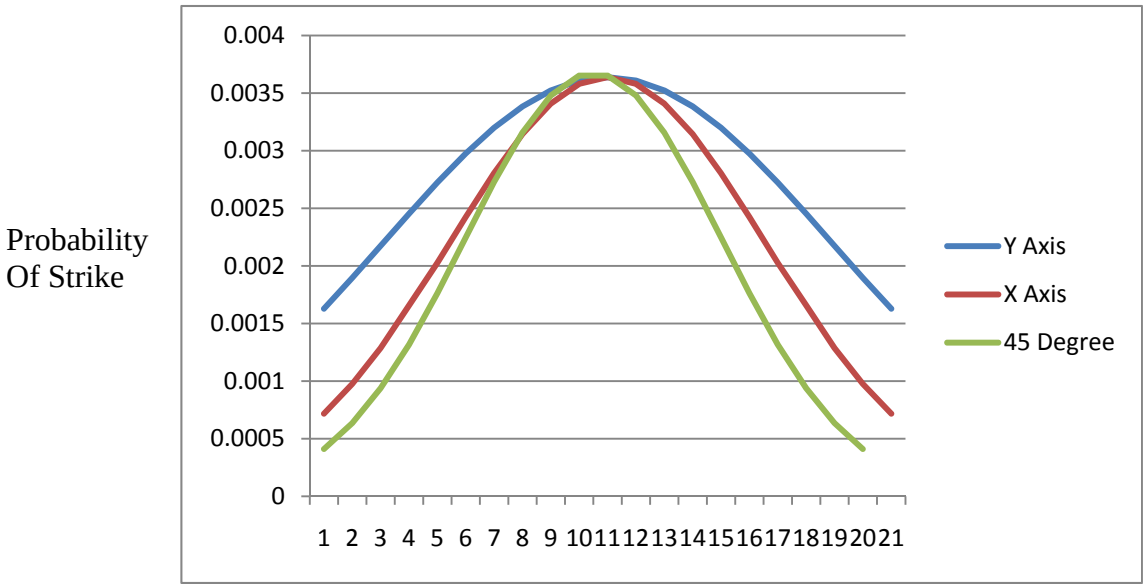

Figure 4.15: Scenario Test Results

As expected and illustrated in Figure 4.10, the probabilities of striking the collateral object display a normal distribution when the collateral object is moved along both the x and y axis as well as through a 45 degree axis.

The results from the comparison of our Excel product and Scientific Workplace outputs from Table 4.5 as well as the results displayed in Figure 4.10 provide validation to the functionality of the Airdrop Collateral Damage Estimator. The file is performing as intended and has the ability to provide numerically integrated probability estimates given a set of inputs.

Example Risk Estimation Scenarios

To show the utility available with our approach to airdrop collateral damage risk estimation using the bivariate normal some realistic scenarios were developed. We will use the Airdrop Collateral Damage Estimator file to calculate the risk of an airdrop striking 10 collateral objects. In the first of 3 scenarios the center bundle of a 9 bundle airdrop will be aimed at a collateral object. The airdrop altitude will be 3000 feet and low velocity chutes are used giving a standard deviation in the X dimension of 191.8 yards and a standard deviation in the Y dimension of 205.8 yards based on the data analyzed in this thesis. The airdrop speed is 135 knots and an assumed timing of 0.5 seconds between bundles is used.

In the second scenario we keep all of the variables the same as the first with one exception. Each bundle's aimpoint is moved along the DZ axis 400 yards. In the third and final scenario all of the variables from the second scenario will be retained with the exception of a change in chute type to the high velocity chute resulting in a standard deviation (x) of 129.9 yards and a standard deviation of (y) of 138.0 yards.

Our Excel tool can handle multiple bundle airdrops quite simply. With an example airspeed of 135 knots and 0.5 seconds between each bundle's exit from the aircraft we would expect each bundle's aimpoint to be 37.98 yards apart along the DZ axis. Once we have calculated the probabilities of each (j) bundle striking each of the (i) collateral objects we can calculate the probability of a strike to collateral object (i) or the probability that at least one of the bundles will strike to any of the collateral objects as follows:

P_{ij} = the probability of airdrop bundle (j)striking collateral object (i)

$1 - \left(\prod_j \left(1 - P_{ij}\right)\right)$ = the probability of any airdrop bundle (j) striking collateral object (i)

$1 - \left(\prod_j \left(1 - \sum_i P_{ij}\right)\right)$ = the probability of at least one airdrop bundle striking any of the collateral objects

Figure 4.16 and Figure 4.17 show an Excel distribution parameter screenshot and visual representation & summary of the 3 scenarios.

	Inputs	Default Values
Aimpoint(x)	0	0
Aimpoint(y)	551.92	0
Std Dev(x)	129.9	121.1
Std Dev (y)	138	158.3
Correlation (x/y)	0	0
Power	1	1
Stepsize	0.1	0.1

Figure 4.16: Excel Aimpoint Input

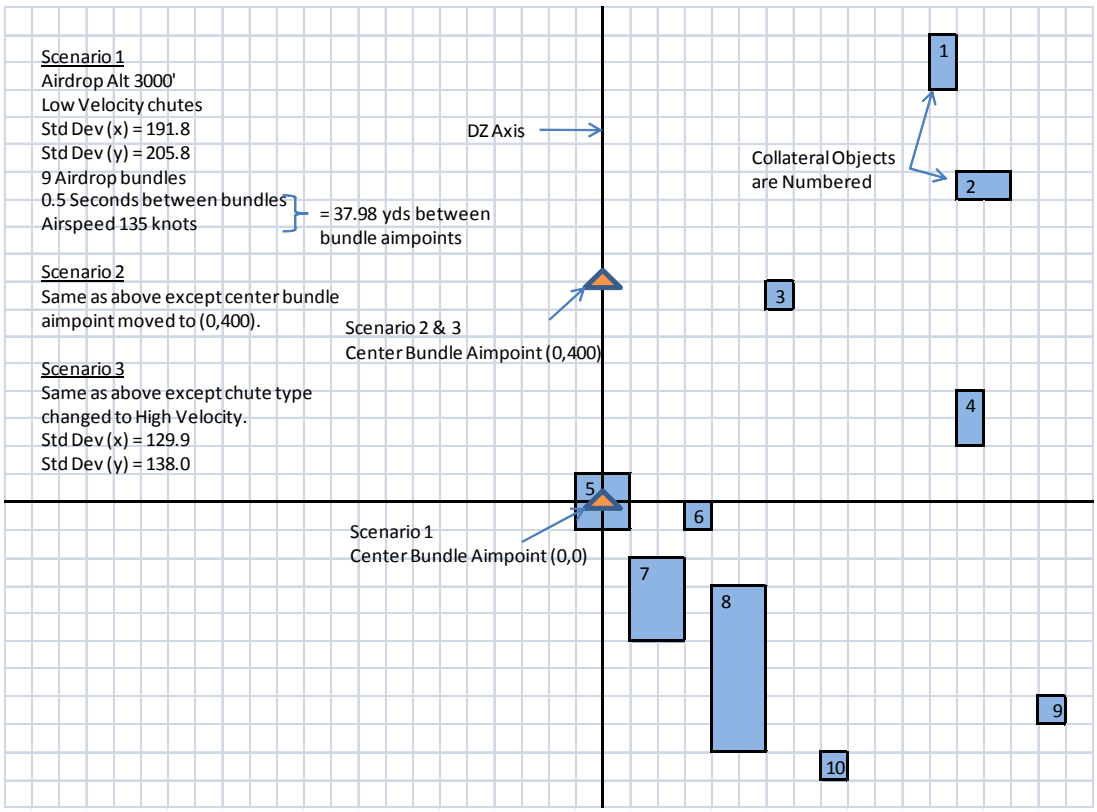

Figure 4.17: Graphic Example of Risk Estimation Scenarios

By comparing the three scenarios it is intuitive that any airdrop collateral damage risk estimate for Scenario 1 should yield a high probability of collateral damage. Scenario 2 should result in a lower probability of damage in comparison to the first scenario as the aimpoint is moved away from most of the large collateral objects.

Scenario 3 should result in the lowest risk estimate due to the improved accuracy of the high velocity chutes.

As Table 4.8 shows, all scenarios resulted in intuitive risk estimations. Scenario 1 results in a very high 60.6% probability of a collateral object strike, Scenario 2 results in a much lower 11.9%, and Scenario 3 returns a very low 5.1%. Further inspection reveals expected behavior between individual bundle probabilities within and across scenarios.

As an example in Scenario 1 the center bundle has the highest probability of striking collateral object 5 and preceding/trailing bundles have an increasingly less chance of a strike. Additionally the first bundles have the highest probability of striking collateral objects 1 through 4 while the trailing bundles have the highest probability of striking collateral objects 7 through 10.

When comparing Scenarios 2 & 3 it can be noted that in Scenario 2 the last CDS bundle is the most likely bundle to strike collateral objects 3 and 5 through 8. It is also the most likely bundle to strike those same collateral objects in Scenario 3 except with a lower probability compared to Scenario 2. This is the expected behavior because the aimpoint remained the same but a more accurate chute type was chosen.

Scenario 1 Results										
Aim Point	(0,-151.92)	(0, -113.94)	(0,-75.96)	(0,-37.98)	(0,0)	(0,37.98)	(0,75.96)	(0, 113.94)	(0,151.92)	
					CDS Bundle # (j)					**Probability**
Collateral Object # (i)	**9**	**8**	**7**	**6**	**5**	**4**	**3**	**2**	**1**	**of Strike**
1	0.0000%	0.0000%	0.0000%	0.0000%	0.0000%	0.0000%	0.0001%	0.0001%	0.0002%	0.0004%
2	0.0000%	0.0000%	0.0000%	0.0001%	0.0001%	0.0002%	0.0003%	0.0004%	0.0006%	0.0017%
3	0.0166%	0.0250%	0.0364%	0.0512%	0.0696%	0.0914%	0.1161%	0.1425%	0.1692%	0.7158%
4	0.0015%	0.0019%	0.0023%	0.0028%	0.0032%	0.0036%	0.0040%	0.0042%	0.0042%	0.0277%
5	3.0224%	3.3971%	3.6929%	3.8826%	3.9480%	3.8826%	3.6929%	3.3971%	3.0224%	27.7646%
6	0.5486%	0.6040%	0.6429%	0.6615%	0.6580%	0.6327%	0.5881%	0.5284%	0.4589%	5.1991%
7	5.0919%	4.9114%	4.5855%	4.1439%	3.6248%	3.0690%	2.5150%	1.9949%	1.5315%	27.4599%
8	3.8541%	3.3992%	2.9127%	2.4245%	1.9600%	1.5386%	1.1726%	0.8674%	0.6226%	17.3075%
9	0.0002%	0.0001%	0.0001%	0.0001%	0.0001%	0.0000%	0.0000%	0.0000%	0.0000%	0.0006%
10	0.0256%	0.0189%	0.0134%	0.0093%	0.0062%	0.0040%	0.0025%	0.0015%	0.0009%	0.0821%
Total Probability	12.5609%	12.3577%	11.8863%	11.1759%	10.2699%	9.2221%	8.0914%	6.9364%	5.8104%	
(1-P)	87.4391%	87.6423%	88.1137%	88.8241%	89.7301%	90.7779%	91.9086%	93.0636%	94.1896%	**60.6404%**
Scenario 2 Results	Moved aimpoint 400 yards from original along the DZ axis									
Aim Point	(0,248.08)	(0, 286.06)	(0,324.04)	(0,362.02)	(0,400)	(0,437.98)	(0,475.96)	(0, 513.94)	(0,551.92)	
					CDS Bundle # (j)					**Probability**
Collateral Object # (i)	**9**	**8**	**7**	**6**	**5**	**4**	**3**	**2**	**1**	**of Strike**
1	0.0005%	0.0008%	0.0012%	0.0018%	0.0025%	0.0033%	0.0043%	0.0053%	0.0064%	0.0262%
2	0.0012%	0.0015%	0.0018%	0.0022%	0.0025%	0.0027%	0.0029%	0.0029%	0.0029%	0.0206%
3	0.2244%	0.2363%	0.2405%	0.2367%	0.2252%	0.2071%	0.1841%	0.1582%	0.1314%	1.8288%
4	0.0038%	0.0034%	0.0030%	0.0025%	0.0020%	0.0016%	0.0012%	0.0009%	0.0006%	0.0191%
5	1.9363%	1.5310%	1.1708%	0.8659%	0.6194%	0.4285%	0.2867%	0.1855%	0.1161%	6.9331%
6	0.2760%	0.2127%	0.1584%	0.1141%	0.0794%	0.0534%	0.0348%	0.0219%	0.0133%	0.9602%
7	0.6776%	0.4635%	0.3068%	0.1965%	0.1218%	0.0731%	0.0424%	0.0238%	0.0130%	1.9044%
8	0.2348%	0.1513%	0.0945%	0.0572%	0.0336%	0.0191%	0.0105%	0.0056%	0.0029%	0.6081%
9	0.0000%	0.0000%	0.0000%	0.0000%	0.0000%	0.0000%	0.0000%	0.0000%	0.0000%	0.0000%
10	0.0002%	0.0001%	0.0000%	0.0000%	0.0000%	0.0000%	0.0000%	0.0000%	0.0000%	0.0004%
Total Probability	**3.3549%**	**2.6007%**	**1.9772%**	**1.4769%**	**1.0863%**	**0.7887%**	**0.5668%**	**0.4041%**	**0.2866%**	
(1-P)	96.6451%	97.3993%	98.0228%	98.5231%	98.9137%	99.2113%	99.4332%	99.5959%	99.7134%	**11.9063%**
Scenario 3 Results	Moved aimpoint 400 yards from original along the DZ axis and changed chute type to High Velocity.									
Aim Point	(0,248.08)	(0, 286.06)	(0,324.04)	(0,362.02)	(0,400)	(0,437.98)	(0,475.96)	(0, 513.94)	(0,551.92)	
					CDS Bundle # (j)					**Probability**
Collateral Object # (i)	**9**	**8**	**7**	**6**	**5**	**4**	**3**	**2**	**1**	**of Strike**
1	0.0000%	0.0000%	0.0000%	0.0000%	0.0000%	0.0000%	0.0000%	0.0000%	0.0000%	0.0000%
2	0.0000%	0.0000%	0.0000%	0.0000%	0.0000%	0.0000%	0.0000%	0.0000%	0.0000%	0.0000%
3	0.0855%	0.0958%	0.0997%	0.0962%	0.0861%	0.0715%	0.0551%	0.0394%	0.0262%	0.6537%
4	0.0000%	0.0000%	0.0000%	0.0000%	0.0000%	0.0000%	0.0000%	0.0000%	0.0000%	0.0000%
5	1.8043%	1.0830%	0.6044%	0.3136%	0.1513%	0.0678%	0.0283%	0.0109%	0.0039%	4.0099%
6	0.1291%	0.0725%	0.0378%	0.0183%	0.0082%	0.0034%	0.0013%	0.0005%	0.0002%	0.2711%
7	0.1283%	0.0570%	0.0236%	0.0091%	0.0033%	0.0011%	0.0003%	0.0001%	0.0000%	0.2227%
8	0.0101%	0.0041%	0.0015%	0.0005%	0.0002%	0.0001%	0.0000%	0.0000%	0.0000%	0.0164%
9	0.0000%	0.0000%	0.0000%	0.0000%	0.0000%	0.0000%	0.0000%	0.0000%	0.0000%	0.0000%
10	0.0000%	0.0000%	0.0000%	0.0000%	0.0000%	0.0000%	0.0000%	0.0000%	0.0000%	0.0000%
Total Probability	**2.1573%**	**1.3125%**	**0.7671%**	**0.4377%**	**0.2490%**	**0.1439%**	**0.0851%**	**0.0510%**	**0.0303%**	
(1-P)	97.8427%	98.6875%	99.2329%	99.5623%	99.7510%	99.8561%	99.9149%	99.9490%	99.9697%	**5.1341%**

Table 4.8: Scenario 1, 2, & 3 Results

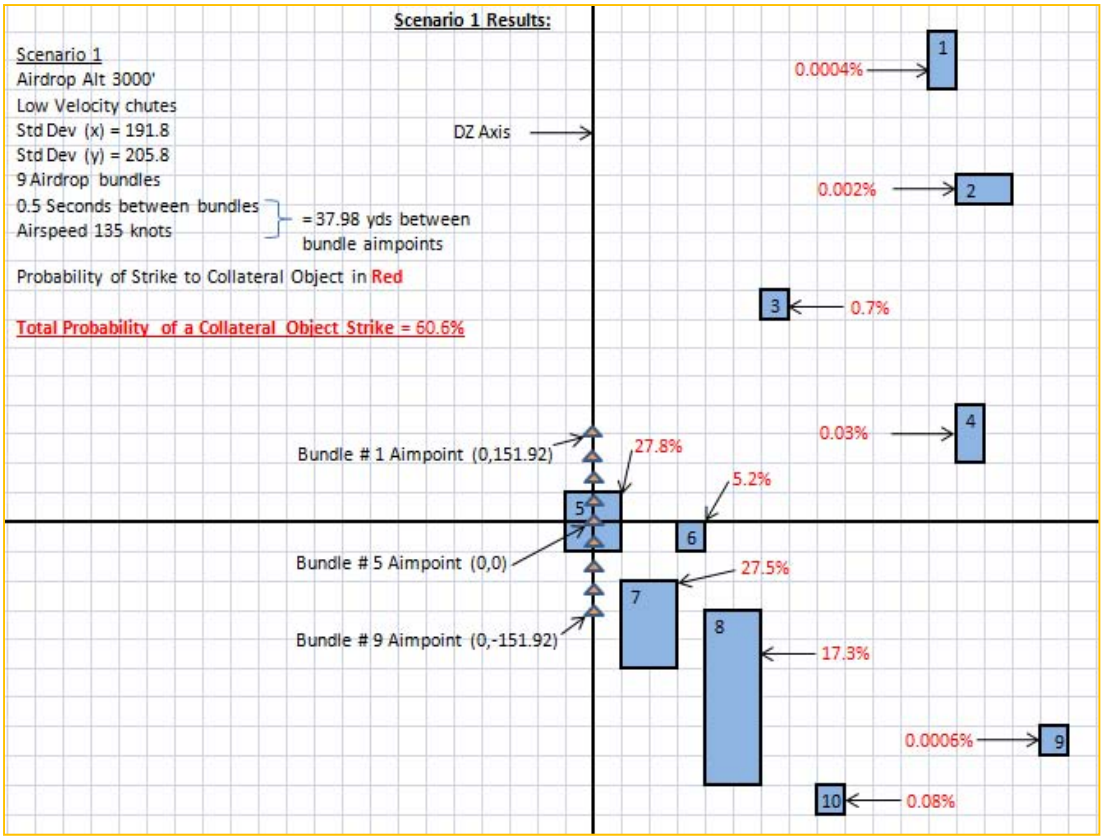

Figure 4.18: Graphic of Scenario 1 Results

The graphic in Figure 4.18 provides a visual example of how the excel tool can provide insights into collateral damage risks. As expected, aiming the center of a 9 bundle airdrop near the center of several large collateral objects is ill-advised. A collateral object's size and location in reference to each bundle's aimpoint determines its probability of being struck. The closer and larger the object is, the higher the risk. As expected object #5 has a high probability of being struck. Its risk is nearly identical to the larger object #7 and is greater than the much larger object #8. Again, an object's probability of being struck is a function of its size and its location relative to the airdrop's aimpoints. Notice object #6's relatively low risk despite its proximity to the aimpoints. This is owing to its relatively small size.

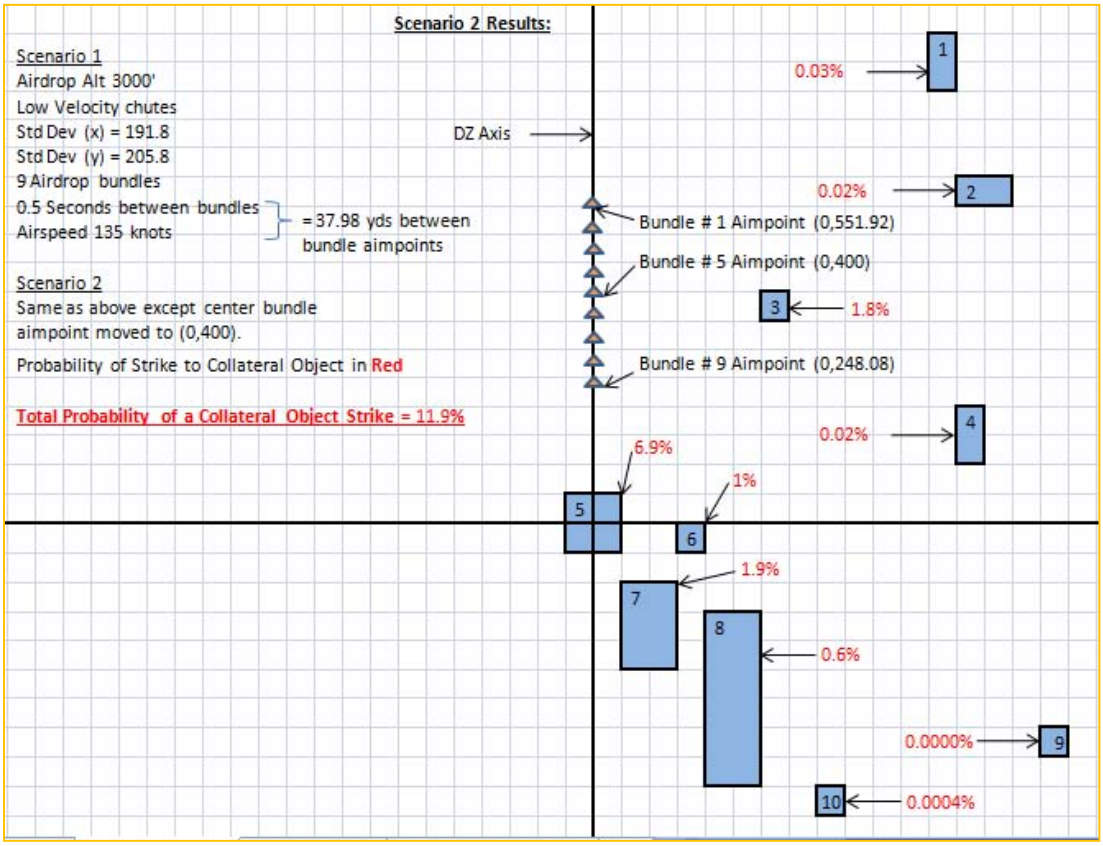

Figure 4.19: Graphic of Scenario 2 Results

In Figure 4.19 we see the results of Scenario 2 where we are still using low velocity chutes but have moved the bundle aimpoints 400 yards further along the DZ axis. Notice how appreciably smaller the risks for each object have become. Object #5 still stands a fair chance of being struck owing to its size and location along the DZ axis. The standard deviations in the Y dimension are larger than those in the X dimension; therefore objects close to the DZ axis will stand a higher chance of strike.

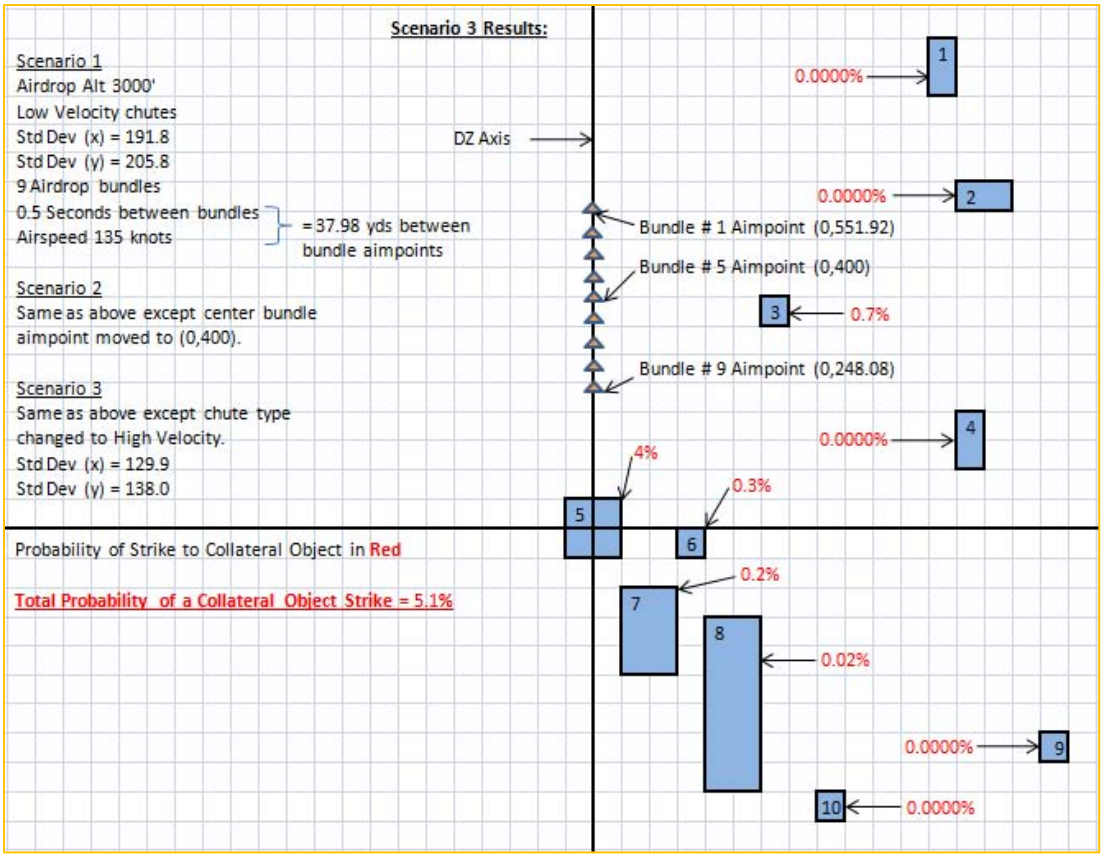

Figure 4.20: Graphic of Scenario 3 Results

In Figure 4.20 we see the results of Scenario 3 where we are using the same aimpoints as Scenario 2 but have switched to the more accurate high velocity chute type. The main collateral object strike concern, object #5's probability of being struck has nearly been cut in half. The lower standard deviations in the X and Y dimension show the higher accuracy of the high velocity chute type and the reduced collateral damage risks are reflected in the Excel tool's output.

V. Conclusions

Conclusions Summary

This thesis began with the seemingly simple question: How can mission planners accurately predict airdrop collateral damage risk? A review of the literature and a statistical examination of recent airdrop data were conducted in order to answer this question. In the previous chapters the literature review and research have provided the basis for the following conclusions:

- The true error distribution pattern for cargo airdrops is most probably elliptical in nature.
    - Examination of the airdrop scoring data set shows that airdrop errors along the DZ axis (Y dimension) tend to be slightly larger than those perpendicular to the DZ axis (X dimension). This could be caused by different factors affecting the airdrop errors in the two dimensions. For example, the timing of the cargo drop from the aircraft would tend to have a significant effect on the Y dimension while wind currents could tend to be more responsible for errors in the X dimension.
- An average cargo airdrop strikes its intended aimpoint.
    - This conclusion is intuitive and suggests that the current CARP models and cargo airdrop methods result in the intended outcome. This also means there is no systematic problem with the CARP models and airdrop methods.

- Cargo airdrop errors in the X dimension are uncorrelated from those in the Y dimension.
    - The airdrop scoring data does not display any correlation between X and Y and the axes of the elliptical error pattern are in line with the X and Y axes.
- The true error distribution pattern for cargo airdrops is reasonably symmetrical.
    - The K-S testing of the airdrop scoring data showed that when comparing distance data along the clock radials the data appeared to be from the same distribution indicating symmetry. This indicates that some sort of symmetrical pattern should be used to model the airdrop errors.
- The bivariate normal is an appropriate distribution to use as the basis for modeling cargo airdrop errors in order to estimate collateral damage risk.
    - Based mainly on theoretical evidence, the bivariate normal distribution is used as the foundation of cargo airdrop risk estimation employed in this research. The bivariate normal is used in similar applications such as gunfire ballistics, naval aircraft ballistic simulations, and bomb drop errors. Additionally, in any situation where a model is fitted and measures of unexplained variation in the form of a set of residuals (errors) are available for examination the residuals should have zero mean and be normally distributed (Draper/Smith, 1966).

- Chute type makes a statistical difference in cargo airdrop error distribution patterns.
    - The data were grouped by chute type and homogeneity of variance tests were conducted. The results provide evidence that suggests that High Velocity chutes are statistically superior to Low Velocity chutes and provide a smaller standard deviation of error. This suggests that different models parameters should be used to estimate cargo airdrop collateral damage risk for low vs. high velocity chutes.
- Airdrop altitude makes a statistical difference in cargo airdrop error distribution patterns.
    - The data were grouped by airdrop altitude and homogeneity of variance tests were conducted. The results provide evidence that suggests that the lower airdrop altitudes provide a smaller standard deviation of error when all other factors are held constant. This suggests that different models parameters should be used to estimate cargo airdrop collateral damage risk for different altitudes.
- The type of aircraft used for a cargo airdrop does not appear to make a statistical difference in cargo airdrop error distribution patterns.
    - The data were grouped by aircraft type and homogeneity of variance tests were conducted. The results provide evidence that suggests that the type of aircraft conducting an airdrop <u>does</u> <u>not</u> make a statistical difference in the airdrop error pattern when all other factors are held constant.

- Grouping cargo airdrop scoring data by chute type and airdrop altitude provides the clearest differences among cargo airdrop error distribution patterns.
    - The data were grouped by chute type and then by airdrop altitude and homogeneity of variance tests were conducted on the grouped data. These groupings showed clear distinctions in both the standard deviation of X and Y. This level of data grouping is recommended for modeling airdrop errors and estimating cargo airdrop collateral damage risk.

In an effort to make the results of this research applicable to mission planning an airdrop collateral damage risk estimation tool was also developed for consideration. The Airdrop Collateral Damage Estimator was coded into Microsoft's Excel spreadsheet tool and can provide reliable risk estimates (Dillenburger, 2011). The tool can be used with only simple, easy to understand inputs and provides clear outputs in the form of a percentage risk of an airdrop striking a collateral object concern.

Limitations

This research focused on determining the appropriate way to model and determines the collateral damage risk associated with one piece of airdropped cargo. The scoring data that was collected is based on the center bundle of a string of bundles that are typically dropped from an aircraft. Therefore the true risk to a collateral object is the probability of any one of a string of airdropped cargo bundles striking it. Therefore this research in its current state only accounts for the risk associated with one object and can only be used to estimate risk in this limited scenario.

Areas for Future Research

This research is the first step towards creating a useful and accurate method for estimating airdrop collateral damage risk but there is much more work that can be done in this area.

- This research was conducted with a limited amount of airdrop scoring data gathered from January to August 2010. Further research using a much larger real world data set or a higher fidelity data set such as testing data can yield higher fidelity in estimating cargo airdrop error distribution patterns and the risk estimations associated with them.
- This research focuses on and provides a tool for estimating collateral damage risk associated with one piece of airdropped cargo. The next logical evolution of this work would be to expand on the capabilities of the Airdrop Collateral Damage Risk Estimator to include multiple airdrop bundles.
- The current methodology assumes the drop zone and all collateral objects are flat and level. Further enhancing the methodology to account for changes in elevation of both the drop zone and collateral objects would improve the fidelity of the risk estimations provided.
- Use and extension of this research to determine constrained optimal aimpoints for cargo airdrops minimizing the risk of a collateral object strike.
- Examine potential Air Force policy implications if this research methodology were adopted by AMC for cargo airdrop mission planning.

Appendix A: Airdrop Data

AIRCRAFT	TYPE	ALT	CHUTES	DISTANCE	CLOCK	X	Y
C-17	CONV	3,000	26'RS	250	7	-125.00	-216.51
C-17	CONV	3,000	26'RS	0	0	0.00	0.00
C-17	CONV	3,000	26'RS				
C-130J	CONV	3,000	26'RS	295	12	0.00	295.00
C-17	CONV	3,000	26'RS	x445	8		
C-130J	CONV	3,000	26'RS	58	4	50.23	-29.00
C-17	CONV	1,000	26'RS				
C-130J	CONV	3,000	26'RS	x17	3		
C-17	CONV	2,500	26'RS	0	0	0.00	0.00
C-17	CONV	2,500	26'RS	133	9	-133.00	0.00
C-130J	CONV	3,300	26'RS	x200	3		
C-130J	CONV	1,500	26'RS	48	4	41.57	-24.00
C-130J	CONV	2,000	26'RS	229	6	0.00	-229.00
C-130J	CONV	2,000	26'RS	50	12	0.00	50.00
C-17	CONV	3,000	26'RS	35	6	0.00	-35.00
C-130J	CONV	2,000	26'RS	59	1	29.50	51.10
C-17	CONV	3,000	26'RS	147	6	0.00	-147.00
C-17	CONV	3,000	26'RS	241	5	120.50	-208.71
C-130J	CONV	1,500	26'RS	134	12	0.00	134.00
C-130J	CONV	2,000	26'RS	219	12	0.00	219.00
C-130H	CONV	2,000	26'RS				
C-130H	CONV	1,500	G12D	x400	3		
C-130J	CONV	3,000	G12E	85	11	-42.50	73.61
C-130J	CONV	1,500	G12E	175	1	87.50	151.55
C-130H	CONV	1,500	G12E	106	11	-53.00	91.80
C-130H	CONV	1,500	G12E	0	12	0.00	0.00
C-17	CONV	1,800	G12E	240	3	240.00	0.00
C-17	CONV	1,500	G12E				
C-130H	CONV	1,500	G12E	500	1	250.00	433.01
C-130H	CONV	1,500	G12E	0	0	0.00	0.00
C-17	CONV	1,500	G12E	105	12	0.00	105.00
C-17	CONV	1,500	G12E	110	6	0.00	-110.00
C-130J	CONV	1,500	G12E	120	4	103.92	-60.00
C-130H	CONV	2,000	G12E	x222	2		
C-17	CONV	1,500	G12E	105	1	52.50	90.93
C-17	CONV	1,500	G12E	120	12	0.00	120.00
C-130H	CONV	1,000	G12E	330	11	-165.00	285.79
C-17	CONV	1,000	G12E	145	1	72.50	125.57
C-17	CONV	1,000	G12E	240	12	0.00	240.00
C-17	CONV	1,000	G12E	200	11	-100.00	173.21
C-130J	CONV	1,000	G12E	215	1	107.50	186.20
C-130J	CONV	3,000	G12E	100	7	-50.00	-86.60
C-17	CONV	2,500	G12E				
C-130H	CONV	1,000	G12E	275	12	0.00	275.00
C-130J	CONV	1,500	G12E	30	1	15.00	25.98
C-17	CONV	1,000	G12E	126	1	63.00	109.12
C-17	CONV	1,000	G12E	85	3	85.00	0.00
C-17	CONV	1,000	G12E	190	11	-95.00	164.54
C-130J	CONV	1,000	G12E	265	12	0.00	265.00
C-130H	CONV	1,000	G12E	75	12	0.00	75.00
C-130J	CONV	1,000	G12E	0	0	0.00	0.00
C-130J	CONV	3,000	G12E	150	11	-75.00	129.90
C-17	CONV	1,000	G12E	0	0	0.00	0.00
C-130H	CONV	1,000	G12E	27	9	-27.00	0.00
C-130H	CONV	1,000	G12E	696	1	348.00	602.75
C-130H	CONV	1,000	G12E	78	6	0.00	-78.00
C-130J	CONV	1,500	G12E	142	6	0.00	-142.00
C-130H	CONV	1,000	G12E	469	10	-406.17	234.50
C-17	CONV	2,100	G12E	147	2	127.31	73.50
C-130J	CONV	1,000	G12E	134	6	0.00	-134.00
C-130J	CONV	1,000	G12E	150	12	0.00	150.00
C-130H	CONV	500	G12E	190	12	0.00	190.00
C-130J	CONV	500	G12E	73	1	36.50	63.22
C-130H	CONV	600	G12E	191	1	95.50	165.41
C-130J	CONV	1,000	G12E	124	6	0.00	-124.00
C-130H	CONV	3,000	G12E	230	10	-199.19	115.00
C-130J	CONV	3,000	G12E	100	3	100.00	0.00
C-130J	CONV	1,000	G12E	114	3	114.00	0.00
C-130H	CONV	2,000	G12E	55	9	-55.00	0.00
C-130H	CONV	3,000	G12E	0			
C-130H	CONV	2,000	G12E	175	12	0.00	175.00
C-130H	CONV	500	G12E	178	3	178.00	0.00
C-130J	CONV	1,500	G12E	0			
C-130J	CONV	1,000	G12E	130	6	0.00	-130.00
C-130H	CONV	1,500	G12E	100	3	100.00	0.00
C-130H	CONV	1,000	G12E	174	11	-87.00	150.69
C-130J	CONV	1,500	G12E	317	12	0.00	317.00
C-130H	CONV	3,000	G12E	88	5	44.00	-76.21
C-130H	CONV	1,500	G12E	0			
C-17	CONV	1,500	G12E	0	0	0.00	0.00
C-130J	CONV	1,500	G12E	x351	6		
C-130H	CONV	1,500	G12E	x262	6		
C-130J	CONV	2,000	G12E				
C-130J	CONV	1,000	G12E	52	12	0.00	52.00

AIRCRAFT	TYPE	ALT	CHUTES	DISTANCE	CLOCK	X	Y
C-130H	CONV	600	G12E	170	2	147.22	85.00
C-130H	CONV	1,500	G12E	90			
C-130H	CONV	1,000	G12E	0			
C-130J	CONV	600	G12E	318	12	0.00	318.00
C-130H	CONV	1,500	G12E	221	12	0.00	221.00
C-130H	CONV	500	G12E	50	12	0.00	50.00
C-130H	CONV	1,000	G12E	37	6	0.00	-37.00
C-130H	CONV	1,000	G12E	X263	X12		
C-130H	CONV	1,000	G12E				
C-130H	CONV	600	G12E	X300	12		
C-130H	CONV	1,000	LCHV	50	12	0.00	50.00
C-130J	CONV	2,000	LCHV				
C-130H	CONV	3,000	LCHV	Unknown	NA		
C-130H	CONV	3,000	LCHV	Unknown	NA		
C-130H	CONV	2,000	LCHV	65	3	65.00	0.00
C-130H	CONV	3,000	LCHV	x34	9		
C-17	CONV	2,000	LCHV	90	1	45.00	77.94
C-130H	CONV	2,000	LCHV	x800	12		
C-17	CONV	2,000	LCHV	X	X		
C-130H	CONV	2,000	LCHV	100	2	86.60	50.00
C-130J	CONV	2,000	LCHV	x300	12		
C-17	CONV	2,000	LCHV	0	0	0.00	0.00
C-17	CONV	2,000	LCHV	57	3	57.00	0.00
C-17	CONV	2,000	LCHV	103	10	-89.20	51.50
C-17	CONV	2,000	LCHV	73	11	-36.50	63.22
C-130J	CONV	2,000	LCHV				
C-17	CONV	2,000	LCHV	100	3	100.00	0.00
C-130J	CONV	3,000	LCHV	25	5	12.50	-21.65
C-130H	CONV	2,000	LCHV	52	6	0.00	-52.00
C-130H	CONV	2,000	LCHV	317	3	317.00	0.00
C-17	CONV	2,100	LCHV	188	1	94.00	162.81
C-130H	CONV	2,000	LCHV	93	3	93.00	0.00
C-130H	CONV	2,000	LCHV	40	11	-20.00	34.64
C-17	CONV	2,500	LCHV	188	8	-162.81	-94.00
C-17	CONV	2,000	LCHV	30	12	0.00	30.00
C-17	CONV	2,000	LCHV	67	12	0.00	67.00
C-17	CONV	2,000	LCHV	63	2	54.56	31.50
C-17	CONV	2,000	LCHV	39	6	0.00	-39.00
C-17	CONV	2,000	LCHV	55	12	0.00	55.00
C-17	CONV	2,000	LCHV	130	12	0.00	130.00
C-17	CONV	2,000	LCHV	122	2	105.66	61.00
C-17	CONV	2,000	LCHV	192	12	0.00	192.00
C-17	CONV	2,000	LCHV	25	8	-21.65	-12.50
C-17	CONV	3,000	LCHV	61	1	30.50	52.83
C-17	CONV	3,000	LCHV	61	1	30.50	52.83
C-17	CONV	3,000	LCHV	40	2	34.64	20.00
C-130J	CONV	2,000	LCHV	108	6	0.00	-108.00
C-130J	CONV	2,000	LCHV	1	3	1.00	0.00
C-17	CONV	2,100	LCHV	84	4	72.75	-42.00
C-130J	CONV	2,000	LCHV	48	6	0.00	-48.00
C-130J	CONV	2,000	LCHV	0	0	0.00	0.00
C-130J	CONV	1,000	LCHV	111	6	0.00	-111.00
C-130J	CONV	2,000	LCHV	59	11	-29.50	51.10
C-130J	CONV	2,000	LCHV	162	4	140.30	-81.00
C-17	CONV	2,000	LCHV	185	6	0.00	-185.00
C-17	CONV	2,000	LCHV	82	7	-41.00	-71.01
C-17	CONV	3,000	LCHV	85	3	85.00	0.00
C-17	CONV	2,100	LCHV	225	5	112.50	-194.86
C-130J	CONV	2,000	LCHV	17	8	-14.72	-8.50
C-17	CONV	3,000	LCHV	201	2	174.07	100.50
C-17	CONV	2,000	LCHV	142	7	-71.00	-122.98
C-17	CONV	2,000	LCHV	188	2	162.81	94.00
C-130J	CONV	2,000	LCHV	37	9	-37.00	0.00
C-17	CONV	3,000	LCHV	116	2	100.46	58.00
C-130J	CONV	2,000	LCHV				
C-17	CONV	1,000	LCHV	172	12	0.00	172.00
C-17	CONV	3,000	LCHV	92	9	-92.00	0.00
C-130J	CONV	2,000	LCHV	160	10	-138.56	80.00
C-17	CONV	1,500	LCHV				
C-17	CONV	2,000	LCHV				
C-17	CONV	3,000	LCHV	250	3	250.00	0.00
C-130H	CONV	1,000	LCHV				
C-17	CONV	3,000	LCHV	91	9	-91.00	0.00
C-17	CONV	3,000	LCHV	271	2	234.69	135.50
C-17	CONV	2,000	LCHV	145	7	-72.50	-125.57
C-130J	CONV	3,000	LCHV	170	2	147.22	85.00
C-17	CONV	2,000	LCHV				
C-17	CONV	2,000	LCHV	152	2	131.64	76.00
C-17	CONV	2,000	LCHV	212	1	106.00	183.60
C-17	CONV	2,000	LCHV	240	12	0.00	240.00
C-130H	CONV	2,000	LCHV	93	6	0.00	-93.00
C-130H	CONV	1,000	LCHV				
C-17	CONV	2,000	LCHV	122	6	0.00	-122.00
C-17	CONV	3,000	LCHV	58	5	29.00	-50.23
C-130H	CONV	2,000	LCHV	466	5	233.00	-403.57

AIRCRAFT	TYPE	ALT	CHUTES	DISTANCE	CLOCK	X	Y
C-17	CONV	3,000	LCHV	223	6	0.00	-223.00
C-17	CONV	3,000	LCHV				
C-17	CONV	2,000	LCHV	150	6	0.00	-150.00
C-130H	CONV	2,000	LCHV	75	6	0.00	-75.00
C-17	CONV	3,000	LCHV	274	9	-274.00	0.00
C-17	CONV	3,000	LCHV				
C-17	CONV	2,000	LCHV	226	3	226.00	0.00
C-17	CONV	3,000	LCHV	210	3	210.00	0.00
C-130H	CONV	3,000	LCHV	128	3	128.00	0.00
C-130J	CONV	3,000	LCHV	150	12	0.00	150.00
C-17	CONV	3,000	LCHV	30	12	0.00	30.00
C-130J	CONV	3,000	LCHV	159	12	0.00	159.00
C-130J	CONV	3,000	LCHV	248	12	0.00	248.00
C-130H	CONV	2,000	LCHV	225	12	0.00	225.00
C-17	CONV	3,000	LCHV	242	2	209.58	121.00
C-17	CONV	2,000	LCHV	168	6	0.00	-168.00
C-17	CONV	3,000	LCHV	162	5	81.00	-140.30
C-17	CONV	3,000	LCHV	363	6	0.00	-363.00
C-130J	CONV	2,000	LCHV	168	6	0.00	-168.00
C-17	CONV	2,000	LCHV	104	3	104.00	0.00
C-130H	CONV	9,200	LCHV	X	X		
C-17	CONV	2,000	LCHV	130	7	-65.00	-112.58
C-130H	CONV	2,000	LCHV	205	12	0.00	205.00
C-17	CONV	2,000	LCHV	131	9	-131.00	0.00
C-17	CONV	2,151	LCHV	106	11	-53.00	91.80
C-17	CONV	2,000	LCHV	60	6	0.00	-60.00
C-17	CONV	3,000	LCHV	40	12	0.00	40.00
C-17	CONV	2,000	LCHV	27	9	-27.00	0.00
C-130J	CONV	3,000	LCHV	94	3	94.00	0.00
C-130J	CONV	2,000	LCHV	161	9	-161.00	0.00
C-17	CONV	2,000	LCHV	310	6	0.00	-310.00
C-17	CONV	1,000	LCHV	107	11	-53.50	92.66
C-17	CONV	3,000	LCHV	100	12	0.00	100.00
C-17	CONV	3,000	LCHV	176	5	88.00	-152.42
C-130J	CONV	2,000	LCHV	186	11	-93.00	161.08
C-17	CONV	3,000	LCHV	293	5	146.50	-253.75
C-17	CONV	1,000	LCHV	x505	8		
C-17	CONV	3,000	LCHV	294	6	0.00	-294.00
C-17	CONV	1,500	LCHV	158	5	79.00	-136.83
C-130J	CONV	2,000	LCHV	139	12	0.00	139.00
C-17	CONV	3,000	LCHV	146	6	0.00	-146.00
C-17	CONV	3,000	LCHV	260	3	260.00	0.00
C-130J	CONV	2,000	LCHV	408	6	0.00	-408.00
C-17	CONV	3,000	LCHV	495	3	495.00	0.00
C-17	CONV	3,000	LCHV	68	12	0.00	68.00
C-130H	CONV	2,000	LCHV	65	12	0.00	65.00
C-130J	CONV	2,000	LCHV	77	6	0.00	-77.00
C-17	CONV	3,000	LCHV	126	1	63.00	109.12
C-130H	CONV	2,000	LCHV	227	9	-227.00	0.00
C-17	CONV	3,000	LCHV	208	3	208.00	0.00
C-17	CONV	3,000	LCHV	101	6	0.00	-101.00
C-17	CONV	3,000	LCHV	340	2	294.45	170.00
C-130H	CONV	2,000	LCHV				
C-17	CONV	2,000	LCHV	0	0	0.00	0.00
C-17	CONV	1,000	LCHV	221	8	-191.39	-110.50
C-17	CONV	2,000	LCHV	120	7	-60.00	-103.92
C-17	CONV	2,000	LCHV	76	3	76.00	0.00
C-17	CONV	2,000	LCHV	225	5	112.50	-194.86
C-130J	CONV	2,000	LCHV	150	12	0.00	150.00
C-17	CONV	2,000	LCHV	174	9	-174.00	0.00
C-130H	CONV	1,000	LCHV	91	12	0.00	91.00
C-17	CONV	3,000	LCHV	361	12	0.00	361.00
C-17	CONV	3,000	LCHV	399	2	345.54	199.50
C-17	CONV	2,000	LCHV	88	9	-88.00	0.00
C-17	CONV	3,000	LCHV	288	3	288.00	0.00
C-17	CONV	2,100	LCHV	67	9	-67.00	0.00
C-17	CONV	3,000	LCHV	x450	9		
C-17	CONV	2,100	LCHV	41	9	-41.00	0.00
C-17	CONV	2,100	LCHV	110	7	-55.00	-95.26
C-130H	CONV	8,400	LCHV				
C-17	CONV	2,000	LCHV	64	2	55.43	32.00
C-17	CONV	2,100	LCHV	187	6	0.00	-187.00
C-17	CONV	2,100	LCHV	53	11	-26.50	45.90
C-130J	CONV	2,000	LCHV	60	12	0.00	60.00
C-17	CONV	3,000	LCHV	54	3	54.00	0.00
C-17	CONV	3,000	LCHV	X	X		
C-130H	CONV	1,000	LCHV				
C-130J	CONV	2,000	LCHV	50	12	0.00	50.00
C-17	CONV	3,000	LCHV				
C-17	CONV	3,000	LCHV				
C-17	CONV	3,000	LCHV	181	11	-90.50	156.75
C-17	CONV	3,000	LCHV				
C-17	CONV	3,000	LCHV				
C-130J	CONV	2,000	LCHV	100	12	0.00	100.00
C-17	CONV	3,000	LCHV				

AIRCRAFT	TYPE	ALT	CHUTES	DISTANCE	CLOCK	X	Y
C-130H	LCLA	500	LCLA	68	6	0.00	-68.00
C-130H	LCLA	300	LCLA	100	12	0.00	100.00
C-130H	LCLA	300	LCLA	88	9	-88.00	0.00
C-130H	LCLA	300	LCLA				
C-130H	LCLA	300	LCLA				
C-130H	LCLA	300	LCLA	50	12	0.00	50.00
C-130H	LCLA	300	LCLA	x188	12		
C-130H	LCLA	300	LCLA	75	12	0.00	75.00
C-130H	LCLA	300	LCLA	62	1	31.00	53.69
C-130H	LCLA	300	LCLA	x406	6		
C-130H	LCLA	300	LCLA				
C-130H	LCLA	300	LCLA	0	0	0.00	0.00
C-130H	LCLA	300	LCLA	110	6	0.00	-110.00
C-130H	LCLA	300	LCLA	38	6	0.00	-38.00
C-130H	LCLA	300	LCLA	0	0	0.00	0.00
C-130H	LCLA	300	LCLA	0			
C-130H	LCLA	300	LCLA	54	0	0.00	54.00
C-130H	CONV	300	LCLA	0	0	0.00	0.00
C-130H	CONV	300	LCLA	66	2	57.16	33.00
C-130H	CONV	300	LCLA	180	12	0.00	180.00
C-130H	CONV	300	LCLA	55	3	55.00	0.00
C-130H	LCLA	300	LCLA	0	0	0.00	0.00
C-130H	CONV	1,500	LCLA	0	0	0.00	0.00
C-130H	LCLA	300	LCLA	70	3	70.00	0.00
C-130H	LCLA	300	LCLA	0	0	0.00	0.00
C-130H	LCLA	300	LCLA	0	0	0.00	0.00
C-130H	CONV	1,500	LCLV	0	0	0.00	0.00
C-130H	CONV	2,500	LCLV	377	3	377.00	0.00
C-130H	CONV	1,500	LCLV	x675	6		
C-17	CONV	1,500	LCLV	168	1	84.00	145.49
C-17	CONV	1,800	LCLV	168	5	84.00	-145.49
C-130J	CONV	1,500	LCLV	139	6	0.00	-139.00
C-130J	CONV	1,600	LCLV	25	12	0.00	25.00
C-130H	CONV	1,500	LCLV	250	3	250.00	0.00
C-17	CONV	1,500	LCLV	93	7	-46.50	-80.54
C-17	CONV	1,500	LCLV	350	12	0.00	350.00
C-17	CONV	1,500	LCLV				
C-17	CONV	1,500	LCLV	90	6	0.00	-90.00
C-17	CONV	3,000	LCLV	250	6	0.00	-250.00
C-130H	CONV	1,000	LCLV	85	1	42.50	73.61
C-130H	CONV	1,000	LCLV	230	7	-115.00	-199.19
C-130H	CONV	1,000	LCLV	180	12	0.00	180.00
C-130H	CONV	1,000	LCLV	x630	10		
C-17	CONV	1,500	LCLV				
C-17	CONV	3,000	LCLV	400	11	-200.00	346.41
C-17	CONV	2,000	LCLV	380	4	329.09	-190.00
C-130H	CONV	1,500	LCLV	125	5	62.50	-108.25
C-130H	CONV	1,500	LCLV	315	1	157.50	272.80
C-130H	CONV	1,000	LCLV	140	9	-140.00	0.00
C-130H	CONV	1,000	LCLV	225	12	0.00	225.00
C-130H	CONV	1,000	LCLV	65	11	-32.50	56.29
C-17	CONV	1,000	LCLV	82	3	82.00	0.00
C-130J	CONV	1,000	LCLV				
C-17	CONV	1,000	LCLV	65	5	32.50	-56.29
C-130H	CONV	1,000	LCLV	174	10	-150.69	87.00
C-17	CONV	1,000	LCLV	170	6	0.00	-170.00
C-17	CONV	1,000	LCLV	55	12	0.00	55.00
C-130H	CONV	1,000	LCLV	150	12	0.00	150.00
C-17	CONV	1,000	LCLV	115	7	-57.50	-99.59
C-130H	CONV	1,000	LCLV				
C-17	CONV	1,000	LCLV				
C-130H	CONV	1,000	LCLV	85	10	-73.61	42.50
C-130J	CONV	1,000	LCLV				
C-130J	CONV	1,000	LCLV				
C-130H	CONV	1,000	LCLV	164	6	0.00	-164.00
C-17	CONV	3,000	LCLV				
C-130H	CONV	1,000	LCLV	300	3	300.00	0.00
C-130H	CONV	1,500	LCLV				
C-17	CONV	1,500	LCLV	x381	6		
C-17	CONV	3,000	LCLV		2	0.00	0.00
C-130J	CONV	3,000	LCLV	0	0	0.00	0.00
C-130H	CONV	1,000	LCLV	0	0	0.00	0.00
C-130H	CONV	1,000	LCLV	28	12	0.00	28.00
C-17	CONV	1,000	LCLV	72	6	0.00	-72.00
C-130H	CONV	1,000	LCLV	112	9	-112.00	0.00
C-130H	CONV	1,000	LCLV	664	12	0.00	664.00
C-17	CONV	2,200	LCLV	74	5	37.00	-64.09
C-130H	CONV	2,000	LCLV				
C-17	CONV	1,000	LCLV	30	6	0.00	-30.00
C-17	CONV	1,000	LCLV	55	5	27.50	-47.63
C-17	CONV	2,600	LCLV	x324	6		
C-130H	CONV	1,000	LCLV	192	3	192.00	0.00
C-17	CONV	3,000	LCLV	x440	10		
C-130H	CONV	1,000	LCLV	66	6	0.00	-66.00
C-130H	LCLA	500	LCLV	60	1	30.00	51.96

AIRCRAFT	TYPE	ALT	CHUTES	DISTANCE	CLOCK	X	Y
C-130J	CONV	1,500	LCLV				
C-17	CONV	1,000	LCLV	189	6	0.00	-189.00
C-17	CONV	2,100	LCLV	70	6	0.00	-70.00
C-17	CONV	1,000	LCLV	x202	12		
C-17	CONV	1,000	LCLV	220	12	0.00	220.00
C-130H	CONV	1,000	LCLV	31	6	0.00	-31.00
C-130H	CONV	1,500	LCLV	70	9	-70.00	0.00
C-130J	CONV	1,000	LCLV				
C-130H	CONV	1,000	LCLV				
C-17	CONV	1,000	LCLV				
C-130H	CONV	1,000	LCLV				
C-130H	CONV	3,000	LCLV	382	6	0.00	-382.00
C-130J	CONV	1,000	LCLV				
C-17	CONV	1,000	LCLV				
C-130J	CONV	1,500	LCLV				
C-130H	CONV	1,000	LCLV	150	4	129.90	-75.00
C-17	CONV	1,000	LCLV	167	1	83.50	144.63
C-130H	CONV	1,000	LCLV	72	1	36.00	62.35
C-130J	CONV	1,500	LCLV	200	1	100.00	173.21
C-130J	CONV	1,000	LCLV	440	6	0.00	-440.00
C-130H	CONV	1,000	LCLV	20	12	0.00	20.00
C-17	CONV	1,500	LCLV				
C-130J	CONV	1,000	LCLV	104	8	-90.07	-52.00
C-130H	CONV	1,500	LCLV	74	10	-64.09	37.00
C-17	CONV	2,100	LCLV	317	11	-158.50	274.53
C-17	CONV	1,000	LCLV	150	5	75.00	-129.90
C-130J	CONV	2,000	LCLV	218	12	0.00	218.00
C-17	CONV	1,000	LCLV	165	12	0.00	165.00
C-130H	CONV	1,000	LCLV				
C-130H	CONV	1,000	LCLV	150	6	0.00	-150.00
C-130H	CONV	1,000	LCLV	30	5	15.00	-25.98
C-17	CONV	2,100	LCLV	255	2	220.84	127.50
C-17	CONV	1,000	LCLV	76	5	38.00	-65.82
C-17	CONV	2,100	LCLV	50	3	50.00	0.00
C-130J	CONV	1,000	LCLV	32	6	0.00	-32.00
C-130J	CONV	1,000	LCLV	143	12	0.00	143.00
C-130H	CONV	1,000	LCLV	245	11	-122.50	212.18
C-17	CONV	2,100	LCLV	226	1	113.00	195.72
C-130H	CONV	1,500	LCLV				
C-17	CONV	1,000	LCLV	155	12	0.00	155.00
C-130H	CONV	1,500	LCLV				
C-130H	CONV	1,000	LCLV				
C-17	CONV	1,000	LCLV				
C-130H	CONV	1,000	LCLV	100	12	0.00	100.00
C-17	CONV	3,000	LCLV	375	9	-375.00	0.00
C-130H	CONV	1,000	LCLV	176	12	0.00	176.00
C-130H	CONV	2,000	LCLV	100	2	86.60	50.00
C-130J	CONV	1,000	LCLV	331	2	286.65	165.50
C-130H	CONV	1,000	LCLV	65	3	65.00	0.00
C-17	CONV	1,000	LCLV	83	7	-41.50	-71.88
C-17	CONV	1,500	LCLV	88	9	-88.00	0.00
C-17	CONV	1,000	LCLV	53	1	26.50	45.90
C-17	CONV	1,000	LCLV	110	7	-55.00	-95.26
C-130H	CONV	1,000	LCLV	100	3	100.00	0.00
C-17	CONV	3,000	LCLV	0	0	0.00	0.00
C-130H	CONV	1,000	LCLV	336	1	168.00	290.98
C-130H	CONV	1,500	LCLV	85	10	-73.61	42.50
C-17	CONV	3,000	LCLV	277	10	-239.89	138.50
C-17	CONV	1,000	LCLV	263	12	0.00	263.00
C-130H	CONV	1,500	LCLV	x238	6		
C-17	CONV	2,800	LCLV	x68	6		
C-130H	CONV	1,000	LCLV	317	1	158.50	274.53
C-17	CONV	1,000	LCLV	78	7	-39.00	-67.55
C-17	CONV	1,000	LCLV	120	6	0.00	-120.00
C-130H	CONV	1,000	LCLV	100	3	100.00	0.00
C-17	CONV	3,000	LCLV	320	11	-160.00	277.13
C-130H	CONV	1,000	LCLV	128	1	64.00	110.85
C-130H	CONV	1,000	LCLV	521	12	0.00	521.00
C-17	CONV	1,500	LCLV	x235	6		
C-130H	CONV	1,000	LCLV	63	3	63.00	0.00
C-17	CONV	1,000	LCLV	28	6	0.00	-28.00
C-17	CONV	1,000	LCLV	225	2	194.86	112.50
C-130H	CONV	3,000	LCLV	197	11	-98.50	170.61
C-17	CONV	1,000	LCLV				
C-130H	CONV	1,000	LCLV	168	12	0.00	168.00
C-17	CONV	1,000	LCLV	75	7	-37.50	-64.95
C-17	CONV	1,000	LCLV	33	2	28.58	16.50
C-17	CONV	1,000	LCLV	161	3	161.00	0.00
C-130H	CONV	2,500	LCLV	191	10	-165.41	95.50
C-17	CONV	1,500	LCLV	325	12	0.00	325.00
C-17	CONV	2,000	LCLV				
C-130H	CONV	1,000	LCLV	260	3	260.00	0.00
C-17	CONV	2,100	LCLV	313	3	313.00	0.00
C-17	CONV	1,000	LCLV	108	2	93.53	54.00
C-17	CONV	1,000	LCLV	146	12	0.00	146.00

AIRCRAFT	TYPE	ALT	CHUTES	DISTANCE	CLOCK	X	Y
C-130J	CONV	1,500	LCLV	242	5	121.00	-209.58
C-17	CONV	1,000	LCLV	75	7	-37.50	-64.95
C-130J	CONV	1,000	LCLV	112	3	112.00	0.00
C-130H	CONV	1,000	LCLV	127	6	0.00	-127.00
C-130J	CONV	1,000	LCLV	86	4	74.48	-43.00
C-130H	CONV	1,500	LCLV	16	7	-8.00	-13.86
C-17	CONV	1,000	LCLV	194	6	0.00	-194.00
C-130J	CONV	1,000	LCLV	100	10	-86.60	50.00
C-130H	CONV	1,000	LCLV	82	2	71.01	41.00
C-130J	CONV	2,000	LCLV	148	12	0.00	148.00
C-130J	CONV	1,000	LCLV	258	12	0.00	258.00
C-17	CONV	1,000	LCLV	46	3	46.00	0.00
C-17	CONV	1,000	LCLV	48	9	-48.00	0.00
C-130H	CONV	1,000	LCLV	182	1	91.00	157.62
C-130J	CONV	2,100	LCLV	0	0	0.00	0.00
C-130H	CONV	1,000	LCLV	139	3	139.00	0.00
C-130H	CONV	1,500	LCLV	202	2	174.94	101.00
C-17	CONV	1,500	LCLV	107	8	-92.66	-53.50
C-17	CONV	1,000	LCLV	235	12	0.00	235.00
C-130J	CONV	2,000	LCLV	61	1	30.50	52.83
C-130H	CONV	3,000	LCLV	359	11	-179.50	310.90
C-17	CONV	1,000	LCLV	31	5	15.50	-26.85
C-17	CONV	1,000	LCLV	90	6	0.00	-90.00
C-130H	CONV	1,000	LCLV	115	2	99.59	57.50
C-130H	CONV	1,000	LCLV	152	8	-131.64	-76.00
C-17	CONV	1,500	LCLV	x290	6		
C-130H	CONV	1,000	LCLV	141	9	-141.00	0.00
C-130J	CONV	1,000	LCLV	188	12	0.00	188.00
C-17	CONV	1,000	LCLV	178	3	178.00	0.00
C-17	CONV	1,000	LCLV	100	6	0.00	-100.00
C-17	CONV	1,000	LCLV	144	6	0.00	-144.00
C-17	CONV	1,000	LCLV		6	0.00	0.00
C-130J	CONV	1,000	LCLV	93	9	-93.00	0.00
C-17	CONV	1,000	LCLV	105	8	-90.93	-52.50
C-17	CONV	1,500	LCLV	101	9	-101.00	0.00
C-130H	CONV	3,000	LCLV	500	11	-250.00	433.01
C-17	CONV	1,000	LCLV	25	6	0.00	-25.00
C-17	CONV	1,000	LCLV	219	12	0.00	219.00
C-17	CONV	1,000	LCLV	86	12	0.00	86.00
C-17	CONV	1,500	LCLV	40	7	-20.00	-34.64
C-17	CONV	1,000	LCLV	167	9	-167.00	0.00
C-130J	CONV	1,000	LCLV	139	8	-120.38	-69.50
C-17	CONV	3,000	LCLV	720	5	360.00	-623.54
C-17	CONV	1,000	LCLV	180	9	-180.00	0.00
C-130H	CONV	3,000	LCLV	272	12	0.00	272.00
C-17	CONV	1,000	LCLV	117	6	0.00	-117.00
C-17	CONV	1,000	LCLV	53	7	-26.50	-45.90
C-130J	CONV	1,000	LCLV	144	9	-144.00	0.00
C-17	CONV	2,500	LCLV	0	0	0.00	0.00
C-17	CONV	1,000	LCLV	337	5	168.50	-291.85
C-130H	CONV	1,000	LCLV	387	12	0.00	387.00
C-130H	CONV	1,500	LCLV	211	10	-182.73	105.50
C-130J	CONV	1,000	LCLV	263	4	227.76	-131.50
C-130H	CONV	1,000	LCLV	x548	9		
C-17	CONV	1,000	LCLV	x501	6		
C-17	CONV	1,500	LCLV	185	4	160.21	-92.50
C-130H	CONV	1,000	LCLV	0			
C-130H	CONV	3,000	LCLV	218	10	-188.79	109.00
C-17	CONV	2,500	LCLV				
C-130H	CONV	1,000	LCLV				
C-17	CONV	1,000	LCLV	460	12	0.00	460.00
C-17	CONV	1,000	LCLV	0	0	0.00	0.00
C-130H	CONV	2,400	LCLV	214	12	0.00	214.00
C-130J	CONV	1,000	LCLV	130	3	130.00	0.00
C-130H	CONV	1,000	LCLV	90	12	0.00	90.00
C-130H	CONV	1,000	LCLV	115	1	57.50	99.59
C-130H	CONV	1,000	LCLV	115	1	57.50	99.59
Unknown	CONV	1,000	LCLV				
C-130H	CONV	1,000	LCLV	24	1	12.00	20.78
C-17	CONV	1,000	LCLV	250	9	-250.00	0.00
C-17	CONV	1,500	LCLV	260	9	-260.00	0.00
C-130H	CONV	1,000	LCLV	0	0	0.00	0.00
C-17	CONV	1,500	LCLV				
C-130H	CONV	1,000	LCLV	218	12	0.00	218.00
C-130H	CONV	1,500	LCLV	50	12	0.00	50.00
C-17	CONV	1,000	LCLV	437	3	437.00	0.00
C-130H	CONV	1,000	LCLV	105	3	105.00	0.00
C-17	CONV	1,500	LCLV	x652	6		
C-17	CONV	1,500	LCLV	222	8	-192.26	-111.00
C-17	CONV	1,000	LCLV	178			
C-130H	CONV	1,000	LCLV	80	8	-69.28	-40.00
C-130H	CONV	1,500	LCLV	x550	5		
C-130H	CONV	1,500	LCLV	x710	4		
C-130J	CONV	1,500	LCLV	550	6	0.00	-550.00
C-17	CONV	3,000	LCLV	50	7	-25.00	-43.30

AIRCRAFT	TYPE	ALT	CHUTES	DISTANCE	CLOCK	X	Y
C-130H	CONV	1,000	LCLV	8	20		
C-130J	CONV	3,000	LCLV	345	6	0.00	-345.00
C-130H	CONV	1,500	LCLV	294	11	-147.00	254.61
C-17	CONV	3,000	LCLV	533	7	-266.50	-461.59
C-130H	CONV	1,000	LCLV	x6000	6		
C-17	CONV	1,500	LCLV	35	3	35.00	0.00
C-130J	CONV	1,000	LCLV	5	3	5.00	0.00
C-17	CONV	1,000	LCLV				
C-17	CONV	1,000	LCLV	0	0	0.00	0.00
C-17	CONV	1,500	LCLV	81	2	70.15	40.50
C-130J	CONV	1,000	LCLV	199	11	-99.50	172.34
C-130H	CONV	1,000	LCLV	199	11	-99.50	172.34
C-17	CONV	1,000	LCLV				
C-130H	CONV	1,000	LCLV				
C-17	CONV	1,500	LCLV	300	7	-150.00	-259.81
C-130H	CONV	1,000	LCLV	150	12	0.00	150.00
C-130H	CONV	1,000	LCLV	x800	12		
C-130J	CONV	1,000	LCLV	115	2	99.59	57.50
C-130J	CONV	1,500	LCLV	50	12	0.00	50.00
C-17	CONV	1,000	LCLV	20	3	20.00	0.00
C-130J	CONV	1,000	LCLV	30	3	30.00	0.00
C-130H	CONV	1,000	LCLV	25	3	25.00	0.00
C-130H	CONV	1,000	LCLV				
C-17	CONV	1,500	LCLV	185	2	160.21	92.50
C-130H	CONV	1,000	LCLV	568	5	284.00	-491.90
C-130H	CONV	3,000	LCLV	38	3	38.00	0.00
C-130H	CONV	3,000	LCLV	38	11	-19.00	32.91
C-17	CONV	1,500	LCLV	72	12	0.00	72.00
C-130J	CONV	1,000	LCLV	18	11	-9.00	15.59
C-17	CONV	1,500	LCLV	330	11	-165.00	285.79
C-130H	CONV	1,000	LCLV	18	11	-9.00	15.59
C-130H	CONV	1,000	LCLV	430	6	0.00	-430.00
C-130H	CONV	1,000	LCLV	260	1	130.00	225.17
C-130H	CONV	1,500	LCLV	0	0	0.00	0.00
C-130H	CONV	1,000	LCLV	58	7	-29.00	-50.23
C-17	CONV	2,000	LCLV	180	3	180.00	0.00
C-130H	CONV	1,500	LCLV	300	11	-150.00	259.81
C-130H	CONV	1,500	LCLV	380	2	329.09	190.00
C-130H	CONV	1,500	LCLV	150	6	0.00	-150.00
C-130J	CONV	3,000	LCLV				
C-130J	CONV	3,000	LCLV	350	9	-350.00	0.00
C-130H	CONV	1,500	LCLV	150	4	129.90	-75.00
C-130J	CONV	1,500	LCLV	142	2	122.98	71.00
C-130J	CONV	1,500	LCLV	152	11	-76.00	131.64
C-130J	CONV	1,500	LCLV	420	12	0.00	420.00
C-130H	CONV	1,000	LCLV	x686	2		
C-130H	CONV	1,000	LCLV	285	12	0.00	285.00
C-130H	CONV	1,000	LCLV	80	6	0.00	-80.00
C-130H	CONV	1,500	LCLV	135	1	67.50	116.91
C-130H	CONV	1,000	LCLV	555	7	-277.50	-480.64
C-17	CONV	1,500	LCLV				
C-130H	CONV	1,000	LCLV				
C-130H	CONV	1,000	LCLV	212	12	0.00	212.00
C-130H	CONV	1,000	LCLV	x1239	10		
C-130H	CONV	1,000	LCLV				
C-130J	CONV	2,000	LCLV	30	9	-30.00	0.00
C-17	CONV	3,000	LCLV	90	9	-90.00	0.00
C-130J	CONV	1,000	LCLV	309	3	309.00	0.00
C-130J	CONV	1,000	LCLV	235	12	0.00	235.00
C-17	CONV	3,000	LCLV	568	8	-491.90	-284.00
C-130H	CONV	1,000	LCLV	0	0	0.00	0.00
C-130H	CONV	1,000	LCLV	80	12	0.00	80.00
C-130J	CONV	1,000	LCLV	343	2	297.05	171.50
C-17	CONV	3,000	LCLV	171	11	-85.50	148.09
C-17	CONV	3,000	LCLV	320	11	-160.00	277.13
C-17	CONV	1,500	LCLV	165	9	-165.00	0.00
C-130H	CONV	1,000	LCLV	187	3	187.00	0.00
C-130J	CONV	1,000	LCLV				
C-17	CONV	1,500	LCLV	703	6	0.00	-703.00
C-130J	CONV	1,000	LCLV	53	6	0.00	-53.00
C-17	CONV	3,000	LCLV	287	8	-248.55	-143.50
C-130J	CONV	1,000	LCLV	194	11	-97.00	168.01
C-130H	CONV	1,500	LCLV	125	3	125.00	0.00
C-130H	CONV	1,000	LCLV	0	0	0.00	0.00
C-130J	CONV	1,000	LCLV				
C-17	CONV	1,500	LCLV	216	5	108.00	-187.06
C-130H	CONV	1,000	LCLV	129	12	0.00	129.00
C-17	CONV	1,000	LCLV	131	11	-65.50	113.45
C-130J	CONV	2,500	LCLV	191	9	-191.00	0.00
C-17	CONV	1,000	LCLV	115	12	0.00	115.00
C-130H	CONV	1,000	LCLV	200	9	-200.00	0.00
C-17	CONV	1,500	LCLV	60	3	60.00	0.00
C-130H	CONV	1,000	LCLV				
C-130J	CONV	1,000	LCLV	135	12	0.00	135.00
C-17	CONV	1,000	LCLV	242	12	0.00	242.00

AIRCRAFT	TYPE	ALT	CHUTES	DISTANCE	CLOCK	X	Y
C-130H	CONV	1,000	LCLV	316	4	273.66	-158.00
C-130J	CONV	1,000	LCLV	80	1	40.00	69.28
C-17	CONV	1,000	LCLV	663	6	0.00	-663.00
C-130J	CONV	1,000	LCLV	161	3	161.00	0.00
C-17	CONV	2,000	LCLV				
C-17	CONV	1,000	LCLV	152	2	131.64	76.00
C-130H	CONV	1,000	LCLV	382	12	0.00	382.00
C-130J	CONV	1,000	LCLV	71	11	-35.50	61.49
C-17	CONV	1,500	LCLV	235	2	203.52	117.50
C-130J	CONV	1,000	LCLV	278	2	240.76	139.00
C-17	CONV	1,000	LCLV	106	3	106.00	0.00
C-130H	CONV	1,500	LCLV				
C-130H	CONV	1,500	LCLV	600	12	0.00	600.00
C-130H	CONV	1,500	LCLV	100	12	0.00	100.00
C-17	CONV	2,000	LCLV	239	1	119.50	206.98
C-130J	CONV	1,000	LCLV				
C-17	CONV	1,000	LCLV	60	6	0.00	-60.00
C-130J	CONV	1,000	LCLV	435	6	0.00	-435.00
C-130J	CONV	1,000	LCLV	5	3	5.00	0.00
C-130J	CONV	1,500	LCLV	256	12	0.00	256.00
C-17	CONV	1,000	LCLV	0	12	0.00	0.00
C-17	CONV	1,500	LCLV	181	11	-90.50	156.75
C-130J	CONV	1,000	LCLV	148	1	74.00	128.17
C-17	CONV	3,000	LCLV				
C-17	CONV	2,000	LCLV				
C-130H	CONV	1,000	LCLV	89	5	44.50	-77.08
C-130J	CONV	1,000	LCLV	104	7	-52.00	-90.07
C-130J	CONV	1,000	LCLV	258	9	-258.00	0.00
C-130H	CONV	1,000	LCLV	50	6	0.00	-50.00
C-130J	CONV	1,000	LCLV	250	7	-125.00	-216.51
C-130J	CONV	1,000	LCLV	291	7	-145.50	-252.01
C-130J	CONV	1,000	LCLV	90	12	0.00	90.00
C-17	CONV	1,500	LCLV	56	3	56.00	0.00
C-130H	CONV	1,000	LCLV				
C-17	CONV	2,151	LCLV	296	12	0.00	296.00
C-17	CONV	1,500	LCLV	217	2	187.93	108.50
C-17	CONV	1,000	LCLV	152	10	-131.64	76.00
C-130J	CONV	1,000	LCLV				
C-130H	CONV	3,000	LCLV	325	6	0.00	-325.00
C-130J	CONV	1,000	LCLV				
C-130J	CONV	1,000	LCLV				
C-130H	CONV	1,000	LCLV	156	3	156.00	0.00
C-130H	CONV	1,000	LCLV	159	3	159.00	0.00
C-17	CONV	1,000	LCLV	223	12	0.00	223.00
C-130H	CONV	1,000	LCLV				
C-130H	CONV	1,000	LCLV	324	2	280.59	162.00
C-17	CONV	2,151	LCLV				
C-130J	CONV	1,500	LCLV	x465	x1		
C-17	CONV	1,000	LCLV	402	6	0.00	-402.00
C-130H	CONV	1,000	LCLV	410	3	410.00	0.00
C-17	CONV	1,000	LCLV	150			
C-130H	CONV	3,000	LCLV	100	12	0.00	100.00
C-130J	CONV	1,086	LCLV	212	7	-106.00	-183.60
C-17	CONV	3,000	LCLV				
C-130H	CONV	1,500	LCLV	63	7	-31.50	-54.56
C-130J	CONV	1,286	LCLV	130	7	-65.00	-112.58
C-130J	CONV	1,286	LCLV	48	3	48.00	0.00
C-130H	CONV	1,500	LCLV	69	3	69.00	0.00
C-17	CONV	1,000	LCLV	114	7	-57.00	-98.73
C-130H	CONV	3,000	LCLV				
C-130H	CONV	1,000	LCLV	207	3	207.00	0.00
C-130H	CONV	1,000	LCLV	10	3	10.00	0.00
C-130H	CONV	1,000	LCLV	433	5	216.50	-374.99
C-17	CONV	3,000	LCLV	116	3	116.00	0.00
C-130H	CONV	1,000	LCLV	117	3	117.00	0.00
C-130J	CONV	1,000	LCLV	135	12	0.00	135.00
C-130H	CONV	1,000	LCLV	0	3	0.00	0.00
C-17	CONV	1,000	LCLV	122	9	-122.00	0.00
C-130J	CONV	1,000	LCLV	0	0	0.00	0.00
C-130J	CONV	1,000	LCLV	165	6	0.00	-165.00
C-130H	CONV	1,000	LCLV				
C-17	CONV	1,500	LCLV	107	11	-53.50	92.66
C-17	CONV	1,000	LCLV	84	10	-72.75	42.00
C-130H	CONV	1,000	LCLV	61	8	-52.83	-30.50
C-130H	CONV	1,000	LCLV	10	12	0.00	10.00
C-130H	CONV	1,000	LCLV				
C-130H	CONV	1,000	LCLV	0	0	0.00	0.00
C-130H	CONV	1,000	LCLV	0	0	0.00	0.00
C-17	CONV	1,500	LCLV	167	9	-167.00	0.00
C-17	CONV	1,000	LCLV	248	4	214.77	-124.00
C-130H	CONV	1,000	LCLV	437	5	218.50	-378.45
C-130H	CONV	1,000	LCLV	0	0	0.00	0.00
C-17	CONV	1,000	LCLV	112	8	-96.99	-56.00
C-130J	CONV	1,000	LCLV	98	9	-98.00	0.00
C-17	CONV	1,500	LCLV	146	5	73.00	-126.44

AIRCRAFT	TYPE	ALT	CHUTES	DISTANCE	CLOCK	X	Y
C-130J	CONV	1,000	LCLV	270	1	135.00	233.83
C-130J	CONV	1,000	LCLV	168	6	0.00	-168.00
C-130J	CONV	1,000	LCLV	227	8	-196.59	-113.50
C-130J	CONV	1,000	LCLV	3	12	0.00	3.00
C-130H	CONV	1,000	LCLV	0	0	0.00	0.00
C-130H	CONV	1,000	LCLV	0	0	0.00	0.00
C-130J	CONV	1,000	LCLV	178	12	0.00	178.00
C-130H	CONV	1,000	LCLV	50	3	50.00	0.00
C-17	CONV	1,500	LCLV	234	6	0.00	-234.00
C-17	CONV	1,000	LCLV	32	12	0.00	32.00
C-130J	CONV	1,000	LCLV	389	12	0.00	389.00
C-130H	CONV	1,000	LCLV	0	0	0.00	0.00
C-130H	CONV	1,000	LCLV	300	2	259.81	150.00
C-17	CONV	1,000	LCLV				
C-130H	CONV	1,500	LCLV	0	0	0.00	0.00
C-130H	CONV	1,500	LCLV	42	12	0.00	42.00
C-130H	CONV	3,000	LCLV	103	9	-103.00	0.00
C-17	CONV	1,000	LCLV	0	0	0.00	0.00
C-130H	CONV	1,000	LCLV	x598	11		
C-130H	CONV	1,000	LCLV	96	2	83.14	48.00
C-130J	CONV	1,000	LCLV	250	3	250.00	0.00
C-130H	CONV	1,000	LCLV	95	7	-47.50	-82.27
C-130H	CONV	1,000	LCLV	24	9	-24.00	0.00
C-130H	CONV	1,000	LCLV	0	0	0.00	0.00
C-130H	CONV	1,000	LCLV	346	10	-299.64	173.00
C-130J	CONV	2,500	LCLV	127	3	127.00	0.00
C-130H	CONV	1,000	LCLV	18	3	18.00	0.00
C-17	CONV	1,000	LCLV	174	10	-150.69	87.00
C-17	CONV	1,000	LCLV	289	6	0.00	-289.00
C-130H	CONV	1,000	LCLV	0	0	0.00	0.00
C-130H	CONV	1,000	LCLV	160	2	138.56	80.00
C-130H	CONV	1,000	LCLV	0	0	0.00	0.00
C-130H	CONV	1,500	LCLV	169	6	0.00	-169.00
C-17	CONV	1,000	LCLV	142	4	122.98	-71.00
C-17	CONV	1,000	LCLV	152	7	-76.00	-131.64
C-130H	CONV	1,000	LCLV	162	12	0.00	162.00
C-130J	CONV	1,000	LCLV	0	0	0.00	0.00
C-130J	CONV	1,000	LCLV	135	8	-116.91	-67.50
C-130H	CONV	1,000	LCLV	96	10	-83.14	48.00
C-17	CONV	1,000	LCLV	146	6	0.00	-146.00
C-17	CONV	1,000	LCLV	212	7	-106.00	-183.60
C-17	CONV	3,000	LCLV	X694	7		
C-17	CONV	1,500	LCLV				
C-130H	CONV	1,000	LCLV	145	12	0.00	145.00
C-17	CONV	1,500	LCLV	193	7	-96.50	-167.14
C-130H	CONV	1,500	LCLV	107	3	107.00	0.00
C-130H	CONV	1,000	LCLV	133	8	-115.18	-66.50
C-17	CONV	2,151	LCLV	256	8	-221.70	-128.00
C-130H	CONV	1,000	LCLV	294	2	254.61	147.00
C-17	CONV	1,000	LCLV	133	3	133.00	0.00
C-130J	CONV	1,000	LCLV	114	9	-114.00	0.00
C-130J	CONV	1,000	LCLV	244	12	0.00	244.00
C-130H	CONV	1,000	LCLV	296	2	256.34	148.00
C-17	CONV	3,000	LCLV	40	11	-20.00	34.64
C-17	CONV	1,000	LCLV	145	4	125.57	-72.50
C-130J	CONV	1,000	LCLV	X560	10		
C-130H	CONV	1,000	LCLV				
C-130H	CONV	1,500	LCLV	20	4	17.32	-10.00
C-130H	CONV	1,000	LCLV	50	12	0.00	50.00
C-130H	CONV	1,000	LCLV	X456	3		
C-17	CONV	2,500	LCLV	132	6	0.00	-132.00
C-130H	CONV	1,000	LCLV	190	2	164.54	95.00
C-17	CONV	3,000	LCLV	79	9	-79.00	0.00
C-17	CONV	1,000	LCLV	355	6	0.00	-355.00
C-17	CONV	3,000	LCLV	615	3	615.00	0.00
C-130H	CONV	1,000	LCLV	190	2	164.54	95.00
C-130H	CONV	3,000	LCLV	105	11	-52.50	90.93
C-17	CONV	3,000	LCLV	465	12	0.00	465.00
C-130J	CONV	3,000	LCLV	284	8	-245.95	-142.00
C-130H	CONV	3,000	LCLV	123	3	123.00	0.00
C-130H	CONV	1,000	LCLV	42	12	0.00	42.00
C-17	CONV	3,000	LCLV	77	8	-66.68	-38.50
C-130J	CONV	1,000	LCLV	154	3	154.00	0.00
C-130J	CONV	1,000	LCLV	109	9	-109.00	0.00
C-17	CONV	3,000	LCLV	X956	7		
C-17	CONV	1,000	LCLV	51	9	-51.00	0.00
C-130H	CONV	1,000	LCLV	145	12	0.00	145.00
C-17	CONV	1,500	LCLV	127	3	127.00	0.00
C-130H	CONV	1,000	LCLV	183	12	0.00	183.00
C-130H	CONV	1,000	LCLV	47	12	0.00	47.00
C-17	CONV	3,000	LCLV	75	12	0.00	75.00
C-130J	CONV	1,000	LCLV	X0	0		
C-17	CONV	1,000	LCLV	X669	6		
C-130H	CONV	2,000	LCLV	58	3	58.00	0.00
C-17	CONV	3,000	LCLV	X500	9		

AIRCRAFT	TYPE	ALT	CHUTES	DISTANCE	CLOCK	X	Y
C-130J	CONV	1,000	LCLV	228	3	228.00	0.00
C-17	CONV	1,000	LCLV	111	3	111.00	0.00
C-130J	CONV	1,000	LCLV				
C-130J	CONV	1,000	LCLV	x0	12		
C-130H	CONV	1,000	LCLV	182	11	-91.00	157.62
C-130H	CONV	3,000	LCLV	X			
C-130J	CONV	1,000	LCLV	0	12	0.00	0.00
C-130H	CONV	1,000	LCLV	192	12	0.00	192.00
C-17	CONV	1,000	LCLV	111	9	-111.00	0.00
C-17	CONV	1,500	LCLV	280	10	-242.49	140.00
C-17	CONV	1,000	LCLV	0	0	0.00	0.00
C-17	CONV	3,000	LCLV	129	6	0.00	-129.00
C-130H	CONV	1,000	LCLV	0	12	0.00	0.00
C-130J	CONV	1,000	LCLV	207	2	179.27	103.50
C-130H	CONV	3,000	LCLV	346	3	346.00	0.00
C-17	CONV	1,000	LCLV	150	6	0.00	-150.00
C-130H	CONV	1,000	LCLV	125	9	-125.00	0.00
C-130H	CONV	1,000	LCLV	238	6	0.00	-238.00
C-130H	CONV	2,000	LCLV	0	0	0.00	0.00
C-130H	CONV	3,000	LCLV	366	12	0.00	366.00
C-130J	CONV	1,000	LCLV	150	12	0.00	150.00
C-130J	CONV	1,000	LCLV	145	3	145.00	0.00
C-130H	CONV	1,000	LCLV	0	0	0.00	0.00
C-130H	CONV	1,000	LCLV	0	0	0.00	0.00
C-130J	CONV	1,000	LCLV	223	11	-111.50	193.12
C-17	CONV	3,000	LCLV	354	7	-177.00	-306.57
C-130H	CONV	3,000	LCLV	484	12	0.00	484.00
C-130H	CONV	2,000	LCLV	275	3	275.00	0.00
C-17	CONV	2,000	LCLV	115	3	115.00	0.00
C-130H	CONV	1,000	LCLV	342	12	0.00	342.00
C-17	CONV	1,500	LCLV	72	12	0.00	72.00
C-130J	CONV	1,000	LCLV				
C-17	CONV	1,500	LCLV	132	6	0.00	-132.00
C-17	CONV	3,000	LCLV	175	9	-175.00	0.00
C-130H	CONV	3,000	LCLV	X900	X		
C-130H	CONV	3,000	LCLV	714	9	-714.00	0.00
C-130H	CONV	1,000	LCLV	430	8	-372.39	-215.00
C-130H	CONV	1,000	LCLV	0	0	0.00	0.00
C-17	CONV	1,000	LCLV	35	9	-35.00	0.00
C-17	CONV	3,000	LCLV	220	12	0.00	220.00
C-17	CONV	1,500	LCLV	53	12	0.00	53.00
C-17	CONV	1,000	LCLV	216	6	0.00	-216.00
C-130J	CONV	1,000	LCLV	0	0	0.00	0.00
C-130J	CONV	1,000	LCLV	0	12	0.00	0.00
C-130J	CONV	3,000	LCLV	X1019	12		
C-17	CONV	3,000	LCLV	X676	12		
C-130H	CONV	1,000	LCLV	80	1	40.00	69.28
C-17	CONV	1,000	LCLV				
C-17	CONV	3,000	LCLV	245	12	0.00	245.00
C-130J	CONV	1,000	LCLV	X396	9		
C-130J	CONV	1,000	LCLV	0	0	0.00	0.00
C-130H	CONV	1,000	LCLV	0	0	0.00	0.00
C-130H	CONV	1,000	LCLV	0	0	0.00	0.00
C-130H	CONV	1,000	LCLV	119	12	0.00	119.00
C-17	CONV	1,500	LCLV	226	6	0.00	-226.00
C-17	CONV	2,100	LCLV	260	6	0.00	-260.00
C-17	CONV	1,500	LCLV	57	7	-28.50	-49.36
C-130H	CONV	1,000	LCLV	300	12	0.00	300.00
C-130J	CONV	1,000	LCLV				
C-130J	CONV	1,000	LCLV	X438	6		
C-17	CONV	1,500	LCLV	X	X		
C-17	CONV	3,000	LCLV	99	3	99.00	0.00
C-17	CONV	1,000	LCLV				
C-130H	CONV	1,000	LCLV	121	12	0.00	121.00
C-17	CONV	1,000	LCLV				
C-17	CONV	2,000	LCLV				
C-130J	CONV	1,000	LCLV	0	0	0.00	0.00
C-17	CONV	1,000	LCLV				
C-130J	CONV	1,000	LCLV	326	11	-163.00	282.32
C-130H	CONV	1,000	LCLV	203	11	-101.50	175.80
C-130H	CONV	2,000	LCLV				
C-17	CONV	2,000	LCLV				
C-17	CONV	1,500	LCLV				
C-17	CONV	1,500	LCLV				
C-130J	CONV	1,000	LCLV	X	X		
C-17	CONV	1,500	LCLV				
C-17	CONV	1,000	LCLV				

Appendix B: Airdrop Collateral Damage Risk Estimator

VBA Program:

Module 1:

```
Dim i As Integer
Dim j As Integer

Sub populate()

k = 1
highi = Round(Cells(9, 3), 2)
lowi = Round(Cells(9, 2), 2)
highj = Round(Cells(10, 3), 2)
lowj = Round(Cells(10, 2), 2)



For i = 50 To 69
   For j = -70 To -61
      Cells(1, 2) = i / 100
      Cells(2, 2) = j / 100
      Cells(k, 8) = i / 100
      Cells(k, 9) = j / 100
      Cells(k, 10) = Cells(7, 2)
      k = k + 1
   Next j
Next i




End Sub
```

Module 2:

```
Dim collateral(1 To 20, 1 To 6) As Variant
Dim aimpoint_x As Double
Dim aimpoint_y As Double
Dim sigma_x As Double
Dim sigma_y As Double
Dim rho As Double
Dim power As Double
Dim squaresize As Double


Sub cammarano()

Application.ScreenUpdating = False

Sheets("Distribution Parameters").Activate
aimpoint_x = Cells(2, 2)
aimpoint_y = Cells(3, 2)
sigma_x = Cells(4, 2)
sigma_y = Cells(5, 2)
rho = Cells(6, 2)
power = Cells(7, 2)
stepsize = Cells(8, 2)

Sheets("Collateral Objects").Activate
numcollateral = 0
For i = 1 To 20
   If Cells(i + 1, 2) <> "" Then
      numcollateral = numcollateral + 1
   End If
Next i
For i = 1 To numcollateral
   For j = 1 To 5
      collateral(i, j) = Cells(i + 1, j + 1)
   Next j
Next i

For activecollateral = 1 To numcollateral
   m = 0
   targetsum = 0
   Do Until collateral(activecollateral, 1) + m * stepsize + 0.5 * stepsize >
collateral(activecollateral, 2)

      n = 0
```

```
        Do Until collateral(activecollateral, 3) + n * stepsize + 0.5 * stepsize >
collateral(activecollateral, 4)
            currentpos_x = collateral(activecollateral, 1) + m * stepsize + 0.5 * stepsize
            currentpos_y = collateral(activecollateral, 3) + n * stepsize + 0.5 * stepsize
            pdfvalue = power / (2 * 3.1415928 * sigma_x * sigma_y * (1 - rho ^ 2) ^ 0.5) *
Exp((-1) / (2 * (1 - rho ^ 2)) * ((currentpos_x - aimpoint_x) ^ 2 / sigma_x ^ 2 - 2 * rho *
(currentpos_x - aimpoint_x) * (currentpos_y - aimpoint_y) / sigma_x / sigma_y +
(currentpos_y - aimpoint_y) ^ 2 / sigma_y ^ 2))
            targetsum = targetsum + pdfvalue
            n = n + 1
        Loop
        m = m + 1
    Loop
    collateral(activecollateral, 6) = targetsum
Next activecollateral

Sheets("Collateral Objects").Activate
For i = 1 To numcollateral
    Cells(i + 1, 7) = collateral(i, 6) * stepsize ^ 2
Next i

Application.ScreenUpdating = False

End Sub
```

Module 3:

```
Sub Macro1()
'
' Macro1 Macro
'

'
    Range("B2:C6").Select
    ActiveSheet.Shapes.AddChart.Select
    ActiveChart.SetSourceData Source:=Range("'collateral'!$B$2:$C$6")
    ActiveChart.ChartType = xlXYScatterLines
    ActiveChart.PlotArea.Select
    ActiveSheet.ChartObjects("Chart 2").Activate
    ActiveChart.Axes(xlCategory).Select
    ActiveChart.Axes(xlCategory).MinimumScale = -10
    ActiveChart.Axes(xlCategory).MinimumScale = -100
    ActiveChart.Axes(xlCategory).MaximumScale = 15
    ActiveChart.Axes(xlCategory).MaximumScale = 100
    ActiveSheet.ChartObjects("Chart 2").Activate
    ActiveChart.PlotArea.Select
    ActiveSheet.ChartObjects("Chart 2").Activate
    ActiveChart.Axes(xlValue).Select
    ActiveChart.Axes(xlValue).MaximumScale = 35
    ActiveChart.Axes(xlValue).MinimumScale = 0
    ActiveChart.Axes(xlValue).MinimumScale = 10
    ActiveChart.Axes(xlValue).MaximumScale = 100
    ActiveChart.Axes(xlValue).MinimumScale = -100
End Sub
```

Appendix C. Quad Chart

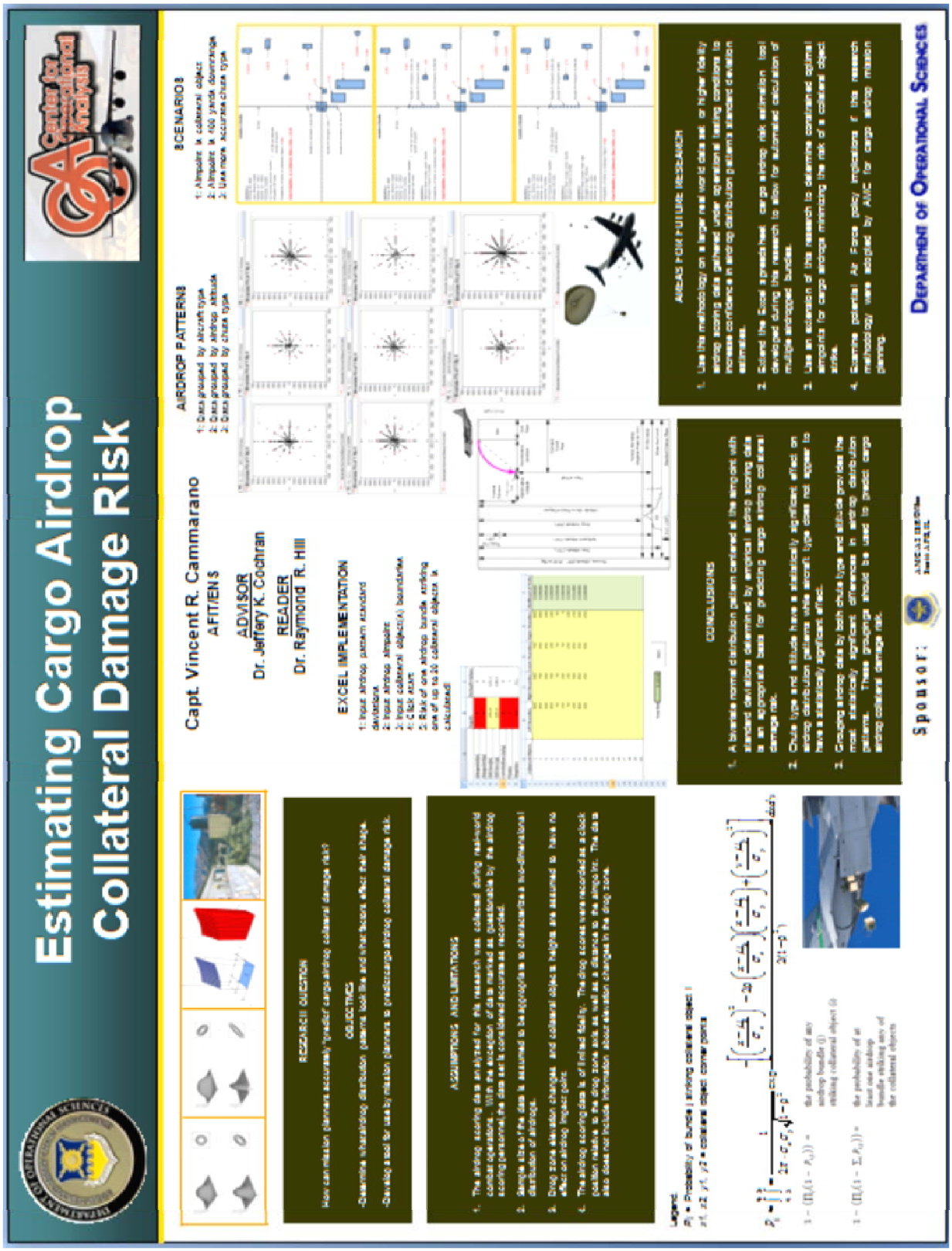

Appendix D: Blue Dart

Since the early days of aviation the art and science of resupply via airdrop has been in a state of constant evolution inspired by mission requirements. The early lessons of aerial resupply at Dien Bien Phu, Khe Sanh, and An Loc during the Vietnam War lead to improved equipment and procedures such as the Low Altitude Parachute Extraction System, Ground Proximity Extraction System, two stage parachutes, high-velocity airdrops, and high-altitude low-opening methods. These early improvements were just the beginning and have culminated in our ultimate achievement in airdrop accuracy to date, the GPS-enabled Joint Precision Airdrop System or JPADS. JPADS has enabled airdrops to be conducted in ways and in locations that would not have been possible prior to its development. But there is one problem with JPADS…it's expensive. The costs of a JPADS airdrop can be prohibitive and as a result most airdrops today are still delivered via the less accurate conventional high or low-velocity chutes.

These conventional chutes are released at an optimum point over a drop zone to maximize the probability that the cargo will land on its desired aimpoint. These optimal points are determined through calculations known as Compute Air Release Points or CARPs. The optimal points developed by these calculations should result in the airdropped cargo landing on its intended aimpoint. Of course, that is the plan. But what happens when the best location to aim an airdrop has a school nearby or a small pond or river? Should the airdrop be executed as planned? What is the chance that the airdrop will strike a collateral object? What is a safe stand-off distance for receiving personnel? This leads us to the research question this thesis aims to answer: How can mission planners accurately predict airdrop collateral damage risk?

Through a comprehensive literature review and a thorough examination of a data set of real world airdrop scoring data this thesis aims to first describe what theoretical airdrop error distribution patterns look like. After a satisfactory description of the theoretical airdrop error distribution pattern is identified it will be used as the basis for a rudimentary planning tool. This tool will be developed for consideration by airdrop planners as a method of estimating cargo airdrop error risk.

This research first determined that a typical airdrop error pattern develops a confidence region that takes on the shape of a symmetrical ellipse. This elliptical confidence region generally has a larger standard deviation along the drop zone or Y axis compared to the X axis. It is also shown that bivariate normal distributions with $\mu_x = 0, \mu_y = 0,\ \rho_{x,y} = 0$ and σ_x & σ_y determined by empirical data are appropriate for modeling cargo airdrop errors. The parameters of these error patterns were determined to be affected by chute type and airdrop altitude. As expected, the empirical data suggest that airdrops using the more accurate high-velocity chutes result in a tighter error pattern than their low-velocity counterparts. Also, as expected, airdrops from lower altitudes generally display tighter error patterns than higher altitudes when all other factors are held constant. Perhaps not as intuitive, the data suggests that airdrops from different aircraft types that use different methods of calculating CARPs do not show significant differences in their cargo airdrop error patterns. These findings suggest that when estimating airdrop collateral damage risk the airdrop error patterns differ mainly by altitude and chute type and any differences associated with aircraft type should be negligible.

This research developed a simple to use spreadsheet tool incorporating the bivariate normal distribution pattern to estimate collateral damage risk. Operators of the tool can select the airdrop error distribution parameters provided in the spreadsheet based on the mission planning parameters. After selecting and entering the distribution parameters, up to 20 collateral objects can be entered on the spreadsheet. The spreadsheet tool will output the probability of the airdropped cargo striking each of the collateral objects as well as the total probability of a collateral object strike. With the output collateral object strike probability, mission planners can make decisions such as changing airdrop altitude or chute type or changing the aimpoint in an effort to balance the risk of collateral damage, the risk to the aircraft from ground-based threats and the risk of not being able to recover the airdropped cargo.

Bibliography

"AFI 11-231, Computed Air Release Point Procedures." *AFDPO webpage*. 31 August 2005. http://www.epublishing.af.mil

Banks, Jerry and John S. Carson II, Barry L. Nelson and David M. Nicol. *Discrete-Event System Simulation* (5th Edition). New Jersey: Pearson Education Inc, 2010

Bartlett, M.S. and D.G. Kendall "The Statistical Analysis of Variances-Heterogeneity and the Logarithmic Transformation," Journal of the Royal Statistical Society, Suppl 8: 128-138 (1946).

Benney, Richard and Justin Barber, Joseph McGrath, Jaclyn McHugh, Greg Noetscher, and Steve Tavan. "The Joint Precision Airdrop System Advanced Concept Technology Demonstration." 18th AIAA Aerodynamic Decelerator Systems Technology Conference and Seminar paper. 2005
http://faculty.nps.edu/oayakime/ADSC/PATCAD%20-%20Benney%20-%20The%20Joint%20Precision%20Airdrop%20System%20Advanced%20Concept%20Technology%20Demonstration.pdf

Berry, William G. and Leon W. Laugginger. *A Computer Simulation of Release Parameter Effects Upon Bomb Impact Distributions.* MS thesis. AFIT/SLGR. Graduate Education Division, School of Systems and Logistics, Air Force Institute of Technology (AU), Wright-Patterson AFB OH, January 1975 (AD-A006347)

Bingham, Origen K. "Air-to-Ground Gunnery Simulation; CAN Computer Program 6-70 (Program AIRTOGR)" Center for Naval Analyses, CNA Research Contribution No. 158, November 1970
http://www.cna.org/documents/0200015800.PDF

Brown, M.B. and Forsythe, A.B. "The Small Sample Behavior of Some Statistics Which Test the Equality of Several Means," *Technometrics*, 16:1, 129-132 (1974).

Box, George E. and Norman R. Draper/Smith, *Empirical Model-Building and Response Surfaces.* John Wiley & Sons, Inc, 1987.

Clarke, Bruce A. and Ralph L. Disney, *Probability and Random Processes: A First Course with Applications.* John Wiley & Sons, Inc, 1985.

CSBSJU. *Kolmogorov-Smirnov Test*. Online Computer Software provided by the College of Saint Benedict & Saint John's University. Accessed: 26 Nov 2010.
http://www.physics.csbsju.edu/stats/KS-test.n.plot_form.html
Dawkins, Paul. "Paul's Online Math Notes." Lamar University. Beaumont, Texas. Accessed: 28 January 2011.
http://tutorial.math.lamar.edu/Classes/CalcIII/DoubleIntegrals.aspx

Devore, Jay L. *Probability and Statistics for Engineering and the Sciences.* Wadsworth, Inc. 1987

Dillenburger, Steve. AFIT PhD Student, The Air Force Institute of Technology, Wright-Patterson AFB, OH. Personal communication. January 2011.

Draper/Smith, N. R. and H. Smith, *Applied Regression Analysis*. John Wiley & Sons, Inc, 1966.

Duchateau, Luc. "Appendix D: The Normal Distribution." Center for Statistics, Limburgs University Center, Diepenbeek, Belgium. Accessed: 28 January 2011. http://agtr.ilri.cgiar.org/Library/docs/Linear_Mixed_Models/AppendixD.htm

Ebeling, Charles E., *An Introduction to Reliability and Maintainability Engineering.* Waveland Press Inc., 2005

"Factsheets." *Air Force Link Webpage.* November 2010. http://www.af.mil/information/factsheets/index.asp

Feltus, Pamela. "U.S. Centennial of Flight Commission: The Berlin Airlift." *Centennial of Flight webpage*. 11 December 2007. http://www.centennialofflight.gov/essay/Air_Power/berlin_airlift/AP35.htm

Frame, J. Davidson. *Managing Risk in Organizations: A Guide for Managers.* Jossey-Bass, A Wiley Imprint., 2003.

Friedman, Linda Weiser and Hershey H. Friedman. "The Probability Distribution as a Performance Criterion When Comparing Alternative Systems" *Simulation*, Vol. 45 no. 5: 262-264 (November 1985)

Garvey, Paul R. *Analytical Methods for Risk Management: A Systems Engineering Perspective.* Chapman & Hall/CRC., 2009.

JMP 8.0 Help Guide. Version 8.0, SAS. Statistics computer software package. SAS Institute Inc. Cary, NC. 2008.

Kogler, Thomas R. *Modeling the Effects of the Use of GPS Derived Altitude Indication in the C-17A Airdrop System.* MS thesis, AFIT/GSO/ENS/89D-9. Graduate School of Management and Engineering, Air Force Institute of Technology (AU), Wright-Patterson AFB OH, December 1989 (AD-A215 366)

KSmrq. "Plot of Function with Rectangle, Trapezoid, Romberg, and Gauss Quadrature," Image created: 2 July 2007. Accessed: 28 January 2011. http://en.wikipedia.org/wiki/File:Numerical_quadrature_4up.png

Levene, H. "Robust Tests for the Equality of Variances" In I. Olkin (ed), *Contributions to Probability and Statistics*, Stanford Univ. Press, (1960).

Mathematical Analysis Research Corp (MARC). *Technical Memo 31: Calculation of the CEP*. Prepared by the Jet Propulsion Laboratory at the California Institute of Technology for the US Army Intelligence Center and School's Combat Developer's Support Facility. Aug 1987.

McClave, James T, P. George Benson, and Terry L. Sincich. *Statistics for Business and Economics (8th Edition).* Prentice Hall, 2000.

McGowen, Laura. "Airdrop System Resupplies Ground Troops." *Defense Department's Transformation webpage.* 16 Aug 2006. http://www.defense.gov/transformation/articles/2006-08/ta081606a.html

O'Brien, R.G., "A General ANOVA Method for Robust Tests of Additive Models for Variances," *Journal of the American Statistical Association*, 74: 877-880 (1979).

Olejnik, S.F. and Algina, J., "Type I Error Rates and Power Estimates of Selected Parametric and Nonparametric Tests of Scale," *Journal of Educational Statistics*, 12, 45-61 (1987).

Tokar, John A. *Provide by Parachute: Airdrop in Vietnam, 1954-1972.* Monograph. School of Advanced Military Studies, United States Army Command and General Staff College, Fort Leavenworth, Kansas. 1998.

Vaughan, David and Donoho, James. "From Stalingrad to Khe Sanh: Factors in the Successful Use of Tactical Airlift to Support Isolated Land Battle Areas." Air & Space Power Journal. October 2000. http://www.airpower.au.af.mil/airchronicles/cc/vaughan.html

Wilson, James "Modeling Dependencies in Stochastic Simulation Inputs." *Proceedings of the 1997 Winter Simulation Conference.* Pg 47-52. IEEE Computer Society Washington, DC, USA. 1997.

Vita

Captain Vincent R. Cammarano graduated from River Ridge High School in New Port Richey, Florida in 1993. He enlisted in the U.S. Air Force in 1997 as a Communications and Navigations Systems Apprentice. Attending Embry Riddle Aeronautical University while on active duty he earned his baccalaureate degree in Professional Aeronautics in 2004. He gained an officer commission through the Air Force Officer Training School in 2005 where he graduated with honors.

His previous assignments were at Dyess AFB, Texas; RAF Mildenhall, UK; and Charleston AFB, South Carolina prior to his assignment to Wright-Patterson AFB, Ohio as an AFIT student. He has performed as an on-equipment and off -equipment avionics technician, Maintenance Operations Center coordinator, Maintenance Group duty officer, assistant flight officer in charge and flight officer in charge. He has experience on C-130H, KC-135R, and C-17A aircraft in various capacities.

Upon graduation from AFIT he will be assigned to the 62nd Maintenance Group at Joint Base Lewis-McChord in Tacoma, Washington.

REPORT DOCUMENTATION PAGE

Form Approved
OMB No. 074-0188

The public reporting burden for this collection of information is estimated to average 1 hour per response, including the time for reviewing instructions, searching existing data sources, gathering and maintaining the data needed, and completing and reviewing the collection of information. Send comments regarding this burden estimate or any other aspect of the collection of information, including suggestions for reducing this burden to Department of Defense, Washington Headquarters Services, Directorate for Information Operations and Reports (0704-0188), 1215 Jefferson Davis Highway, Suite 1204, Arlington, VA 22202-4302. Respondents should be aware that notwithstanding any other provision of law, no person shall be subject to an penalty for failing to comply with a collection of information if it does not display a currently valid OMB control number.
PLEASE DO NOT RETURN YOUR FORM TO THE ABOVE ADDRESS.

1. REPORT DATE *(DD-MM-YYYY)*
24-3-2011

2. REPORT TYPE
Master's Thesis

3. DATES COVERED *(From – To)*
Sep 2009 - Mar 2011

4. TITLE AND SUBTITLE
Estimating Cargo Airdrop Collateral Damage Risk

5a. CONTRACT NUMBER

5b. GRANT NUMBER

5c. PROGRAM ELEMENT NUMBER

6. AUTHOR(S)
Cammarano, Vincent R., Captain, U.S. Air Force

5d. PROJECT NUMBER

5e. TASK NUMBER

5f. WORK UNIT NUMBER

7. PERFORMING ORGANIZATION NAMES(S) AND ADDRESS(S)
Air Force Institute of Technology
Graduate School of Engineering and Management (AFIT/EN)
2950 Hobson Street, Building 642
WPAFB OH 45433-7765

8. PERFORMING ORGANIZATION REPORT NUMBER
AFIT-LSCM-ENS-11-02

9. SPONSORING/MONITORING AGENCY NAME(S) AND ADDRESS(ES)
AMC/A2 Attn: Col MacNabb / Maj Birdwell
420 Scott Drive Unit 1L8 DSN: 779-4403
Acott AFB IL 62225 e-mail: Michael.birdwell@scott.af.mil

10. SPONSOR/MONITOR'S ACRONYM(S)

11. SPONSOR/MONITOR'S REPORT NUMBER(S)

12. DISTRIBUTION/AVAILABILITY STATEMENT
DISTRIBUTION STATEMENT A. APPROVED FOR PUBLIC RELEASE; DISTRIBUTION IS UNLIMITED.

13. SUPPLEMENTARY NOTES

14. ABSTRACT
The purpose of this research is to determine an appropriate method for estimating cargo airdrop collateral damage risk. Specifically, this thesis answers the question: How can mission planners accurately predict airdrop collateral damage risk? The question is answered through a literature review and a thorough examination of a data set of real world airdrop scoring data. The data were examined to determine critical factors that affect airdrop error risks as well as to determine the characteristics of airdrop error patterns. Through this research it was determined that bivariate normal distributions with parameters of $\mu_x = 0, \mu_y = 0,\ \rho_{x,y} = 0$ and σ_x & σ_y pairs determined by empirical data are appropriate for modeling cargo airdrop errors patterns. Collateral risk is estimated by summing numerical integrations of a fit bivariate normal distribution for each drop type across rectangular representations of drop field objects in the field of concern. Airdrop altitude and chute type are found to make a statistically significant difference in airdrop error patterns while airdrop aircraft type does not appear to have a significant effect. This research methodology is implemented in an EXCEL spreadsheet tool that can be easily used by airdrop mission planners including an extension, requested by the research sponsors, to handle bundled drops that fall in a linear spread.

15. SUBJECT TERMS
Airdrop, Airdrop Patterns, Airdrop Distributions, Collateral Damage, Risk Estimation

16. SECURITY CLASSIFICATION OF:			17. LIMITATION OF ABSTRACT	18. NUMBER OF PAGES	19a. NAME OF RESPONSIBLE PERSON
a. REPORT	b. ABSTRACT	c. THIS PAGE			Dr. Jeffery Cochran, Professor of Operations Research
U	U	U	UU	108	**19b. TELEPHONE NUMBER** *(Include area code)* (937) 255-3636, ext 4521; e-mail: Jeffery.cochran@afit.edu

Standard Form 298 (Rev. 8-98)
Prescribed by ANSI Std. Z39-18